THEORETICAL INVESTIGATION OF THE EFFECT OF INTRAMOLECULAR

INTERACTIONS ON THE CONFIGURATION

OF POLYMERIC CHAINS

Thesis by

John Gillett Curro

In Partial Fulfillment of the Requirements

For the Degree of

Doctor of Philosophy

California Institute of Technology

Pasadena, California

1969

(Submitted April 27, 1969)

ACKNOWLEDGMENTS

ABSTRACT

A theoretical investigation of the effect of intramolecular interactions on the configurational statistics of a polymer molecule is presented. This problem has been studied by many authors and is known as the "excluded volume problem" in the literature. A statistical mechanical approach is used. Many of the similarities between the theory of "classical fluids" and the excluded volume problem are exploited.

The configurational statistics of 2 and 3 segment chains are computed exactly for the "hard sphere potential". The integrations were performed by introducing bipolar and tripolar coordinate systems. It was found that the mean square end-to-end distance for these cases was $n^{1.33}$ where n is the number of segments. These results are of no practical use in predicting the properties of real polymer chains which are much longer. It is instructive, however, to compare these exact results with approximate theories in the limit of short chain length.

A "cluster expansion" is written for the partition function of a polymer chain with the ends of the chain fixed. This is analogous to the cluster expansion for the partition function of an imperfect gas. The first-order term in this expansion is evaluated for the hard core potential. In the limit of small hard core diameters, the first-order term leads to the well-known first-order perturbation theory for the mean square end-to-end distance. The exact results of this first-order correction term are used to construct higher-order terms of a specified

"isolated topology". If only these terms are used in the cluster expansion, incorrect results are obtained for the mean square end-to-end distance. This indicates that higher-order terms of complicated topology are significant for longer chain length.

Various approximate integral equations for the restricted partition function of a polymer chain are presented. The most promising of these equations is the analog of the well-known Percus-Yevick equation in the theory of liquids. In deriving this equation two topologically distinct types of graphs are defined. These are the "nodal and elementary" graphs. An exact equation relating these types of graphs is presented. The analog of the Percus-Yevick approximation is made which leads to an integro-difference equation. This equation is solved exactly using the hard core potential for the special case of the hard core diameter equal to the polymer segment length. Results of numerical calculations are given for other intermediate values of this diameter ranging from zero to the segment length (the "pearl necklace" model). This leads to values of γ ranging correspondingly from 1.0 to 2.0 where $\langle r^2_{1N} \rangle \propto M^{\gamma}$ with $\langle r^2_{1N} \rangle$ the mean square end-to-end distance and M the molecular weight. The numerical results for $\langle r^2_{1N} \rangle$ as a function of chain length are in good agreement with the second-order perturbation theory of Fixman for small hard core diameters.

TABLE OF CONTENTS

TABLE OF CONTENTS--Continued

TABLE OF CONTENTS--Continued

1. INTRODUCTION

The field of polymer physics has expanded greatly since 1940. The motivation for the study of polymers has come from two sources. With the advent of industrially important synthetic polymers came the need for a basic understanding of polymer structure and behavior. Biochemists also realized that many of the biologically important compounds such as proteins and nucleic acids are polymeric in nature. Thus the study of polymer physics is important to both the engineer and the biologist.

Theoretical polymer physics can be divided into phenomenological and molecular theories. In phenomenological theory one attempts to describe the physical behavior of polymers in terms of a minimum number of experimentally determinable parameters. Examples of this approach are the fields of thermodynamics, fluid mechanics and elasticity. In molecular theory, on the other hand, one attempts to describe the behavior of polymers in terms of molecular parameters. These molecular parameters are in principle calculable from quantum mechanics. Practically this is often not possible, and some rigor is necessarily sacrificed in finding these molecular parameters.

Many of the unique physical properties of polymers are due to the fact that the polymer chains are capable of assuming a very large number of configurations. Molecular theories to deduce these properties necessarily involve the use of statistical mechanical methods. The configurational statistics of a polymer chain are the starting points

for theories on polymer elasticity, viscoelasticity, polymer solutions and molecular weight determination. A simplified model of a non-interacting polymer chain has been solved exactly and has been successful in approximating the actual behavior of polymeric chains. In order to refine this simplified theory, the interactions of the polymer molecule with itself and with other molecules must be incorporated into the theory. The effect of intramolecular interactions or the interaction of a polymer chain with itself has been a subject of considerable interest. The effect of intramolecular interactions on the configurational statistics of the chain is commonly known as the "excluded volume" effect. This problem has been studied by many polymer physicists in the past with very limited success (1-13).

The excluded volume problem has many similarities to many-body problems in other areas of physics. The equations from the theory of imperfect gases and liquids, in particular, are similar in form to the polymer chain equations. In this thesis, the excluded volume problem will be investigated in detail and some mathematical techniques used in liquid state theory will be applied to this problem.

2. SUMMARY OF PREVIOUS WORK

In this chapter I will give a brief summary of some previous work on the problem of computing the configurational statistics of a freely-jointed polymer chain with intramolecular interactions.

The excluded volume effect in polymers was first treated by Flory (1). Flory assumed that the distribution of segments about the center of mass and the end-to-end distance of the chain was Gaussian, although the width of these Gaussian distributions is enlarged by the excluded volume effect. In order to. find the amount of enlargement, the influence of intramolecular interactions is treated as a swelling phenomenon for which thermodynamic formulas for solvent-polymer systems exist. Flory found the result,

$$\alpha^5 - \alpha^3 = Cn^{1/2} \qquad (2.1)$$

for a chain of 2n segments. α is the ratio of the root mean square end-to-end distance of the chain to the corresponding end-to-end distance in the absence of intramolecular effects (random walk problem). Thus for large n, Flory's theory predicts that the mean square end-to-end distance is proportional to $n^{6/5}$. The physical significance of Flory's method is somewhat vague, and his assumption that the distribution remains Gaussian is certainly questionable.

Hermans, Klamkin and Ullman (2) derived a generalized Fokker-Planck type of equation for the distribution function of a chain with excluded volume. This entailed the assumption of a specific form for

the conditional probability of the nth segment being at $\vec{r}_n$, given that the first n-1 segments are held fixed. These authors found that the mean square end-to-end distance differed by only a constant from the corresponding value for a non-interacting chain (i.e. α = constant). Rubin (3) has given evidence that the Herman, Klamkin, Ullman choice of the conditional probability is not correct. In another paper Rubin (4) presented arguments that the mean square end-to-end distance is proportional to n raised to a power which has an upper bound of 3/2.

Zimm, Stockmayer, and Fixman (5) derived an integral equation of the Markoff form for the pair distribution function of a polymer chain. The kernel of this integral equation is the conditional probability. This function is an extremely complicated multiple integral which involves the pair potential between any two points on the chain. A first-order approximation to this conditional probability was obtained using the so-called "single contact" approximation, which considers only those configurations in which a single pair of segments is interacting. Since the potential between nonadjacent segments $v(r_{ij})$ is short range, Zimm, Stockmayer, and Fixman approximated this potential by

$$h(r_{ij}) = 1 - \exp\ [-v(r_{ij})/kT] = X\delta(r_{ij}) \qquad (2.2)$$

where $\delta(r_{ij})$ is a three-dimensional delta function and

$$X = \int [1 - \exp(-v(r_{ij})/kT)]\ d\vec{r}_{ij}.$$

With this form for the potential these authors found that the mean square end-to-end distance $<r_{1N}^2>$ was a function of the parameter,

$$z = X(3/2\pi a^2)^{3/2} n^{1/2} \tag{2.3}$$

where a is a segment length in the chain. Zimm, Stockmayer and Fixman found the first term in the expansion of $<r_{1N}^2>$ in terms of z.

$$\alpha^2 = \frac{<r_{1N}^2>}{<r_{1N}^2>_o} = [1 + 4/3z + \ldots] \tag{2.4}$$

$<r_{1N}^2>_o$ is the corresponding mean square end-to-end distance for a chain with no excluded volume. This equation was also obtained by Yamamoto (6) and Grimely (7). The next higher-order term in this expansion was obtained by Fixman (8)

$$\alpha^2 = [1 + 4z/3 - (16/3 - 28\pi/27)z^2 + \ldots]. \tag{2.5}$$

In deriving this equation Fixman also approximated the potential by Eq. (2.2).

Notable progress was made recently by Edwards (9) and Reiss (10), who decoupled the many-body problem by a self-consistent field technique similar to the Hartree Fock (11) method for many electron atoms. Edwards solved his equations asymptotically and found that $<r_{1N}^2> \propto n^{6/5}$ Edwards' treatment, although original, is very difficult to read and, as Reiss points out in his paper, is somewhat incomplete. In his treatment, Reiss replaced the sum over pair interactions $1/2 \sum_{i \neq j} v_{ij}$ by $\sum_i \phi_i$ where the ϕ_i are chosen to satisfy a variational principle. That the ϕ_i

rigorously satisfy the variational principle is questionable (11).

Reiss was able to obtain a zeroth-order approximation to ϕ_i from his

equations. This was used to obtain an integral equation of the Markoff

type for the probability distribution. He then passed to a differential

equation which he was able to solve in one limit. Reiss found that

$\langle r_{1N}^2 \rangle \propto n^{4/3}$.

Yamakawa (12) has shown that Reiss left out a term in deriving

the integral equation. Yamakawa used Reiss' self-consistent potential

with a somewhat different integral equation to obtain $\langle r_{1N}^2 \rangle \propto n^{6/5}$ as $n \to \infty$.

This treatment also entailed the approximation of the potential as in

Eq. (2.2).

One of the drawbacks to using a self-consistent field is that it

is not known how good the approximation is. Since the ϕ_i are chosen

to satisfy the variational principle they represent the best set (there

may be more than one set) of functions ϕ_i under the restriction 1/2

$\sum_{i \neq j} v_{ij} = \sum_i \phi_i$. The variational principle says nothing about the error

involved in the original approximation however. It should also be pointed

out that only a zeroth-order approximation to the ϕ_i which satisfies

the variational principle is actually used in the treatments of Reiss,

Edwards and Yamakawa.

Naghizadeh (13) derived a Born-Green-Kirkwood (14, 15) type of

integral equation for the distribution function. The Born-Green and

Kirkwood equations were originally derived for the radial distribution

function in liquids. Naghizadeh's equation for the n element distribution

function contains the (n+1) element distribution function. In order to

truncate this hierarchy of equations, Naghizadeh made the analog of the

"Kirkwood Superposition" approximation. The resulting equations are

very similar in form to Reiss' equations. This is not very surprising

since the Kirkwood Superposition principle involves the averaging of

forces, which is essentially what the self-consistent central field

does.

3. GENERAL THEORY

In this chapter the basic equations for the distribution function of a freely-jointed polymer chain with intramolecular inter-actions is derived. The methods used in the literature are usually based on random walk theory, however, I will use a statistical mechanical argument to derive an equation for the probability distribution function for the ends of the chain. The concept of an ordering potential between adjacent chain elements is introduced. This enables one to proceed in a manner analogous to the statistical mechanics of real gases (17).

Choose as a model a chain of N-1 (N subsystems) "freely-jointed" segments which are allowed to interact (see Fig. 3.1).
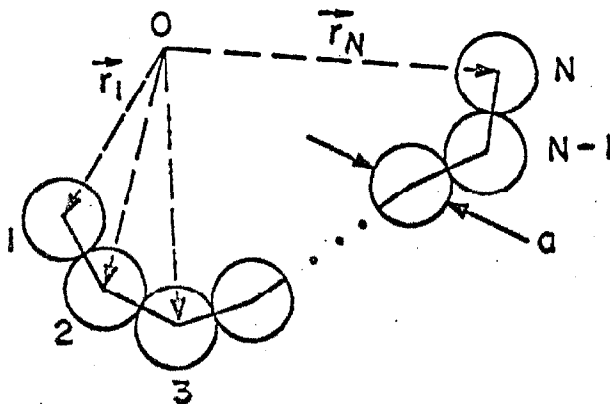
Fig. (3.1)

One chain in an ensemble of chains.

The term "freely-jointed" implies that there is no fixed bond angle or hindered rotation between segments. In effect the segments behave as if they were connected by universal joints. Assume further that the temperature and masses are large enough so that quantum effects can be neglected and the problem can be handled classically. From statistical mechanics the probability of observing the system in a particular energy state is given by,

$$P[\vec{p}_1...\vec{p}_N,\vec{\rho}_1...\vec{\rho}_N] \, d\vec{p}_1...d\vec{p}_N d\vec{\rho}_1...d\vec{\rho}_N \qquad (3.1)$$

$$= Q_N^{-1} h^{-3N} \exp[-\beta H(\vec{p}_1...\vec{p}_N,\vec{\rho}_1...\vec{\rho}_N)] d\vec{p}_1...d\vec{p}_N d\vec{\rho}_1...d\vec{\rho}_N$$

$\beta = 1/kT$ and $\vec{p}_j$ is the momentum of the jth subsystem. $\vec{\rho}_j$ is the position of the jth particle, which for convenience has been scaled by the segment length a (i.e. $\vec{\rho}_j = \vec{r}_j/a$). H is the classical Hamiltonian defined by the sum of a kinetic and configurational energies

$$H(\vec{p}_1...\vec{p}_N,\vec{\rho}_1...\vec{\rho}_N) = \sum_i p_i^2/2m + V(\vec{\rho}_1...\vec{\rho}_N). \qquad (3.2)$$

V is the configurational or potential energy of the system. Q_N is the canonical partition function.

$$Q_N = h^{-3N} \int...\int \exp(-\beta H) d\vec{p}_1...d\vec{p}_N d\vec{\rho}_1...d\vec{\rho}_N \qquad (3.3)$$

If the Hamiltonian in Eq. (3.2) is substituted into Eq. (3.3), the momentum integrations are factorable and are easily performed to give a factor which depends on temperature.

$$Q_N = (2\pi mkT/h^2)^{3N/2} Z \qquad (3.4)$$

Z is the configuration integral,

$$Z = \int \ldots \int \exp(-\beta V) d\vec{\rho}_1 \ldots d\vec{\rho}_N. \qquad (3.5)$$

The probability that two subsystems i and j have positions $\vec{\rho}_i$ and $\vec{\rho}_j$ respectively is obtained by integrating Eq. (3.1) over all variables except $\vec{\rho}_i$ and $\vec{\rho}_j$.

$$P[\vec{\rho}_i, \vec{\rho}_j] d\vec{\rho}_i d\vec{\rho}_j = (Z_{ij} (\vec{\rho}_i \vec{\rho}_j, N)/Z) d\vec{\rho}_i d\vec{\rho}_j \qquad (3.6)$$

Z_{ij} can be considered to be a restricted configuration integral in which subsystems i and j are held fixed in configuration space.

$$Z_{ij} (\vec{\rho}_i, \vec{\rho}_j, N) = \int \ldots \int \exp(-\beta V) \prod_{k \neq ij} d\vec{\rho}_k \qquad (3.7)$$

Integration over $\vec{\rho}_i$ and $\vec{\rho}_j$ in Eq. (3.7) yields the unrestricted configuration integral Z defined by Eq. (3.5)

$$Z = \int \int Z_{ij} (\vec{\rho}_i, \vec{\rho}_j, N) d\vec{\rho}_i d\vec{\rho}_j.$$

The probability that the ends of the chain have positions $\vec{\rho}_1$ and $\vec{\rho}_N$ is,

$$P[\vec{\rho}_1 \vec{\rho}_N] d\vec{\rho}_1 d\vec{\rho}_N = (Z_{1N} (\vec{\rho}_1 \vec{\rho}_N)/Z) d\vec{\rho}_1 d\vec{\rho}_N . \qquad (3.8)$$

Assuming pairwise additivity of forces, the potential V can be regarded as the sum of pair potentials between adjacent subsystems and nonadjacent subsystems.

$$V = \sum_i w_{ii+1} + 1/2 \sum_{i \neq j} \sum v_{ij} \qquad (3.9)$$

ρ_{ij} is the distance between points i and j (i.e. $\rho_{ij} = |\vec{\rho}_j - \vec{\rho}_i|$).
Choose the potential between adjacent subsystems w_{ii+1} so that the
segments are connected, thereby forming a chain. This condition is
satisfied by choosing

$$\exp\,(-\beta w_{ii+1}) = \delta(\rho_{ii+1}-1). \qquad (3.10)$$

This potential is essentially an infinite potential well since,

$$w_{ii+1} \to +\infty \text{ for } \rho_{ii+1} \neq 1$$
$$w_{ii+1} \to -\infty \text{ for } \rho_{ii+1} = 1$$

Thus the configuration of the system is constrained so that the dis-
tance between adjacent subsystems i and i+1 is always $\rho_{ii+1} = 1$ (or
$r_{ii+1} = a$). The potential w_{ii+1} is effectively an "ordering" potential
which ensures that a chain of subsystems is generated in the order 1,
2 . . . N (see Fig. 3.1). The potential between nonadjacent subsystems
v_{ij} is short range. v_{ij} becomes infinitely large for small ρ_{ij} and
approaches zero rapidly for ρ_{ij} of the order of unity or larger. Using
Eqs. (3.9) and (3.10), the restricted configuration integral can be
written as,

$$Z_{ij}(\rho_{ij},N) = \int...\int \prod_k \delta(\rho_{kk+1}-1) \prod_{k\ell}\exp(-\beta v_{k\ell}) \prod_{\ell \neq ij} d\vec{\rho}_\ell. \qquad (3.11)$$

Note that the potential V does not depend on the choice of the origin,
hence the origin is arbitrary. As a result, the argument of Z_{ij} can be
taken to be ρ_{ij}. In other words Z_{ij} depends only on the scalar distances
between fixed points i and j. For the ends of the chain fixed, we have

$$Z_{1N}(\rho_{1N}) = \int \cdots \int \prod_k \delta(\rho_{kk+1}-1) \prod_{ij} \exp(-\beta v_{ij}) d\vec{\rho}_2 \cdots d\vec{\rho}_{N-1}. \quad (3.12)$$

It is convenient to define a set of functions, similar to the Mayer functions used in the theory of imperfect gases.

$$h_{ij} = 1 - \exp(-\beta v_{ij}) \quad (3.13)$$

$$\text{as } h_{ij} \to 1 \quad \rho_{ij} \to 0$$

$$\text{as } h_{ij} \to 0 \quad \rho_{ij} \to \infty$$

Eq. (3.12) can be rewritten in terms of these functions.

$$Z_{1N} = \int \cdots \int \prod_k \delta(\rho_{kk+1}-1) \prod_{ij}(1-h_{ij}) d\vec{\rho}_2 \cdots d\vec{\rho}_{N-1} \quad (3.14)$$

Eq. (3.14) represents the configuration integral for a freely-jointed chain with excluded volume. The factor involving $\delta-$ functions is due to the ordering of the chain segments (i.e. adjacent segments are connected). The factors involving h_{ij} arise from the excluded volume effect. This configuration integral is of prime importance, since the end-to-end distribution functions can be obtained from it using Eq. (3.8). Because the product of $\delta-$ functions appears frequently in this work, it is convenient to define

$$\Gamma_N = \prod_{i=1}^{N-1} \delta(\rho_{ii+1}-1). \quad (3.15)$$

The symbol Γ_N will be used in this thesis where no ambiguity can arise. Eq. (3.14) can then be written as

$$Z_{1N} = \int \cdots \int \Gamma_N \prod_{ij}(1-h_{ij}) d\vec{\rho}_2 \cdots d\vec{\rho}_{N-1}. \quad (3.16)$$

4. SOME SPECIAL CASES

The general equation, Eq. (3.14), will now be solved for some special cases of interest. The simplest postulate one can make is that there is no interaction between segments of the chain (no excluded volume). This model is equivalent to the random walk problem in three dimensions and has been used extensively in the theory of rubber elasticity and polymers in solution. Eq. (3.14) will then be solved for very short chains (2 and 3 links) exactly for the hard sphere potential. Although these short chain solutions are of no practical value in predicting the behavior of real polymer chains, these solutions have been worked out because they are the only cases in which Eq. (3.14) can be solved exactly with our present knowledge of many-body problems. Later on it will be interesting to compare the results of our more general theory with these exact solutions in the limit of short chain length.

A. Non - Excluded Volume Problem

If the effect of intramolecular interactions is neglected (i.e. $v_{ij} = 0$), Eq. (3.14) becomes,

$$Z_{1N} = \int \ldots \int \prod_{k=1}^{N-1} \delta(\rho_{kk+1}-1) d\vec{\rho}_2 \ldots d\vec{\rho}_{N-1}. \qquad (4.1)$$

These integrations can be simplified by introducing the Fourier transform of the δ- function. Define the transform pair,

$$f(k) = \int \delta(\rho-1) \exp(-i\vec{k}\cdot\vec{\rho}) d\vec{\rho} \qquad (4.2a)$$

$$8\pi^3\delta(\rho_{ii+1}-1) = \int f(k) \exp(i\vec{k}\cdot\vec{\rho}_{ii+1})d\vec{k}. \qquad (4.2b)$$

This representation for $\delta(\rho_{N-1N}-1)$ is introduced into Eq. (4.1) and the order of integration interchanged to give,

$$8\pi^3 Z_{1N} = \int f(k) \exp(i\vec{k}\cdot\vec{\rho}_N)d\vec{k}\int\ldots\int\Gamma_{N-1}\exp(-i\vec{k}\cdot\vec{\rho}_{N-1})d\vec{\rho}_2\ldots d\vec{\rho}_{N-1}. \qquad (4.3)$$

Since $\vec{\rho}_{N-2}$ is fixed in the $\vec{\rho}_{N-1}$ integration, we have from Eq. (4.2a) that

$$\int\delta(\rho_{N-2N-1}-1) \exp(-i\vec{k}\cdot\vec{\rho}_{N-1})d\vec{\rho}_{N-1} = f(k) \exp(-i\vec{k}\cdot\vec{\rho}_{N-2}). \qquad (4.4)$$

Substitution of Eq. (4.4) into Eq. (4.3) leads to

$$8\pi^3 Z_{1N} = \int f^2(k) \exp(i\vec{k}\cdot\vec{\rho}_N)d\vec{k}\int\ldots\int\Gamma_{N-2}\exp(-i\vec{k}\cdot\vec{\rho}_{N-2})d\vec{\rho}_2\ldots d\vec{\rho}_{N-2}.$$

If this procedure is repeated (N-1) times, the multiple integral of Eq. (4.1) is reduced to a single integration.

$$8\pi^3 Z_{1N} = \int [f(k)]^{N-1}\exp(i\vec{k}\cdot\vec{\rho}_{1N})d\vec{k} \qquad (4.5)$$

Inserting spherical coordinates into Eq. (4.2a) enables us to evaluate $f(k)$. Substitution of this result into Eq. (4.5) and integration over the angular variables (see Appendix I for details) leads to the result

$$2\pi^2 Z_{1N} = (4\pi)^{N-1}\int_0^\infty (\sin k/k)^{N-1}k^2(\sin k\rho_{1N}/k\rho_{1N})dk . \qquad (4.6)$$

This procedure for the reduction of the multiple integral in Eq. (4.1) to a single integral is a special case of the technique used by Montroll (18) for evaluating certain types of cluster integrals.

Eq. (4.6) is the same (within a normalization constant) as the probability distribution for a random walk in three dimensions, first derived by Rayleigh (19). A simplified random walk theory was applied to polymer chains by James and Guth (20). The more general theory is due to Wang and Guth (21), who obtained various representations for the inversion of the Fourier integral. Following Wang and Guth, the function $(\sin k/k)^{N-1}$ in Eq. (4.6) can be expanded as,

$$(\sin k/k)^{N-1} = \exp[-(N-1)k^2/6][1-(N-1)k^2/180 + \ldots]. \qquad (4.7)$$

Substituting this expansion into Eq. (4.6) and integrating term by term yields,

$$z_{1N} = (4\pi)^{N-1}[3/2\pi(N-1)]^{3/2}\exp[-3\rho_{1N}^2/2(N-1)]. \qquad (4.8)$$

Eq. (4.8) is a Gaussian approximation to the distribution function Eq. (4.6). It is applicable when $\rho_{1N} \ll N$ and $N \gg 1$. Other approximations for the inversion of the Fourier integral which apply to other ranges of ρ_{1N} and N are derived by Wang and Guth. The exact distribution function for a three dimensional random walk has been obtained in the form of a series by Irwin and Hall (22). For practical calculations the simple Gaussian form is usually adequate.

Mean square end-to-end distance

The mean square end-to-end distance of a noninteracting chain can now be computed using the configurational integral we have just evaluated. From Eq. (3.8) we have

$$\langle \rho^2_{1N} \rangle = \int \rho^2_{1N} Z_{1N} d\vec{\rho}_{1N} / \int Z_{1N} d\vec{\rho}_{1N}. \tag{4.9}$$

Substitution of the Gaussian form for Z_{1N} into Eq. (4.9) leads to

$$\langle \rho^2_{1N} \rangle = \int_0^\infty \rho^4 \exp[-3\rho^2/2(N-1)] d\rho / \int_0^\infty \rho^2 \exp[-3\rho^2/2(N-1)] d\rho. \tag{4.10}$$

where the upper limit of the integration has been approximated by infinity. The integrals in Eq. (4.10) are simple gamma functions and can be performed to give,

$$\langle \rho^2_{1N} \rangle = (N-1) = n$$

$$\langle r^2_{1N} \rangle = na^2. \tag{4.11}$$

This same result is obtained if one calculates the mean square end-to-end distance using the more general expression Eq. (4.6) (see Appendix II for details).

Mean square radius of gyration

Another parameter of interest in describing the average configuration of a polymer chain is the mean square radius of gyration. This value can be determined absolutely (independent of any model) from light scattering measurements. The center of mass $\vec{r}_m$ of a chain of ($n = N-1$) segments of equal mass is defined to be

$$\vec{r}_m = N^{-1} \sum_i \vec{r}_i \tag{4.12}$$

where $\vec{r}_i$ is measured from an arbitrary origin 0 (see Fig. 3.1). The square of the radius of gyration $\vec{R}_G$ for such a chain is,

$$R_G^2 = N^{-1} \sum_i S_i^2 \qquad (4.13)$$

$\vec{S}_i$ is the distance from the center of mass to point i on the chain.

$$S_i^2 = (\vec{r}_i - \vec{r}_m) \cdot (\vec{r}_i - \vec{r}_m) \qquad (4.14)$$

Substitution of Eq. (4.12) into Eq. (4.14) yields,

$$S_i^2 = r_i^2 + N^{-2} \sum_{kj} \vec{r}_k \cdot \vec{r}_j - 2N^{-1} \sum_j \vec{r}_i \cdot \vec{r}_j.$$

Since,

$$r_{ij}^2 = r_i^2 + r_j^2 - 2\vec{r}_i \cdot \vec{r}_j$$

we have,

$$S_i^2 = r_i^2 - (1/2N^2) \sum_{kj} (r_{kj}^2 - r_k^2 - r_j^2) + N^{-1} \sum_{j=1}^{N} (r_{ij}^2 - r_i^2 - r_j^2).$$

Substitution of this result into Eq. (4.13) gives the radius of gyration as

$$R_G^2 = (1/2N^2) \sum_{ij} r_{ij}^2 .$$

The mean square radius of gyration is thus

$$\langle R_G^2 \rangle = (a^2/2N^2) \sum_{ij} \langle \rho_{ij}^2 \rangle. \qquad (4.15)$$

The mean square radius of gyration can now be computed for the noninteracting chain. Since the chain is noninteracting, the mean square distance between two points i and j on the chain depends only on that part of the chain between points i and j. In other words, the ends of the

chain $(1 \rightarrow i, j \rightarrow N)$ do not affect the distribution between the points i and j. Thus $<r^2_{ij}>$ for a noninteracting chain of N-1 segments is the same as $<r^2_{ij}>$ computed for a noninteracting chain of $|j-i|$ segments. From Eq. (4.11) we have,

$$<r^2_{ij}> = a^2 |j-i|. \qquad (4.16)$$

The mean square radius of gyration of a noninteracting chain of n = N-1 segments is

$$<R^2_G> = (a/N)^2 \sum_i \sum_j (j-1).$$

These summations can be performed easily to give the following result for large N:

$$<R^2_G> = (N-1)a^2/6 = <r^2_{1N}>/6. \qquad (4.17)$$

This result was obtained by Zimm and Stockmayer (23) and Debye (24).

B. Short Chains

For a nonzero potential function, it becomes very difficult to compute the configuration integral Eq. (3.12). I will now compute the integrals for 2 and 3 link chains using the "hard sphere" potential.

Three interacting spheres

The shortest chain in which there is an excluded volume effect is a 2-link chain or N = 3 subsystems. For this case, Eq. (3.12) reduces to

$$Z_{13} = \exp(-\beta v_{13}) \int \delta(\rho_{12}-1)\delta(\rho_{23}-1)d\vec{\rho}_2. \qquad (4.18)$$

Note that the term involving the excluded volume potential v_{13} can be removed from under the integral sign in this case. The integral in Eq. (4.18) could be done by inverting the Fourier transform of Eq. (4.6) with $N = 3$. I will use a different method which consists of introducing bipolar coordinates into Eq. (4.18). The Jacobian for bipolar coordinates is obtained in Appendix III. Introducing this into Eq. (4.18) leads to,

$$\rho_{13}Z_{13} = 2\pi \exp(-\beta v_{13}) \int \delta(\rho_{12}-1)\rho_{12}d\rho_{12} \int_{|\rho_{12}-1|}^{\rho_{12}+1} \delta(\rho_{23}-1)\rho_{23}d\rho_{23}.$$

Note that in using bipolar coordinates there are restrictions which have to be placed on the limits of integration. The first integral gives either zero or unity depending on whether or not the variable of integration passes through the zero of the δ-function's argument. Thus,

$$\rho_{13}Z_{13} = 2\pi \exp(-\beta v_{13}) \int_{|\rho_{13}-1|}^{\rho_{13}+1} \delta(\rho_{12}-1)\rho_{12}d\rho_{12}.$$

Performing the last integration gives finally,

$$\rho_{13}Z_{13} = 2\pi \exp(-\beta v_{13}) \quad \text{for } 0 \leq \rho_{13} \leq 2$$
$$= 0 \quad \text{for } \rho_{13} > 2.$$

If we introduce the hard sphere potential,

$$v_{ij} = \infty \text{ for } \rho_{ij} < b \tag{4.19}$$
$$v_{ij} = 0 \text{ for } \rho_{ij} > b.$$

We obtain,

$$Z_{13} = 2\pi/\rho_{13} \text{ for } b \leqq \rho_{13} \leqq 2 \tag{4.20}$$
$$= 0 \text{ for } \rho_{13} < b, \rho_{13} > 2.$$

Using Eq. (4.20) to compute the value of $\langle\rho^2_{13}\rangle$ leads easily to the result,

$$\langle\rho^2_{13}\rangle = (16-b^4)/2(4-b^4). \tag{4.21}$$

Note that when there is no excluded volume $(b = 0)$, Eq. (4.21) becomes

$$\langle\rho^2_{13}\rangle = 2 = n,$$

which agrees with the result obtained for a chain with no excluded volume , Eq. (4.11).

Four interacting spheres (25)

As the chain length increases, the difficulties in computing the configurational integral increase greatly. This is exemplified in the problem of four interacting hard spheres (or equivalently, a 3-link chain). This is very much more difficult than the 3-sphere case discussed in the last section. In order to do this calculation, I will introduce a "tripolar" coordinate system. To my knowledge this coordinate system has not been used before, and it might be useful in other problems such as computing virial coefficients. The configuration integral for a system of four spheres (subsystems) is found by putting N = 4 in Eq. (3.12).

$$Z_{14} = \tag{4.22}$$
$$\exp(-\beta v_{14}) \int \delta(\rho_{34}-1) \exp(-\beta v_{13}) d\vec{\rho}_3 \int \delta(\rho_{12}-1) \delta(\rho_{23}-1) \exp(-\beta v_{24}) d\vec{\rho}_2$$

Note that the term involving v_{14} can be removed from under the integral

sign since subsystem 1 and 4 are held fixed in the integrations. No

appreciable simplification of Eq. (4.22) can be achieved by introducing

Fourier transforms. The multiple integrals do not collapse by this

technique as was found in the non-excluded volume case discussed earlier.

This is due to the presence of the excluded volume terms. Since the

kernel of the interior integral of Eq. (4.22) depends on ρ_{12}, ρ_{23}, ρ_{24},

it seems natural to use these coordinates in the integration. This

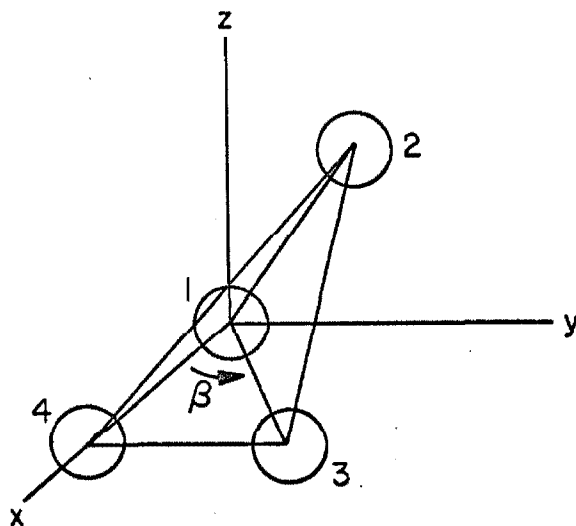tripolar coordinate system is shown in Fig. (4.1).

Fig. (4.1)

Tripolar Coordinate System

In order to compute the Jacobian for this coordinate system

we have to express ρ_{12}, ρ_{23} and ρ_{24} in terms of the cartesian coordi-

nates xyz. From geometrical considerations (see Appendix IV for details), the following relations can be obtained:

$$\rho_{12} = (x^2 + y^2 + z^2)^{1/2} \tag{4.23}$$

$$\rho_{23} = (x^2 + y^2 + z^2 - 2\rho_{13} x \cos \beta - 2\rho_{13}y \sin \beta + \rho^2_{13})^{1/2}$$

$$\rho_{24} = (x^2 + y^2 + z^2 - 2\rho_{14}x + \rho^2_{14})^{1/2}$$

$$\cos \beta = (\rho^2_{14} + \rho^2_{13} - \rho^2_{34})/2\rho_{14}\rho_{13}.$$

Let the Jacobian for this transformation be given by J_T. In this case it is easier to compute J_T^{-1} than J_T directly.

$$J_T^{-1} = \partial(\rho_{12}\rho_{23}\rho_{24})/\partial(xyz) \tag{4.24}$$

This determinant can be worked out using the relations in Eq. (4.23). These details are presented in Appendix IV. The final result is

$$J_T = -\rho_{12}\rho_{23}\rho_{24}/z \sin \beta\rho_{13}\rho_{14} \tag{4.25}$$

where $Z^2\sin^2\beta =$ (4.26)

$$\rho^2_{12} (1-\cos^2\beta) - (\rho^2_{12} + \rho^2_{14} - \rho^2_{24})^2/4 \rho^2_{14} - (\rho^2_{12} + \rho^2_{13} - \rho^2_{23})^2/4 \rho^2_{13}$$
$$+ 2(\rho^2_{12} + \rho^2_{13} - \rho^2_{23})(\rho^2_{12} - \rho^2_{24} + \rho^2_{14})\cos \beta/4\rho_{13}\rho_{14}$$

Note that J_T is singular at the zeros of ρ_{13}, ρ_{14}, ρ_{34} and z. This causes no concern however, since the hard sphere interactions will preclude the possibility of integrating through any of these singularities.

The kernel of the outer integral in Eq. (4.22) will depend on ρ_{13}, ρ_{34} and ρ_{14}. Since ρ_{14} is to be held fixed, the natural coordinate

system for this integration is the bipolar coordinate system (see Fig.(4.2).
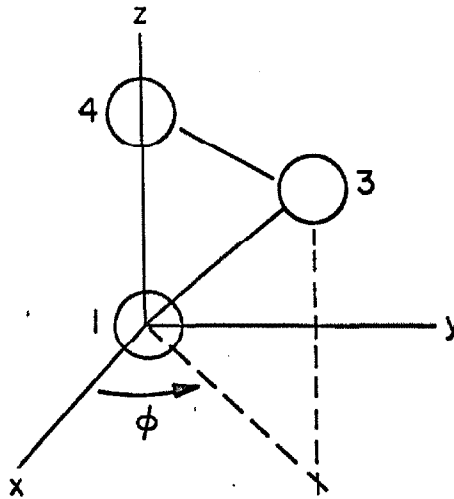
Fig. (4.2)

Bipolar coordinate system.

The Jacobian for this coordinate system J_B is computed in Appendix III.

$$J_B = \rho_{13}\rho_{34}/\rho_{14} \tag{4.27}$$

Using tripolar coordinates for the interior integration and bipolar coordinates for the outer integration, Eq. (4.22) can be written as,

$$\rho^2_{14}z_{14} = \tag{4.28}$$

$$2\pi\exp(-\beta v_{14})\iint \delta(\rho_{34}-1)\exp(-\beta v_{13})\rho_{34}d\rho_{13}d\rho_{34}$$

$$\times\iiint\exp(-\beta v_{24})\delta(\rho_{12}-1)\delta(\rho_{23}-1)\rho_{12}\rho_{23}\rho_{24}(z\sin\beta)^{-1}d\rho_{12}d\rho_{12}d\rho_{12}.$$

Let us now introduce the hard core potential given by Eq. (4.19) into Eq. (4.28). In order to simplify the calculation, take the diameter of the hard core to be exactly equal to the link length of the chain. In other words, take $b = 1^*$. Thus the exponential terms become step functions.

$$\exp(-\beta v_{ij}) = 0 \text{ for } \rho_{ij} < 1 \qquad (4.29)$$
$$= 1 \text{ for } \rho_{ij} > 1$$

or equivalently

$$\exp(-\beta v_{ij}) = H(\rho_{ij}-1)$$

where $H(X)$ is the Heaviside step function.

It would appear that the integrals in Eq. (4.28) are rather simple since the ρ_{12}, ρ_{23} and ρ_{34} integrations involve δ-functions. Replacing ρ_{12}, ρ_{23} and ρ_{34} by unity in Eq. (4.28) implies certain restrictions on the limits of the remaining integrations to insure that we integrate through the zero of the arguments of the δ-functions. These limits can be found by restricting ρ_{14}, ρ_{24} and ρ_{13} so that adjacently numbered spheres are always in contact. Furthermore, it is possible to replace $\exp(-\beta v_{24})$ and $\exp(-\beta v_{13})$ by unity in accordance with Eq. (4.29), provided ρ_{14}, ρ_{13} and ρ_{24} are constrained in such a way that the spheres cannot penetrate each other. The problem of finding

---

*In chapter 2 we scaled all the distances by the link length $a (\vec{\rho} = \vec{r}/a.)$.

all these restrictions is clearly nontrivial. In effect we have cast
the problem in a form where most of the difficulty lies in finding the
restrictions on the limits of integration. These restrictions will
have to be found by a detailed geometrical analysis of the problem.

Let us now attempt to find the restrictions on ρ_{14}, ρ_{24} and ρ_{13}
when we require that the adjacently numbered spheres be in contact and
nonadjacent spheres cannot penetrate each other. Clearly the maximum
value that ρ_{14} can take is $\rho_{14} = 3$, for then the spheres lie along a
straight line. Also the minimum value of ρ_{14} is $\rho_{14} = 1$, since spheres
1 and 4 cannot penetrate.

Consider first the case when $2 \leq \rho_{14} \leq 3$. What are the restric-
tions placed on ρ_{24} and ρ_{13} when ρ_{14} is in this range? The maximum and
minimum values that ρ_{13} can take are 2 and $\rho_{14}-1$ respectively. This can
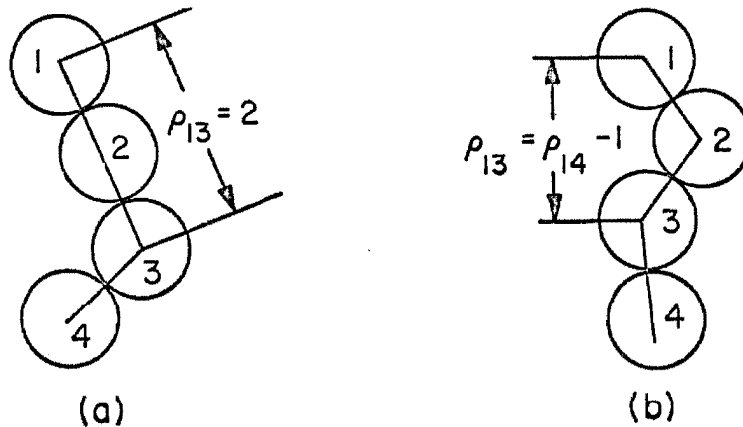be seen easily in Fig. (4.3).

(a)   (b)

Fig. (4.3)
Maximum (a) and minimum (b) values
of ρ_{13} when $2 \leq \rho_{14} \leq 3$

For fixed ρ_{14} and ρ_{13}, the maximum and minimum values that ρ_{24} can be found from the two possible positions of sphere 2 when it lies in the plane defined by spheres 1, 3, and 4 (see Fig. 4.4).
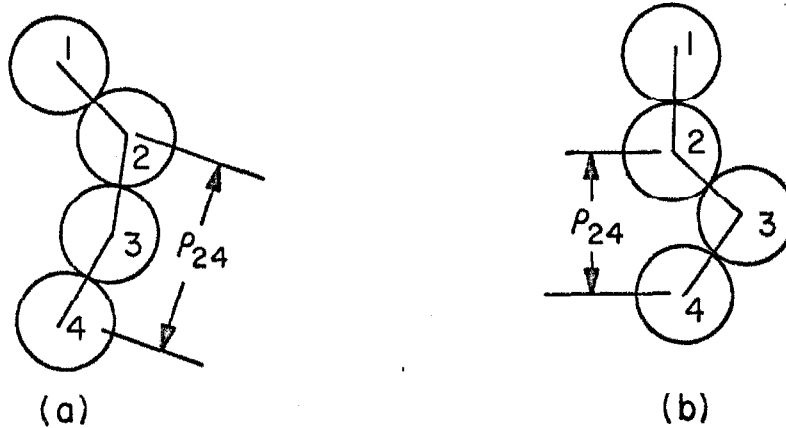
Fig. (4.4)
Maximum (a) and minimum (b) values of ρ_{24} for
fixed ρ_{13} and ρ_{14} when $2 \leq \rho_{14} \leq 3$

If ρ_{14} is in the range $3^{1/2} \leq \rho_{14} \leq 2$, the situation is different. ρ_{13} can take on values $1 \leq \rho_{13} \leq 2$, however, depending on where ρ_{13} is in this range, sphere 2 can bump into sphere 1. This bumping or "libration" when it occurs, causes the minimum to be one. Thus ρ_{13} must be broken up into three different ranges within $3^{1/2} \leq \rho_{13} \leq 2$. These three cases are shown in Fig. (4.5)

When the end-to-end distance ρ_{14} is in the range $1 \leq \rho_{14} \leq 3^{1/2}$, then the maximum value that ρ_{13} can take is something less than two. This is because spheres 1, 2, and 3 cannot be placed with their centers in a straight line without sphere 2 penetrating sphere 4 (see Fig. 4.6). Bumping of spheres 2 and 4 occurs for all possible fixed values

(a)   (b)   (c)
no libration   libration   no libration
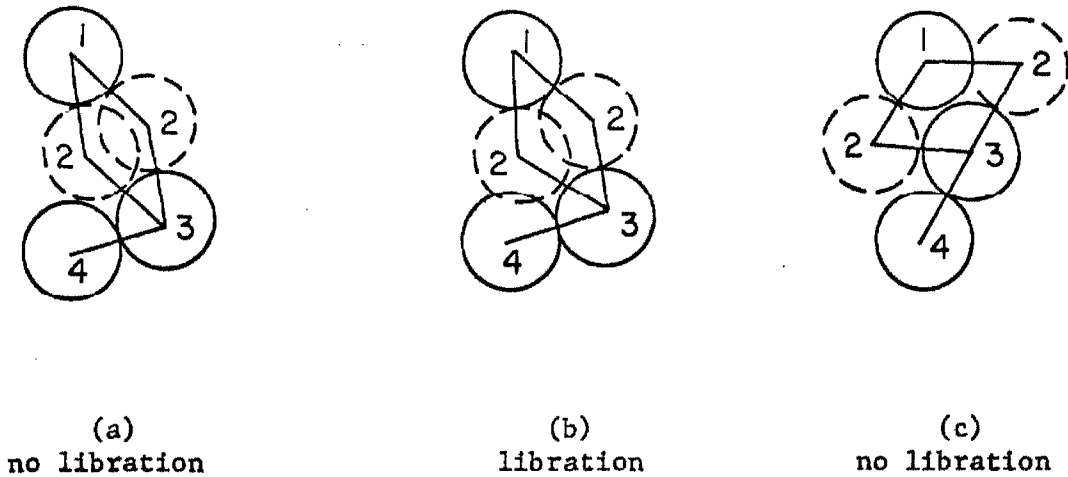
Fig. (4.5)
The maximum and minimum values of ρ_{24} for fixed
ρ_{14} and three different values of ρ_{13}.
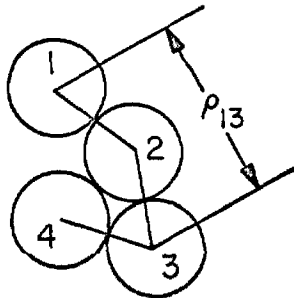
Fig. (4.6)
The maximum value of ρ_{13} when ρ_{14} is
fixed in the range $1 \leq \rho_{14} \leq \sqrt{3}$.

of ρ_{13} in this range of ρ_{14}; consequently the minimum ρ_{24} is one.

All the restrictions on ρ_{13} for fixed ρ_{14} and on ρ_{24} for fixed ρ_{14} and ρ_{13} have been calculated from geometry. These restrictions are summarized in Table 4.1.

We now can perform the integrations over ρ_{12}, ρ_{23} and ρ_{34} in

Table 4.1

A summary of the restrictions on ρ_{13} for fixed ρ_{14} and on ρ_{24} for fixed ρ_{14} and ρ_{13} .

$$2A_{\pm} = 2 + \rho^2_{14} \pm [3(4-\rho^2_{14})]^{1/2} \rho_{14}$$

$$B_{\pm} = (3 - \rho^2_{13} + \rho^2_{14})/2 \pm \{(4 - \rho^2_{13})[1 - (\rho^2_{13} + 1 - \rho^2_{14})^2 /4\rho^2_{13}]\}^{1/2}$$

Range of ρ_{14}	$(\rho_{13})^2_{max}$	$(\rho_{13})^2_{min}$	$(\rho_{24})^2_{max}$	$(\rho_{24})^2_{min}$
$2 \le \rho_{14} \le 3$	4	$(\rho_{14} - 1)^2$	B_+	B_-
$3^{1/2} \le \rho_{14} \le 2$	A_-	1	"	"
"	A_+	A_-	"	1
"	4	A_+	"	B_-
$1 \le \rho_{14} \le 3^{1/2}$	A_+	1	"	1

Eq. (4.28) by simply replacing these variables by one. Also the terms

$\exp(-\beta v_{14})$, $\exp(-\beta v_{13})$, and $\exp(-\beta v_{24})$ can be replaced by one. Note

that in order to make these simplifications, the variables ρ_{13}, ρ_{14} and

ρ_{24} must be restricted according to Table 4.1. Eq. (4.28) becomes,

$$\rho^2_{14}Z_{14} = 2\pi \int d\rho_{13} \int \rho_{24} (z \sin \beta)^{-1} d\rho_{24} \qquad (4.29)$$

where $z \sin \beta$ is given by Eq. (4.26). In order to simplify Eq. (4.29)

make the substitutions,

$$w = (1 + \rho^2_{14} - \rho^2_{24})/2\rho_{14} \qquad (4.30)$$
$$u = (1 + \rho^2_{13} - \rho^2_{14})/2\rho_{13}$$
$$v = (\rho^2_{13} + \rho^2_{14} - 1)/2\rho_{14}.$$

Eq. (4.29) now becomes,

$$\rho_{14}Z_{14} = -2\pi \int d\rho_{13} \int_{w_1}^{w_2} [(1-v^2/\rho^2_{13} - \rho^2_{13}/4) + wv - w^2]^{-1/2} \, dw. \qquad (4.31)$$

The interior integration can be performed by completing the square of

the denominator giving,

$$\rho_{14}Z_{14} = \qquad (4.32)$$

$$2\pi \int_{(\rho_{13})min}^{(\rho_{13})max} \sin^{-1}[(w - v/2)(v^2/4 + 1 - v^2/\rho_{13} - \rho^2_{13}/4)^{-1/2}]_{w_2}^{w_1} \, d\rho_{13}.$$

The limits of the integration can be found from Table 4.1 and are

shown in Table 4.2.

In the range $2 \leq \rho_{14} \leq 3$, Eq. (4.32) can be integrated directly

Table 4.2
Limits of integration to be used in Eq. (4.32)

$$2A_{\pm} = 2 + \rho_{14}^2 \pm \rho_{14}[3(4 - \rho_{14}^2)]^{1/2}$$

$$2\rho_{14}C_{\pm} = \rho_{14}^2 - 1 + \rho_{13}u \pm [(4 - \rho_{13}^2)(1 - u^2)]^{1/2}$$

Range of ρ_{14}	$(\rho_{13})_{max}^2$	$(\rho_{13})_{min}^2$	w_1	w_2
$2 \leq \rho_{14} \leq 3$	4	$(\rho_{14} - 1)^2$	C_+	C_-
$3^{1/2} \leq \rho_{14} \leq 2$	A_-	1	"	"
"	A_+	A_-	"	$\rho_{14}/2$
"	4	A_+	"	C_-
$1 \leq \rho_{14} \leq 3^{1/2}$	A_+	1	"	$\rho_{14}/2$

to give the simple result,

$$Z_{14} = 2\pi^2(3 - \rho_{14})/\rho_{14} \text{ for } 2 \leq \rho_{14} \leq 3. \qquad (4.33)$$

When $3^{1/2} \leq \rho_{14} \leq 2$, the integration can be broken into three integrals, two of which can be done analytically.

$$\rho_{14}Z_{14} = \pi^2[2 + (\rho_{13})_{max} - (\rho_{13})_{min}] \qquad (4.34)$$

$$+ 2\pi \int_{(\rho_{13})_{min}}^{(\rho_{13})_{max}} \sin^{-1}[(\rho_{14} - v)/2(v^2/4 + 1 - v^2/\rho_{13} - \rho^2_{13}/4)^{1/2}]d\rho_{13}$$

In the range $1 \leq \rho_{14} \leq 3^{1/2}$ we have,

$$\rho_{14}Z_{1N} = \qquad (4.35)$$

$$2\pi \int_{1}^{(\rho_{13})max} \{\sin^{-1}[(\rho_{14} - v)/2(v^2/4 + 1 - v^2/\rho_{13} - \rho^2_{13}/4)^{1/2}]+\pi/2\}d\rho_{13}$$

$$\text{for } 1 \leq \rho_{14} \leq 3^{1/2}.$$

The integrals in Eqs. (4.34) and (4.35) were performed numerically using Simpson's rule on an IBM 7094 digital computer. The results were fitted to polynomials using a least square subroutine.

$$Z_{14} = \sum_{i=1}^{5} a_i \rho_{14}^{i-1} \text{ for } 1 \leq \rho_{14} \leq 3^{1/2} \qquad (4.36)$$

$$Z_{14} = \sum_{i=1}^{3} b_i \rho_{14}^{i-1} \text{ for } 3^{1/2} \leq \rho_{14} \leq 2$$

The coefficients a_i and b_i are shown in Table 4.3.

The configurational partition function Z_{14} is discontinuous at $\rho_{14} = 1$ and piecewise smooth in the range $1 \leq \rho_{14} \leq 3$. A plot of

this function is shown in Fig. (4.7).

<div align="center">

Table 4.3
Coefficients in Eqs. (4.36)

</div>

i	a_i	b_i
1	15.024	-12.037
2	-27.794	17.036
3	34.548	-3.041
4	-18.767	---
5	39.236	---

The probability that the end-to-end distance ρ_{14} is in the range $\rho_{14} \rightarrow \rho_{14} + d\rho_{14}$ is found by normalizing Z_{14} according to Eq. (3.8).

$$P[\rho_{14}]d\rho_{14} = \rho^2_{14} Z_{14} d\rho_{14} / \int_0^3 \rho^2 Z_{14} d\rho$$

This normalized probability density $P[\rho_{14}]$ is shown in Fig. (4.8).

The configurational integral Z_{14}^o for a 3-link chain neglecting the interactions can be found by inverting the Fourier transform in Eq. (4.5) for N = 4.

$$Z_{14}^o = 8\pi^2 \text{ for } 0 \leq \rho_{14} \leq 1 \qquad (4.37)$$
$$= 4\pi^2(3 - \rho_{14})/\rho_{14} \text{ for } 1 \leq \rho_{14} \leq 3$$
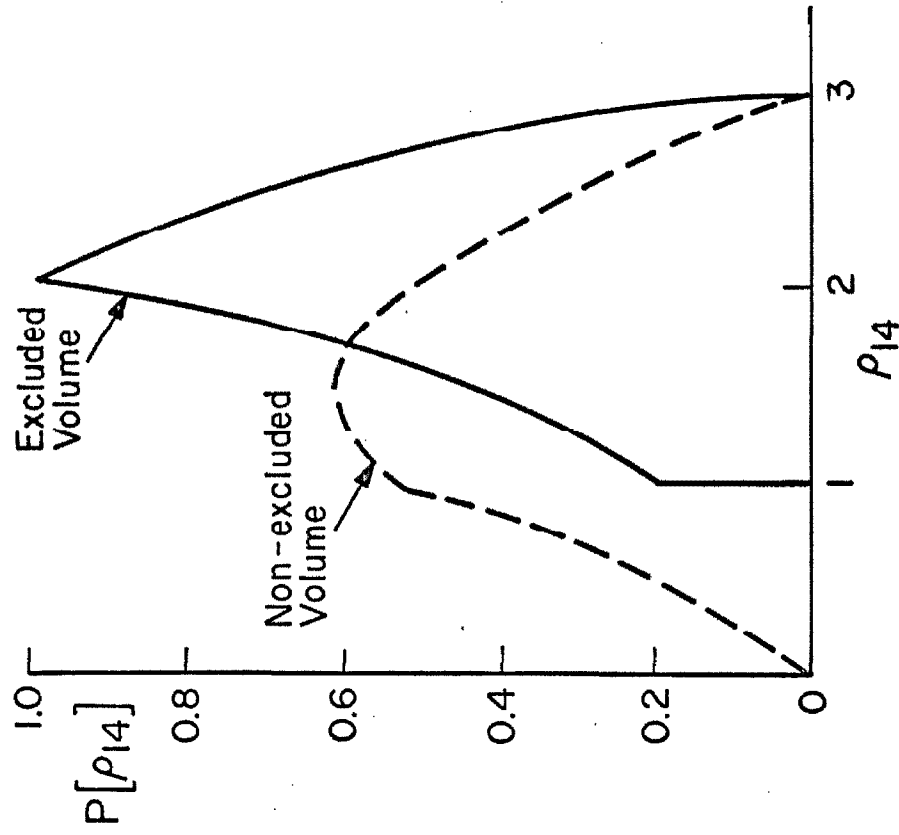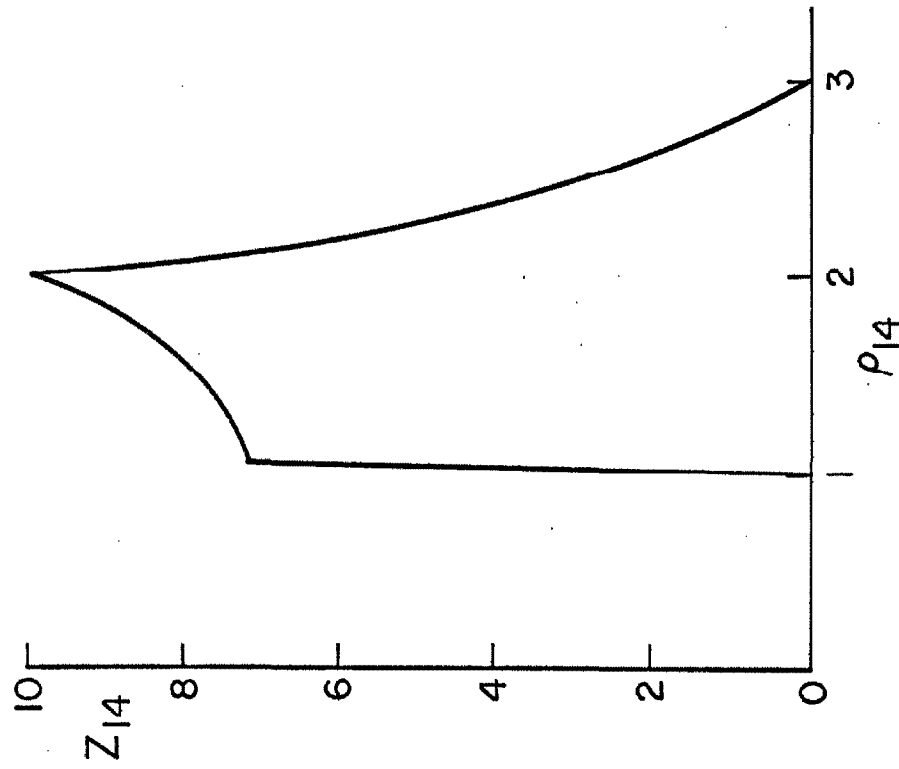
These results can be normalized to give

Fig. (4.8)

Fig. (4.7)

$$P^{\circ}[\rho_{14}] = \rho^2_{14}/2 \text{ for } 0 \leq \rho_{14} \leq 1$$

$$= (3 - \rho_{14})\rho_{14}/4 \text{ for } 1 \leq \rho_{14} \leq 3.$$

This function is also plotted in Fig. (4.8).

It can be seen from Fig. (4.8) that the excluded volume effect tends to shift the peak of the distribution to the right. In other words, the chain is expanded. This is because many of the otherwise available configurations of the chain are eliminated because of the excluded volume. This will be true for longer chains as well.

The mean square end-to-end distance $<\rho^2_{14}>$ can now be computed using Eqs. (4.33) and (4.36).

$$A<\rho^2_{14}> = \int_1^{3^{1/2}} (\sum_{i=1}^5 a_i\rho^{i-1})\rho^4 d\rho + \int_{3^{1/2}}^2 (\sum_{i=1}^3 b_i\rho^{i-1})\rho^4 d\rho$$

$$+ 2\pi^2 \int_2^3 (3 - \rho)\rho^3 d\rho. \tag{4.38}$$

A is a normalization constant and is given by

$$A = \int_1^{3^{1/2}} (\sum_{i=1}^5 a_i\rho^{i-1})\rho^2 d\rho + \int_{3^{1/2}}^2 (\sum_{i=1}^3 b_i\rho^{i-1})\rho^2 d\rho$$

$$+ 2\pi^2 \int_2^3 (3-\rho)\rho \, d\rho. \tag{4.39}$$

These definite integrals can be performed in a straightforward manner to give the result,

$$<\rho^2_{14}> = 4.31 = n^{1.33}. \tag{4.40}$$

When the excluded volume effect is neglected, the corresponding mean square end-to-end distance $<\rho^2_{14}>_0$ is given by Eq. (4.11).

$$\langle \rho^2{}_{14} \rangle_o = 3 = n.$$ (4.41)

Thus the mean square end-to-end distance is expanded by a factor of $n^{.33}$ for a 3-link chain ($N = 4$).

The possibility of extending this procedure to longer chains does not seem feasible. For a 3-link chain, tripolar coordinates were the natural coordinates since the kernel of the configuration integral contained functions of the three distances ρ_{12}, ρ_{23}, ρ_{24}. For longer chains the configurational integral will contain additional functions. The problem of deducing the restrictions on the variables was tedious in the 3-link chain. For longer chains this problem becomes very much more complicated. In order to attack longer chains some approximations must be made. Since the 3-link chain calculation is exact, it will be interesting to compare approximate theories with the exact result when $N = 4$.

5. CLUSTER EXPANSION

A. General Formulas

It does not seem feasible to use the methods of chapter 4 for long chains. In fact an exact solution for the configuration integral, Eq. (3.14) for a nontrivial potential, may indeed be impossible. There is a striking similarity between the configuration integral for a polymer chain

$$Z_{1N} = \int \ldots \int \Gamma_N \prod_i \prod_j (1 - h_{ij}) d\vec{\rho}_2 \ldots d\vec{\rho}_{N-1}. \tag{3.14}$$

and the configuration integral of a classical fluid (17). Although this similarity has been observed by many authors, the analogy has not yet been fully exploited. The methods that have been used in the physics of liquids and gases can be roughly divided into cluster expansions and integral equations. I will discuss the cluster expansion of Eq. (3.14) in this chapter and reserve the derivation of integral equations for later.

A cluster expansion of Eq. (3.14) can be obtained by expanding the double product.

$$\prod_{i=1}^{N-2} \prod_{j=i+2}^{N} (1 - h_{ij}) = 1 - \sum_{i=1}^{N-2} \sum_{j=i+2}^{N} h_{ij} + \ldots \tag{5.1}$$

Substitution of this expansion into Eq. (3.14) and interchanging the orders of summation and integration leads to,

$$Z_{1N} = \sum_{o}^{\binom{N-1}{2}} (-1)^i Z_{1N}^{(i)} \tag{5.2}$$

where:

$$Z_{1N}^{(o)} = \int \ldots \int \Gamma_N \, d\vec{\rho}_2 \ldots d\vec{\rho}_{N-1}$$

$$Z_{1N}^{(1)} = \sum_k \sum_\ell \int \ldots \int \Gamma_N \, h_{k\ell} d\vec{\rho}_2 \ldots d\vec{\rho}_{N-1}$$

$$Z_{1N}^{(2)} = \sum_k \sum_\ell \sum_m \sum_n \int \ldots \int \Gamma_N \, h_{k\ell} h_{mn} d\vec{\rho}_2 \ldots d\vec{\rho}_{N-1}$$

etc.

This type of expansion was suggested by Rubin (4). Inclusion of the first two terms in Eq. (5.2) is equivalent to the "single contact approximation" of Zimm, Stockmayer and Fixman (5) and leads to the well-known first-order perturbation theory for the mean square end-to-end distance after some further approximation (5-7). Fixman's second-order perturbation theory is equivalent to keeping the first three terms of Eq. (5.2). These perturbation theories are the only applications of the cluster expansion technique in the literature.

It is convenient to express Eq. (5.2) in terms of graphs or diagrams. This technique is used in the theory of imperfect gases (17).

$$Z_{1N}(\rho_{1N}) = \underset{\text{pairs}}{\bigcirc\!\!-\!\!\bigcirc\!\!-\!\!\circ \cdots \circ\!\!-\!\!\bigcirc} \quad - \quad \sum_{\text{pairs}} \bigcirc\!\!-\!\!\circ\!\!-\!\!\overbrace{\circ \cdots \circ}\!\!-\!\!\circ \cdots \circ\!\!-\!\!\bigcirc \qquad (5.3)$$

$$+ \quad \sum_{\text{fours}} \bigcirc\!\!-\!\!\circ\!\!-\!\!\circ\!\!-\!\!\overbrace{\circ \cdots \circ\!\!\overbrace{\circ}\!\!-\!\!\circ}\!\!-\!\!\circ \cdots \circ\!\!-\!\!\bigcirc \quad + \quad \ldots$$

Each diagram represents an integral in Eq. (5.2). Each circle can be identified with a subsystem of the chain. The straight line or δ-bond joining circles i and $i+1$ represents the δ-function ordering potential

$\delta(\rho_{ii+1}-1)$ between subsystems i and i+1. A curved line or h-bond between circles i and j represents an h_{ij}-function. The restriction is made that there can be only one bond between any two circles. In addition, only δ-bonds can exist between adjacent circles i, i+1 and h-bonds between nonadjacent circles i,j. If we consider the N circles with (n = N-1) δ-bonds as a "skeleton", then Eq. (5.3) is represented by the sum of all possible combinations of h-bonds on the skeleton. For a chain of N subsystems, the number of graphs in Eq. (5.3) can be shown to be (see Appendix V)

$$\text{Number of graphs in } Z_{1N} = 2^{(N-1)(N-2)/2}. \quad (5.4)$$

For long chains the number of graphs in the expansion of Z_{1N} is approximately given by $2^{N^2/2}$.

In actual practice, the experimentally observed quantity of interest is not the configuration integral itself but some quantity averaged with respect to the weighting function Z_{1N}. It is possible to express the moments of Z_{1N} in terms of the coefficients in the power series expansion of the Fourier transform of Z_{1N}. In particular the mean square end-to-end distance $<\rho^2_{1N}>$ can be found from the first two coefficients in the expansion of $\bar{Z}_{1N}(k)$ (see Appendix II for details).

$$<\rho^2_{1N}> = \frac{\text{coeff. } (-k^2/6) \text{ in } \bar{Z}_{1N}(k)}{\text{coeff. } (1) \text{ in } \bar{Z}_{1N}(k)}$$

where $\bar{Z}_{1N}(k)$ is the Fourier transform of $Z_{1N}(\rho_{1N})$.

$$\bar{Z}_{1N}(k) = \int Z_{1N}(\rho) \exp(-i\vec{k}\cdot\vec{\rho})d\vec{\rho}$$

$$(5.5)$$

$$8\pi^3 Z_{1N}(\rho_{1N}) = \int \bar{Z}_{1N}(k) \exp(i\vec{k}\cdot\vec{\rho}_{1N})d\vec{k}$$

Because the coefficients in the expansion of the Fourier transform $\bar{Z}_{1N}(k)$ determine the moments (in particular $<\rho_{1N}^2>$), it is frequently more useful to work with the Fourier transform rather than the configurational integral itself. In anticipation of this, let us define the Fourier transform pairs for the terms in the cluster expansion Eq. (5.2).

$$\bar{z}_{1N}^{(i)}(k) = \int z_{1N}^{(i)}(\rho) \exp(-i\vec{k}\cdot\vec{\rho})d\vec{\rho}$$

$$(5.6)$$

$$8\pi^3 z_{1N}^{(i)}(\rho_{1N}) = \int \bar{z}_{1N}^{(i)}(k) \exp(i\vec{k}\cdot\vec{\rho}_{1N})d\vec{k}$$

$$\text{where } i=0, 1, \ldots \binom{N-1}{2}$$

If $f(r)$ is an arbitrary function of the scalar r, then the Fourier transform of $f(r)$ defined by

$$\bar{f}(k) = \int f(r) \exp(-i\vec{k}\cdot\vec{r})d\vec{r},$$

can be written in the form (see Appendix I)

$$\bar{f}(k) = 4\pi\int_0^\infty f(r) r^2 (\sin kr/kr)dr.$$

Since $(\sin kr/kr)$ is an even function of k, then $\bar{f}(k)$ must be even. The configuration integral Z_{1N} and the terms in the cluster expansion $z_{1N}^{(i)}$ are functions of the scalar ρ_{1N}. Hence their respective Fourier transforms must be even functions of k. Let us write $\bar{Z}_{1N}$ and $\bar{z}_{1N}^{(i)}$ as power series with coefficients $z_j(N)$ and $z_{ij}(N)$.

$$\bar{Z}_{1N}(k) = \sum_j z_j(N)k^{2j} \tag{5.7}$$

$$\bar{Z}_{1N}^{(i)}(k) = \sum_j z_{ij}k^{2j}$$

Because of Eq.(5.2), an obvious relation exists between z_j and z_{ij}.

$$z_j(N) = \sum_{i=0}^{\binom{N-1}{2}} (-1)^i z_{ij}(N) \tag{5.8}$$

The mean square end-to-end distance can now be written as

$$\langle \rho^2{}_{1N} \rangle = -6 \sum_i (-1)^i z_{i1}(N) / \sum_i (-1)^i z_{i0}. \tag{5.9}$$

For large N there is a great multitude of terms in Eq. (5.9). If all but the zero-order terms (i = 0) are neglected, the mean square end-to-end distance $\langle \rho^2{}_{1N} \rangle$ reduces to n = (N-1). This is the result for the freely jointed chain with no excluded volume which was discussed in chapter 4. Let us now examine the terms in Eq. (5.9) for i = 1. This represents a first-order correction to the idealized, noninteracting chain. If this correction is small compared to the zero-order term, a good approximation might be achieved by including only a small number of terms in Eq. (5.9).

B. First-Order Correction

The first-order correction term to the configurational partition function for noninteracting chains is given by

$$z_{1N}^{(1)} = \sum_i \sum_j \int \ldots \int \Gamma_N \, h_{ij} \, d\vec{\rho}_2 \ldots d\vec{\rho}_{N-1}. \tag{5.10}$$

This can be represented by a summation of graphs of the type

Integrals represented by this type of graph can be factored at the points i and j to give

$$z_{1N}^{(1)} = \sum_i \sum_j \iint z_{1i}^{(0)} z_{ij}^{(0)} h_{ij} z_{ij}^{(0)} d\vec{\rho}_i d\vec{\rho}_j. \tag{5.11}$$

This factorization can be achieved because the graph can be cut into two parts at the points i or j. These points are called "articulation points" or "nodes" in graph theories of the liquid state (26, 27).

The function $z_{ij}^{(0)}$ appearing in Eq. (5.11) is the configuration integral for a chain with no excluded volume. This function is known and was found in chapter 4, Eq. (4.6). The Fourier transform of $z_{1N}^{(0)}(\rho_{1N})$ reduces to

$$\bar{z}_{1N}^{(0)}(k) = (4\pi \sin k/k)^{N-1}. \tag{5.12}$$

The Fourier integral representation of h_{ij} can be written in the form

$$\bar{h}(k) = \int h_{ij} \exp(-i\vec{k}\cdot\vec{\rho}) d\vec{\rho} \tag{5.13}$$

$$8\pi^3 h_{ij} = \int \bar{h}(k) \exp(i\vec{k}\cdot\vec{\rho}_{ij}) d\vec{k}.$$

Using the properties of convolution integrals, the Fourier transform of $z_{1N}^{(1)}$ in Eq. (5.11) reduces to

$$\bar{z}_{1N}^{(0)}(k) = \sum_i \sum_j \bar{z}_{1i}^{(0)}(k) \bar{y}_{ij}(k) \bar{z}_{jN}^{(0)}(k), \tag{5.14}$$

where

$$y_{ij}(k) = \int h_{ij} z_{ij}^{(0)}(\rho_{ij}) \exp(-i\vec{k}\cdot\vec{\rho}_{ij}) d\vec{\rho}_{ij}.$$

If the Fourier representation of $z_{ij}^{(0)}$ is introduced into $y_{ij}(k)$ and the order of integration is interchanged, $y_{ij}(k)$ can be written in the form

$$8\pi^3 y_{ij}(k) = \int \bar{h}(|\vec{k} - \vec{\ell}|) \bar{z}_{ij}^{(0)}(\ell) d\vec{\ell}. \tag{5.15}$$

Eq. (5.15) is valid for any choice of the potential as long as the Fourier transform of h_{ij} exists. I will now specialize this equation by introducing the hard core potential defined in Eq. (4.19). This potential implies that

$$h_{ij} = 1 \text{ for } \rho_{ij} < b \tag{5.16}$$

$$h_{ij} = 0 \text{ for } \rho_{ij} > b.$$

Introduction of this representation for h_{ij} into Eq. (5.13) leads to the result (see Appendix VI)

$$\bar{h}(k) = 4\pi(\sin bk - bk \cos bk)/k^3. \tag{5.17}$$

Eq. (5.15) now becomes,

$$2\pi^2 y_{ij}(k) = (4\pi)^{j-i} \int (\sin \ell/\ell)^{j-i}(\sin bx - bx \cos bx)x^{-3}d\vec{\ell}. \tag{5.18}$$

where x is the absolute value of the difference of the two vectors $\vec{k}$ and $\vec{\ell}$ making an angle with each other of γ.

$$x = |\vec{k} - \vec{\ell}| = (k^2 + \ell^2 - 2k\ell \cos \gamma)^{1/2}$$

If $d\vec{\ell}$ is written in spherical coordinates, the angular integrations in Eq. (5.18) can be performed (see Appendix VI). The final result for $y_{ij}(k)$ for the hard core potential is,

$$\pi k y_{ij}(k) = (4\pi)^{j-i} \int_0^\infty \ell(\sin \ell/\ell)^{j-i} K_1(k,\ell,b)d\ell,$$

where

$$K_1(k, \ell, b) = \sin(k - \ell)b/(k - \ell) - \sin(k + \ell)b/(k + \ell).$$

The Fourier transform of the first correction term $Z_{1N}^{(1)}$ in the cluster expansion of Z_{1N} becomes

$$\pi k \bar{Z}_{1N}(k) =$$

$$(4\pi)^{N-1} \sum_{i=1}^{N-2} \sum_{j=i+2}^{N} (\sin k/k)^{N-i+j-1} \int_0^\infty (\sin \ell/\ell)^{j-i} \ell K_1(k, \ell, b)d\ell.$$

It is possible to replace the sum over i and j in this equation by a single summation over m = j-i, provided we multiply by an appropriate combinatorial coefficient C(m). This factor represents the number of combinations of j and i (consistent with the summation) which lead to the same value for m = j-i. This combinatorial coefficient is found to be (see Appendix VII) C(m) = N - m. Thus $\bar{Z}_{1N}^{(1)}(k)$ can finally be written as

$$\pi k \bar{Z}_{1N}(k) =$$

$$(4\pi)^{N-1} \sum_{m=2}^{N-1} (N-m)(\sin k/k)^{N-1-m} \int_0^\infty (\sin \ell/\ell)^m \ell K_1(k, \ell, b)d\ell \qquad (5.19)$$

Let us now extract the first two coefficients in the power series of $\bar{Z}_{1N}^{(1)}(k)$ in Eq. (5.19). $K_1(k, \ell, b)$ is an analytic function of k for all k, hence this function can be expanded in a Taylor series about k = 0. It can be verified by direct differentiation that,

$$K_1(k, \ell, b) = 2(\sin \ell b/\ell^2 - b \cos \ell b/\ell)k$$

$$-2(b^2 \sin \ell b/2\ell^2 + b \cos \ell b/\ell^3 - \sin \ell b/\ell^4 - b^3 \cos \ell b/6\ell)k^3 + \ldots$$

Substitution of this series into Eq. (5.19) and the interchange of the order of integration and summation enables us to identify the coefficients

$$\pi z_{10} = 2(4\pi)^{N-1} \sum_m (N - m) \int_0^\infty (\sin \ell/\ell)^m K_2(k, \ell, b)d\ell \qquad (5.20a)$$

$$\pi z_{11}[2(4\pi)^{N-1}]^{-1} = \qquad (5.20b)$$

$$- \sum_m (N - m)[(N-1-m)/6 \int_0^\infty (\sin \ell/\ell)^m K_2(k, \ell, b)d\ell - \int_0^\infty (\sin \ell/\ell)^m K_3(k, \ell, b)d\ell]$$

where the functions K_2 and K_3 are defined by

$$K_2(k, \ell, b) = \sin \ell b/\ell - b \cos \ell b \qquad (5.21a)$$

$$K_3(k, \ell, b) = \qquad (5.21b)$$

$$b^3 \cos \ell b/6 - b^2 \sin \ell b/2\ell - b \cos \ell b/\ell^2 + \sin \ell b/\ell^3.$$

Solution for small b

The particular choice of the hard core potential function to represent the potential between elements on the polymer chain involves the parameter b. This parameter represents the diameter of the hard core

which has been scaled by the segment length a. An illustration of
this situation is depicted in Fig. (5.1). b is essentially a measure
of the amount of excluded volume. When b = 0 all terms in the cluster
expansion become zero except the zero-order or non-excluded volume term.
The maximum allowable value of b corresponds to the situation when the
hard core diameters are exactly equal to the segment lengths of the
chain. The mean square end-to-end distance of our model chain can be
estimated in the limit of small excluded volume by expanding the inte-
grands in power series in b followed by term-by-term integration.

The following expansions can be easily verified:

$$K_2(k, \ell, b) = \ell^2 b^3/3 + 0(b^5)$$

$$K_3(k, \ell, b) = 0(b^5).$$

Substitution of these results into Eqs. (5.20a) and (5.20b) yields

$$\pi^z{}_{10} =$$

$$2(4\pi)^{N-1} \sum_m (N - m) \int_0^\infty (\sin \ell/\ell)^m [\ell^2 b^3/3 + 0(b^5)] d\ell, \qquad (5.22a)$$

$$\pi^z{}_{11} =$$

$$-2\pi(4\pi)^{N-1} \sum_m (N - m)(N - 1 - m) \int_0^\infty (\sin \ell/\ell)^m [\ell^2 b^3/3 + 0(b^5)] d\ell. \qquad (5.22b)$$

Let us now make use of the Gaussian approximation discussed in
chapter 4, Eq. (4.7). The integral in Eqs. (5.22a) and (5.22b) reduces
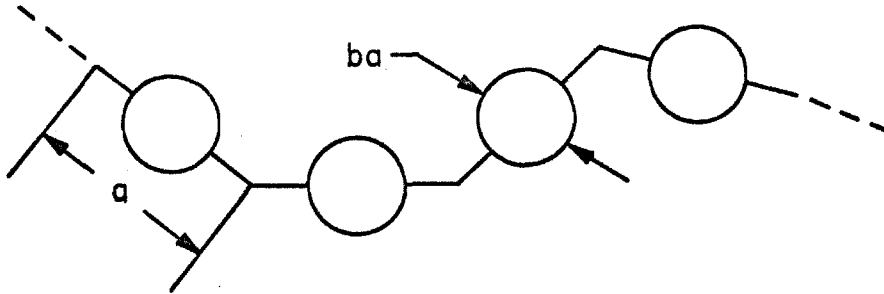to a simple gamma function.

Fig. (5.1)
A portion of the model polymeric chain with a
hard core potential between elements of the
chain (the "pearl necklace" model).

$$(b^3/3) \int_0^\infty \exp(-m\ell^2/6)\ell^2 d\ell = (6\pi/m^3)^{1/2}b^3/2$$

Eqs. (5.20a) and (5.20b) can now be written as

$$z_{10} = (6/\pi)^{1/2}(4\pi)^{N-1}b^3 \sum_{m=2}^{N-1} (N - m)m^{-3/2},$$

$$z_{11} = -(6/\pi)^{1/2}(4\pi)^{N-1}b^3 \sum_{m=2}^{N-1} (N - 1 - m)(N - m)m^{-3/2}.$$

It will be shown later that terms of higher order are of order b^6 or

less. The mean square end-to-end distance Eq. (5.9) becomes

$$\langle \rho^2_{1N} \rangle = \frac{-6[z_{01} - z_{11} + 0(b^6)]}{z_{00} - z_{10} + 0(b^6)} .$$

From chapter 4 it is known that

$$z_{00} = 1$$

$$z_{01} = -(N - 1)/6.$$

Thus for small values of b, the mean square end-to-end distance has the form

$$\langle \rho^2_{1N} \rangle = \frac{(N-1) - (6/\pi)^{1/2}b^3 \sum\limits_{m} (N-m)(N-1-m)/m^{3/2}}{1 - (6/\pi)^{1/2}b^3 \sum\limits_{m} (N-m)/m^{3/2}} . \quad (5.23)$$

If b is chosen sufficiently small, then the second term in the denominator of Eq. (5.23) is less than one. Therefore for sufficiently small b, the denominator in Eq. (5.23) can be expanded as a geometric series. This procedure leads to

$$\langle \rho^2_{1N} \rangle = (N-1) + (6/\pi)^{1/2}b^3 \sum\limits_{m} (N-m)/m^{1/2} + O(b^5). \quad (5.24)$$

The summation in Eq. (5.24) can be estimated using the Euler-Maclaurin Summation Formula (28).

$$\sum\limits_{m=2}^{N-1} (N-m)/m^{1/2} = \int\limits_{x=1}^{N-1} (N-x)/x^{1/2} dx - (N-1)/2$$

$$+ (1/12)[(N-1)/2 + 1 - N^{-1}] - \ldots$$

The integration can be performed easily to give

$$\sum\limits_{m=2}^{N-1} (N-m)/m^{1/2} = 2(N-1)^{1/2}N - (2/3)(N-1)^{3/2} + O(N).$$

For large N this becomes

$$\sum\limits_{m=2}^{N-1} (N-m)/m^{1/2} = (4/3)(N-1)^{3/2}. \quad (5.25)$$

The mean square end-to-end distance Eq. (5.24) simplifies to

$$\langle \rho^2_{1N} \rangle = (N - 1)[1 + (6/\pi)^{1/2} 4b^3/3 + \ldots].$$

In the literature the parameter z defined in Eq. (2.3) is frequently referred to.

$$z = X(3/2\pi a^2)^{3/2} n^{1/2} \qquad (2.3)$$

n is the number of links in the chain (i.e. $n = N-1$) and X is the "binary cluster integral" defined by

$$X = a^3 \int [1 - \exp(-\beta v_{ij})] d\vec{\rho}_{ij}$$

$$= a^3 \int h_{ij} d\vec{\rho}_{ij}.$$

For the hard core potential in Eq. (4.19), X is simply the volume excluded to one sphere by the presence of another.

$$X = (4/3)\pi (ab)^3$$

The parameter z in Eq. (2.3) then becomes

$$z = (6/\pi)^{1/2} b^3 n^{1/2}$$

for the hard core potential. Thus we obtain the result

$$\langle \rho^2_{1N} \rangle = n(1 + 4z/3 + \ldots) \qquad (5.26)$$

in the limit of small hard core diameter b.

The above equation for the mean square end-to-end distance has been obtained by many authors (5-7) by making use of the approximation

$$h_{ij} = X\delta(\vec{r}_{ij}), \qquad\qquad (2.7)$$

where $\delta(\vec{r}_{ij})$ is a three dimensional δ-function. This approximation assumes that h_{ij} is so short range that the only contributions to integrations involving h_{ij} occur at $\vec{r}_{ij} = 0$. Since the true shape of the potential function is not known, Eq.(2.7) can be regarded as the definition of the potential. It approaches the hard core potential as the hard core diameter b becomes small. It is not surprising then that the mean square end-to-end distance of a hard core model chain reduces to the result obtained using Eq. (2.7) as b becomes small.

If Eq. (2.7) is taken as the definition of the potential function, then it is possible to show that the mean square end-to-end distance $<\rho^2_{1N}>$ is solely a function of the parameter z. Eq. (5.26) can then be regarded as a power series in z. The coefficient of the z^2 term has been obtained by Fixman (8) by considering $Z^{(2)}_{1N}$ (ρ_{1N}) in Eq. (5.2), and using Eq. (2.7) for the potential. Fixman obtained

$$<\rho^2_{1N}> = n[1 + 4z/3 - (16/3 - 28\pi/27)z^2 + ...]. \qquad (5.27)$$

It is obvious that $<\rho^2_{1N}>$ cannot be solely a function of the parameter z for the exact hard core potential. Since z is directly proportional to b^3, a power series in z is equivalent to a power series in b^3. Eqs. (5.21a) and (5.21b) indicate that the terms in the expansion of the coefficients z_{10} and z_{11} increase as b^3, b^5, b^7, etc. Only when the potential is sufficiently short range so that terms of higher order than b^3 can be neglected, can $<\rho^2_{1N}>$ be viewed solely as a function of z.

Solution by numerical integration

It will be shown later that some of the higher order graphs in the expansion of $\langle \rho^2_{1N} \rangle$ can be expressed in terms of the first-order correction term. In view of this fact it would be desirable to obtain an accurate representation of the coefficients z_{10} and z_{11} in Eqs. (5.20a) and (5.20b) for $0 \leq b \leq 1$.

The integrals in Eqs. (5.20a) and (5.20b) are uniformly convergent with respect to m for $m \geq 1$. The finite summations can be taken under the integral sign to give

$$\pi z_{10} = 2(4\pi)^{N-1} \int_0^\infty \psi_0(N,\ell)K_2(k, \ell, b)d\ell \qquad (5.28a)$$

$$\pi z_{11} = 2(4\pi)^{N-1} \int_0^\infty [(1/6)\psi_1(N,\ell)K_2(k, \ell, b) - \psi_0(N,\ell)K_3(k, \ell, b)]d\ell \quad (5.28b)$$

where K_2 and K_3 are defined by Eqs. (5.19). The functions ψ_0 and ψ_1 are given by

$$\psi_0(N,\ell) = \sum_{m=2}^{N-1} (N - m)(\sin \ell/\ell)^m \qquad (5.29a)$$

$$\psi_1(N,\ell) = \sum_{m=2}^{N-1} (N - m)(N - 1 - m)(\sin \ell/\ell)^m. \qquad (5.29b)$$

These two series can be summed by using the properties of the geometric series. The details of the summation procedure are outlined in Appendix VIII. The results are

$$(1 - L^2)\psi_0(N,\ell) = L^2[N - 2 - L(1 - L^{N-2})(1 - L)^{-1}], \qquad (5.30)$$

$$(1 - L) \psi_1(N,\ell) = N(N - 1)(L^2 - L^N) + \{L^2[(N - 1)^2L^{N-2} - N(N - 2)L^{N-2} - L]$$

$$+ L^2[2 - L - NL^{N-2} + (N - 1)L^{N-1}][2(1 - L)^{-1} - 2N + 1]\}(1 - L)^{-1}$$

where

$$L = (\sin \ell/\ell).$$

In the limit as $\ell \to 0$, $L \to 1$. Using L'Hospital's rule, the limit of ψ_0 and ψ_1 as $\ell \to 0$ can be found (see Appendix VIII).

$$\lim_{\ell \to 0} \psi_0(N, \ell) = (N - 1)(N - 2)/2 \qquad (5.31a)$$

$$\lim_{\ell \to 0} \psi_1(N, \ell) = (N - 1)(N - 2)(N - 3)/3 \qquad (5.31b)$$

Using Eqs. (5.30) and (5.31), the integrals in Eq. (5.28) were performed numerically on an IBM 7094 digital computer. The program made use of a Simpson rule subroutine. The value of b was arbitrarily fixed at 0.25 in this calculation. The upper limit of these infinite integrals was chosen large enough so that the maximum estimated error is less than one percent. The results from these calculations are shown in Figs. (5.2) and (5.3).

It is difficult to achieve a high degree of accuracy in the numerical integrations of Eqs. (5.28a) and (5.28b). For computational purposes the upper limit of infinity must be replaced by a large finite number. It can be seen from Eqs. (5.28) and (5.30) that the integrands of the two integrations are of order ℓ^{-2} for large values of the integration parameter ℓ. This rather slow convergence of the integrals
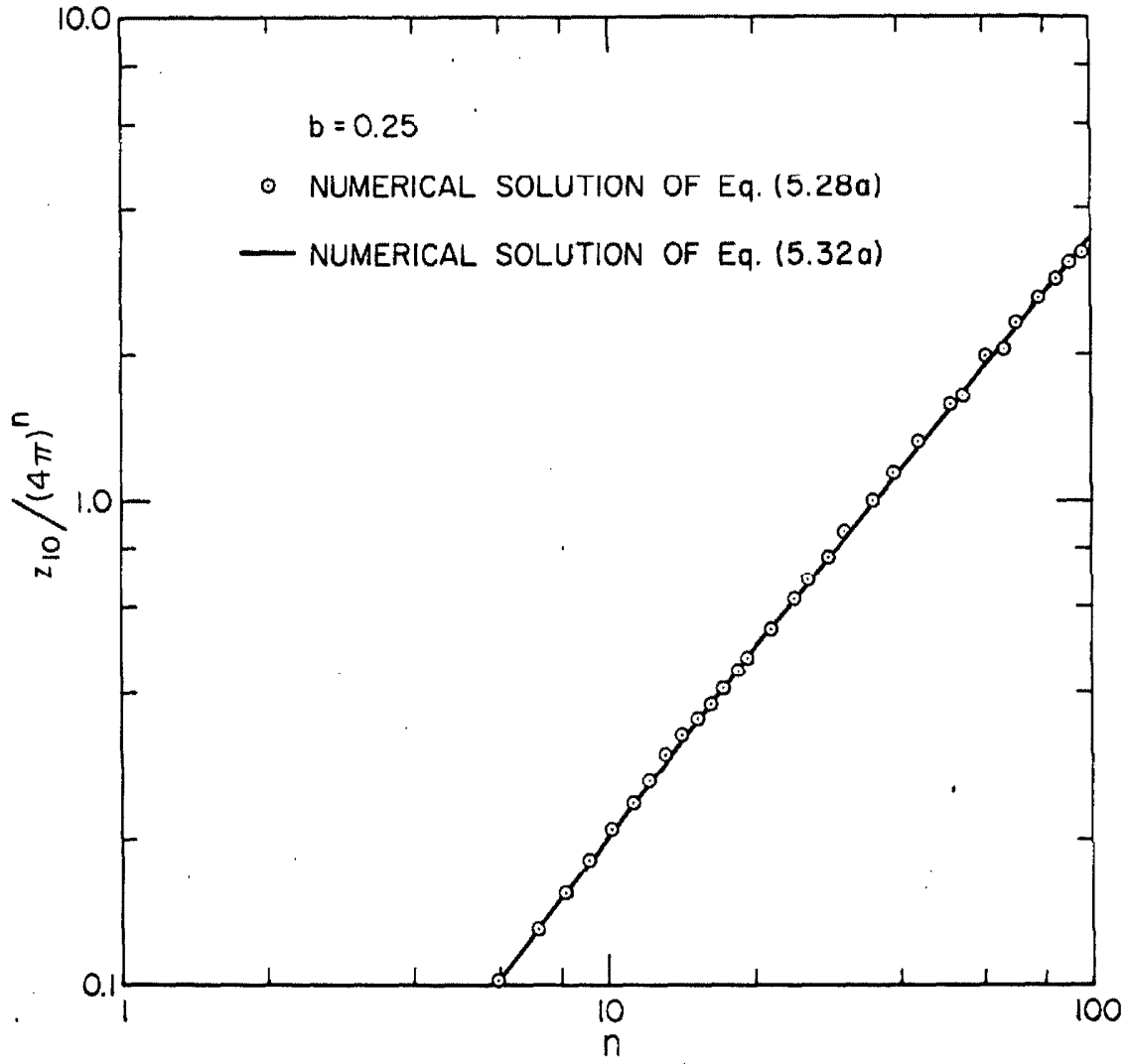
Fig. (5.2)

First-order correction term.
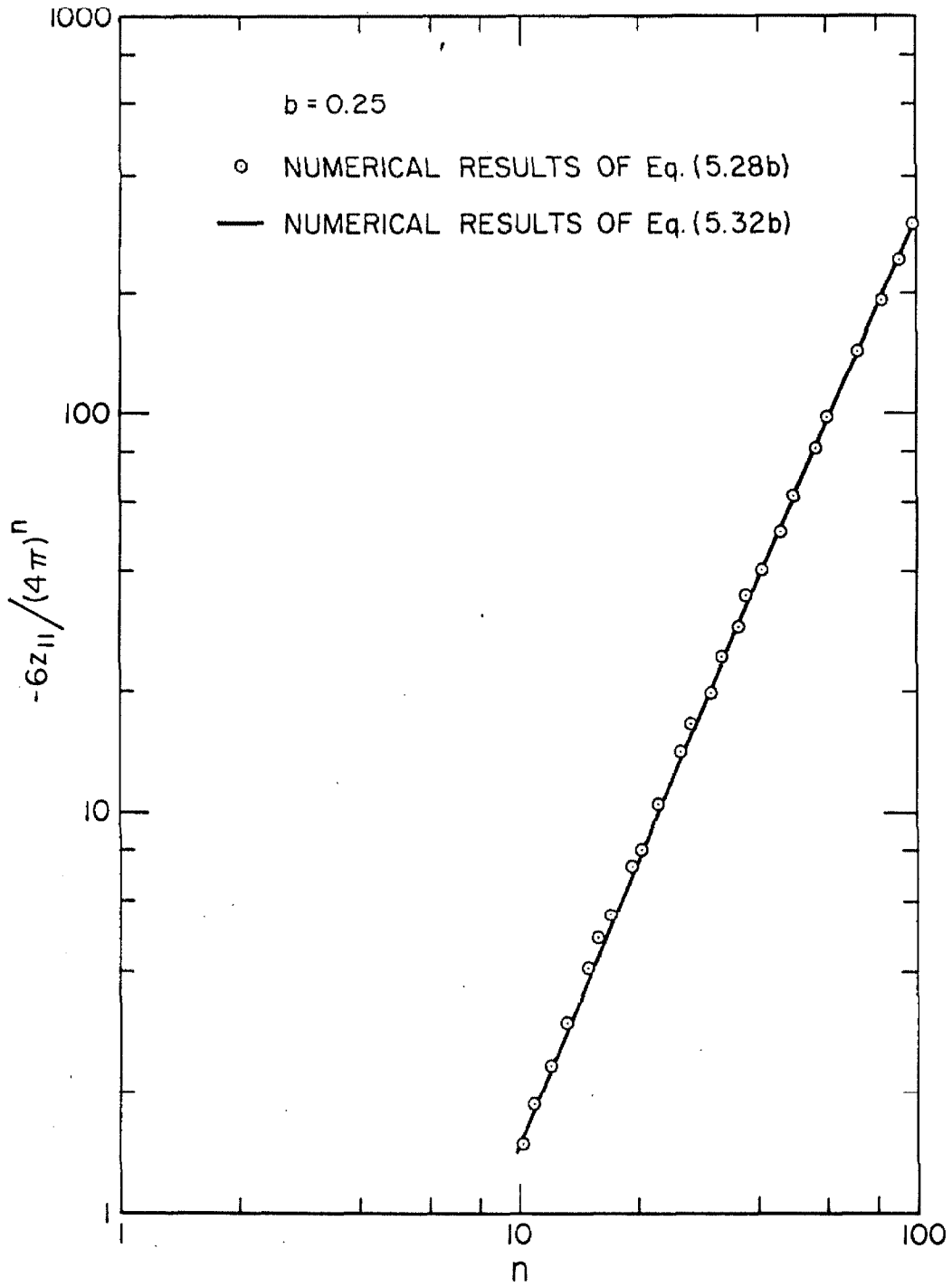
Fig. (5.3)

First-order correction term.

requires that the upper limit of the integrations be chosen to be very large in order to obtain accuracy.

Numerical solution using the Gaussian approximation

An alternative method of evaluating z_{10} and z_{11} in Eqs. (5.20a) and (5.20b) consists of integrating first analytically and then summing the resulting finite series numerically. Eqs. (5.20) for z_{10} and z_{11} can be written as

$$\pi z_{10} = 2(4\pi)^{N-1} \sum_{m=2}^{N-1} (N - m)\Omega_0(b, m) \qquad (5.32a)$$

$$\pi z_{11} = -2(4\pi)^{N-1} \sum_{m=2}^{N-1} (N - m)[(N - 1 - m)\Omega_0(b, m)/6 - \Omega_1(b,m)]. \qquad (5.32b)$$

Ω_0 and Ω_1 are integrals defined by

$$\Omega_0(b, m) = \int_0^\infty (\sin \ell/\ell)^m K_2(k, \ell, b)d\ell \qquad (5.33a)$$

$$\Omega_1(b, m) = \int_0^\infty (\sin \ell/\ell)^m K_3(k, \ell, b)d\ell, \qquad (5.33b)$$

where K_2 and K_3 are defined by Eqs. (5.19). These integrals can be evaluated analytically provided the Gaussian approximation is made for $(\sin \ell/\ell)^m$. With this representation for $(\sin \ell/\ell)^m$, Ω_0 and Ω_1 become

$$\Omega_0(b, m) = \int_0^\infty \exp(-m\ell^2/6)(1-\ell^4 m/180 + \dots)K_2(k, \ell, b)d\ell \qquad (5.34a)$$

$$\Omega_1(b, m) = \int_0^\infty \exp(-m\ell^2/6)(1-\ell^4 m/180 + \dots)K_3(k, \ell, b)d\ell. \qquad (5.34b)$$

Ω_0 in Eq. (5.34a) is the difference between a Fourier sine transform and Fourier cosine transform. The result obtained by integrating

Eq. (5.34a) is found to be (see Appendix IX).

$$\Omega_o = (\pi/2) \text{erf}[(3b^2/2m)^{1/2}] \tag{5.35}$$

$$- (3\pi b^2/2m)^{1/2} \exp(-3b^2/2m)[1 + 0(m^{-1})].$$

Ω_1 can also be put in the form of Fourier sine and cosine transforms (see Appendix IX), which leads to

$$\Omega_1 = (b/6)(b^2 + m)(3\pi/2m)^{1/2} \exp(-3b^2/2m) \tag{5.36}$$

$$- (\pi m/12) \text{erf}[(3b^2/2m)^{1/2}] + 0(1).$$

Eqs. (5.35) and (5.36) are accurate only for large m. This difficulty can be circumvented by finding the first few $\Omega_o(b, m)$ and $\Omega_1(b, m)$ exactly and then using Eqs.(5.35) and (5.36) thereafter. For m = 2 and 3 we have

$$\Omega_o(b, 2) = \pi b^2/8$$

$$\Omega_o(b, 3) = \pi b^3/12$$

$$\Omega_1(b, 2) = -\pi b^4/96$$

$$\Omega_1(b, 3) = -\pi b^5/120 .$$

Eqs. (5.32a) and (5.32b) can now be written as

$$z_{10} \simeq (4\pi)^{N-1}\{(N - 2)b^2/4 + (N - 3)b^3/6 \tag{5.37a}$$

$$+ \sum_{m=4}^{N-1} (N - m)[\text{erf}(3b^2/2m)^{1/2} - (6b^2/\pi m)^{1/2} \exp(-3b^2/2m)]\}$$

$$-6(4\pi)^{-(N-1)} z_{11} \simeq \qquad (5.37b)$$

$$(N - 2)(N - 3)b^2/4 + (N - 3)(N - 4)b^3/6 + (N - 2)b^4/8 + (N - 3)b^5/10$$

$$+ \sum_{m=4}^{N-1} (N - m)[(N - 1)\operatorname{erf}(3b^2/2m)^{1/2} - (6b^2/\pi m)^{1/2}(N - 1 + b^2)\exp(-3b^2/2m)]$$

The summations in Eqs. (5.37a) and (5.37b) were performed numerically using an IBM 7094 computer for the special choice of $b = .25$. The results are shown in Figs. (5.2) and (5.3) and can be seen to agree quite well with the results from the previous section.

The mean square end-to-end distance can now be written including the first-order correction terms. From Eq. (5.9) we have

$$<\rho^2_{1N}> \simeq \frac{6(N - 1) + 6z_{11}}{1 - z_{10}} \qquad (5.38)$$

Using the numerical values of z_{10} and z_{11} exhibited in Figs. (5.2) and (5.3) for $b = .25$, $<\rho^2_{1N}>$ was computed as a function of the chain length n. These results appear in Fig. (5.4) along with Eq. (5.27), obtained by Fixman. The portion of the curve shown is for small enough n so that Eq. (5.27) converges rapidly. It can be seen from Fig. (5.4) that the numerical results of log $<\rho^2_{1N}>$ start to deviate sharply from linearity as a function of log n for $n > 15$. It is known from experiment and from computer generated chains on a lattice that $<\rho^2_{1N}> \propto n^\gamma$ where γ is a constant. Since z_{10} and z_{11} were computed very accurately by several methods, it appears that higher order interaction terms in the cluster expansion Eq. (5.2) must be contributing to $<\rho^2_{1N}>$ for large N.
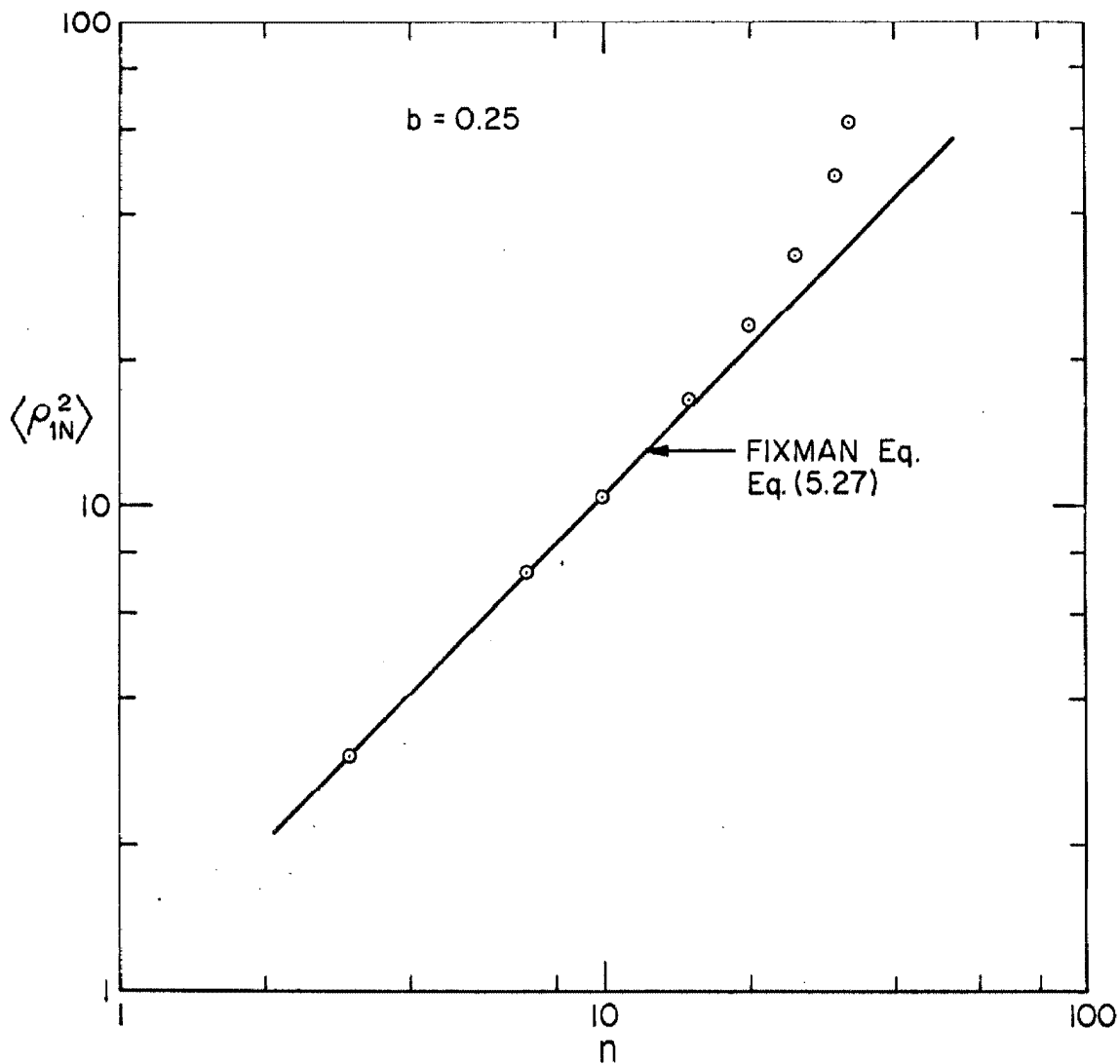
Fig. (5.4) – $\langle \rho_{1N}^2 \rangle$ vs. n CALC. FROM Eq. (5.41)

C. Higher-Order Terms

From the preceding section it appears as if higher-order terms in the cluster expansion of $\langle \rho_{1N}^2 \rangle$ contribute significantly for longer chain lengths. To evaluate all the integrals in the cluster expansion for large N is out of the question. It was shown earlier that there are approximately $2^{N^2/2}$ terms in the cluster expansion for large N. For a chain of 100 links the number of integrals to evaluate is approximately 10^{1500}. Furthermore, the difficulty encountered in evaluating integrals representing many interactions will be much greater than the relatively simple first-order terms discussed in the last section. In developing an approximation to the exact solution it would be useful to know the relative sizes of some of the higher-order terms as a function of chain length. In this section I will present a method for determining certain classes of higher-order graphs in terms of simpler lower-order graphs. I will also give the results of some numerical computations for the contribution of higher-order graphs of a specific topological type.

Current analogy

Many of the higher-order graphs may be simplified by transforming these integrals into Fourier space. As was seen in the previous section the first-order graphs were greatly simplified by this technique. By transforming various higher-order integrals into Fourier space, as was done in part 2 of this chapter, it was noticed that a convenient pnemonic device existed which allows the Fourier transform of an inte-

gral to be written down immediately by examining the topology of the corresponding graph. We have called this procedure the "current analogy." This technique consists of representing the graph as an electrical circuit with current flowing from left to right. An example using the first-order graph is shown below.
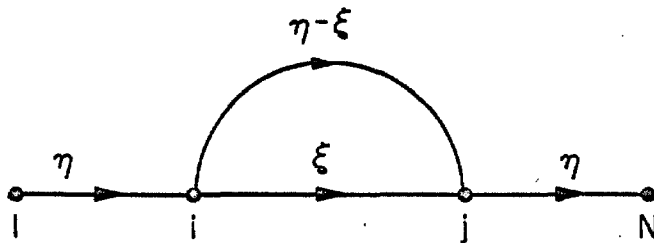
The Fourier transform of the circuit can be written following a set of rules.

1. All currents flow from left to right and obey Kirchoff's first law: the sum of the currents entering and leaving a circuit point is zero.

2. The contribution of the straight portions of the graph to the Fourier transform is $\bar{Z}_{ij}^{(0)}(\eta)$. i and j are circuit points with ξ and $\eta-\xi$ the currents flowing through this section.

3. The contribution of the looped portion to the Fourier transform is a convolution integral of h (loop current) with the contribution of the straight sections of the loop; e.g.

$$(8\pi^3)^{-1} \int \bar{h}(|\vec{\eta} - \vec{\xi}|)\bar{Z}_{ij}^{(0)}(\vec{\xi})d\vec{\xi}$$

4. The total contribution to the Fourier transform is the pro-

duct of the respective contributions from the straight and looped sections.

As an example, consider the first-order graph. The contribution of the straight section is $\bar{z}_{1i}^{(0)}(\eta)\ \bar{z}_{jN}^{(0)}(\eta)$. The looped section contributes

$$(8\pi^3)^{-1} \int \bar{h}(|\vec{\eta} - \vec{\xi}|)\bar{z}_{ij}^{(0)}(\vec{\xi})d\vec{\xi}.$$

The total Fourier transform of this graph is the product of these contributions.

$$(8\pi^3)^{-1}\bar{z}_{1i}^{(0)}(\eta)\bar{z}_{jN}^{(0)}(\eta) \int \bar{h}(|\vec{\eta} -\vec{\xi}|)\bar{z}_{ij}^{(0)}(\vec{\xi})d\vec{\xi}$$

This agrees with the result obtained earlier in this chapter by the direct method.

Now consider the more complicated terms represented by graphs of the form

The circuit for this graph is
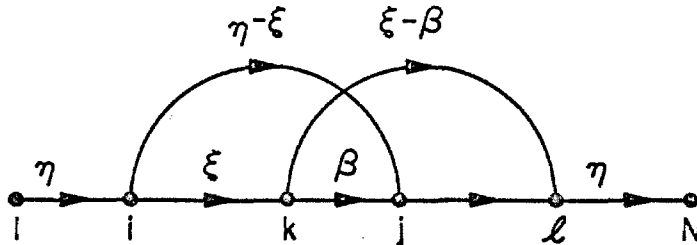
with the currents represented by the Greek letters and the circuit

points represented by i, j, k, ℓ.

Following the rules established, the contributions of the

straight sections to the Fourier transform of the graph are $\bar{Z}_{1i}^{(0)}(\eta)$

and $\bar{Z}_{jN}^{(0)}(\eta)$.

The total Fourier transform of this graph becomes

$$(8\pi^3)^{-1}\bar{Z}_{1i}^{(0)}(\eta)\bar{Z}_{\ell N}^{(0)}(\eta) \int \bar{h}(|\vec{\eta} - \vec{\xi}|)\bar{Z}_{ik}^{(0)}(\xi)d\vec{\xi}$$

$$\times \int \bar{h}(|\vec{\xi} - \vec{\beta}|)\bar{Z}_{kj}^{(0)}(\beta)\bar{Z}_{j\ell}^{(0)}(|\vec{\xi}- \vec{\eta} + \vec{\beta}|)d\vec{\beta}. \qquad (5.39)$$

Using this technique the Fourier transform of any graph, no

matter how complex the topology, can be written down.

Second-order term

The second-order term in the cluster expansion, Eq. (5.2), is

of the form

$$Z_{1N}^{(2)}(\rho_{1N}) = \sum_i \sum_j \sum_m \sum_n \int \ldots \int \Gamma_N h_{ij}h_{mn}d\vec{\rho}_2 \ldots d\vec{\rho}_{N-1}. \qquad (5.40)$$

This can be represented by sums of graphs of three topologically dis-

tinct types

$$Z_{1N}^{(2)}(\rho_{1N}) = W_{1N}^{(2)} + X_{1N}^{(2)} + Y_{1N}^{(2)}, \qquad (5.41)$$

where

$$W_{1N}^{(2)} = \sum \qquad \text{(isolated)}$$

$$X_{1N}^{(2)} = \sum \text{(nested)}$$

$$Y_{1N}^{(2)} = \sum \text{(overlapped)}$$

The integrals represented by the graphs above are of three different types: isolated, nested, and overlapped. Each type must be treated separately.

The isolated graphs are the simplest to evaluate. $W_{1N}^{(2)}$ is defined to be

$$W_{1N}^{(2)} = \Sigma \int \ldots \int \Gamma_N \, h_{ij} h_{mn} \, d\vec{\rho}_2 \ldots d\vec{\rho}_{N-1},$$

[sum over $1 \leq i \leq (j - 2)$, $j \leq m \leq (n - 2)$, $n \leq N$]

Choose a point s in the range $j \leq s \leq m$. $W_{1N}^{(2)}$ can then be factored to give

$$W_{1N}^{(2)} = \sum_{s=3}^{N-2} \int z_{1s}^{(1)}(\rho_{1s}) z_{sN}^{(1)}(\rho_{sN}) \, d\vec{\rho}_s \qquad (5.42)$$

This expression can be simplified further by use of Fourier transforms. Define the Fourier transform pair

$$\bar{W}_{1N}^{(2)}(k) = \int W_{1N}^{(2)}(\rho)\exp(-i\vec{k}\cdot\vec{\rho})d\vec{\rho} \tag{5.43}$$

$$8\pi^3 W_{1N}^{(2)}(\rho_{1N}) = \int \bar{W}_{1N}^{(2)}(k)\exp(i\vec{k}\cdot\vec{\rho}_{1N})d\vec{k}.$$

Introduction of the Fourier transform representation of $Z_{1N}^{(1)}$ into Eq. (5.42) and interchange of the order of integration leads to the result

$$\bar{W}_{1N}^{(2)}(k) = \sum_{s=3}^{N-2} \bar{Z}_{1s}^{(1)}(k)\bar{Z}_{sN}^{(1)}(k). \tag{5.44}$$

It can be seen that the "isolated" graphs of the second-order term in the cluster expansion can be expressed in terms of the first-order term. This will also be true of the "nested" graphs. The current analogy diagram for the type of graphs in $X_{1N}^{(2)}$ is
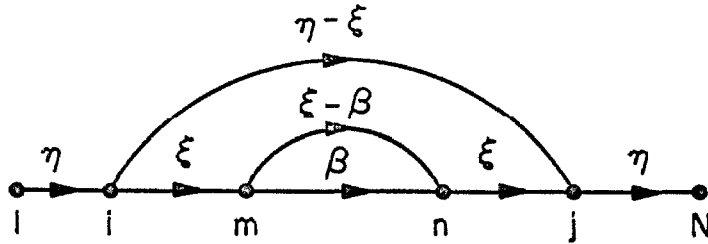
The Fourier transform of $X_{1N}^{(2)}$ becomes

$$\bar{X}_{1N}^{(2)}(n) = \sum \bar{Z}_{1i}^{(0)}(n)\bar{Z}_{jN}^{(0)}(n) \int \bar{h}(|\vec{n} - \vec{\xi}|)\bar{Z}_{im}^{(0)}(\xi)\bar{Z}_{nj}^{(0)}d\xi$$

$$\times \int \bar{h}(|\vec{\xi} - \vec{\beta}|)\bar{Z}_{mn}^{(0)}(\beta)d\vec{\beta} \tag{5.45}$$

$$[\text{sum over } 1 \leq i \leq m \leq (n-2), \ n \leq j \leq N].$$

Observe that

$$\bar{Z}_{ij}^{(1)} (\xi) = \Sigma \ \bar{Z}_{im}^{(0)} \bar{Z}_{nj}^{(0)} \int \bar{h}(|\vec{\xi} - \vec{\beta}|) \bar{Z}_{mn}^{(0)}(\beta) d\vec{\beta}$$

[sum over $i \leq m \leq (n - 2)$, $n \leq j$].

Thus $\bar{X}_{1N}^{(2)}$ can be written as

$$\bar{X}_{1N}^{(2)} (\eta) = \Sigma \ \bar{Z}_{11}^{(0)} \bar{Z}_{jN}^{(0)} \int \bar{h}(|\vec{\eta} - \vec{\xi}|) \bar{Z}_{ij}^{(1)}(\xi) d\vec{\xi} \qquad (5.46)$$
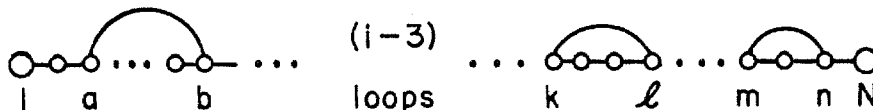
[sum over $1 \leq i \leq (j - 2)$, $j \leq N$].

This expression for $\bar{X}_{1N}^{(2)}$ is more complicated to evaluate than the corresponding relation for $\bar{W}_{1N}^{(2)}$ in Eq. (5.44), since Eq. (5.46) involves an integration.

It is not possible to simplify $\bar{Y}_{1N}^{(2)}$, the overlapping graph contribution to $\bar{Z}_{1N}^{(2)}$, in terms of the lower-order graphs as was done for $\bar{W}_{1N}^{(2)}$ and $\bar{X}_{1N}^{(2)}$. This is due to the overlapping topology of the graphs. The Fourier transform of $\bar{Y}_{1N}^{(2)}$ was obtained in the previous section as an illustration of the current analogy. In order to evaluate this term it is necessary to evaluate a difficult three-center integral.

Third and higher-order terms

It is obvious that higher-order terms with greater numbers of interactions (h-bonds) entail many more graphs of varying topology. Some of these graphs will be able to be expressed in terms of lower-order graphs (i.e. they are reducible). As an example, consider graphs of the "isolated" type.

$$\underset{\text{I}}{\text{O}}-\underset{a}{\text{O}}-\text{O} \cdots \underset{b}{\text{O}}-\text{O}- \cdots \quad (i-3) \quad \cdots \underset{k}{\text{O}}-\text{O}-\underset{\ell}{\text{O}} \cdots \underset{m}{\text{O}}-\text{O}-\underset{n}{\text{O}} \quad \text{loops} \quad k \quad \ell \quad m \quad n \quad N$$

The number of loops or h-bonds represents the order of the graph.

These "isolated" graphs will make a contribution to terms of all orders

in the cluster expansion. Let us denote this contribution by $W_{1N}^{(i)}$ where

i is the order of the term.

$$W_{1N}^{(i)} = \Sigma \int \cdots \int \Gamma_N \overbrace{h_{ab} h_{cd} \cdots h_{k\ell} h_{mn}}^{\text{i terms}} d\vec{\rho}_2 \cdots d\vec{\rho}_{N-1} \qquad (5.47)$$

[sum over $1 \leq a \leq (b-2)$, ..., $\ell \leq m \leq (n-2)$, $n \leq N$]

From the current analogy, the Fourier transform of Eq. (5.47) can be

written,

$$\bar{W}_{1N}^{(i)}(k) = \Sigma \overbrace{\bar{Z}_{1a}^{(0)} \bar{Z}_{bc}^{(0)} \cdots \bar{Z}_{\ell m}^{(0)} \bar{Z}_{nN}^{(0)}}^{\text{i terms}}$$

$$\times \int \bar{h}(|\vec{n} - \vec{\xi}|) \bar{Z}_{ab}^{(0)}(\xi) d\vec{\xi} \cdots \int \bar{h}(|\vec{n} - \vec{\beta}|) \bar{Z}_{mn}^{(0)}(\beta) d\vec{\beta}.$$
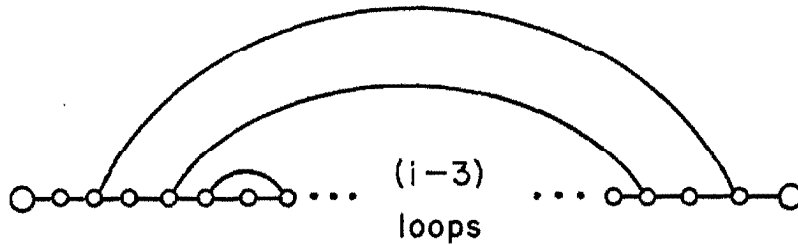
Choose a point s in the range $\ell \leq s \leq m$ then

$$\bar{Z}_{\ell m}^{(0)}(\eta) = \bar{Z}_{ms}^{(0)}(\eta) \bar{Z}_{sn}^{(0)}(\eta).$$

$\bar{W}_{1N}^{(i)}$ can then be factored into two parts which can be identified with

$\bar{W}_{1s}^{(i-1)}(\eta)$ and $\bar{Z}_{sN}^{(1)}(\eta)$ to give the simple relation

$$\bar{W}_{1N}^{(i)}(\eta) = \sum_{s=2i-1}^{N-2} \bar{W}_{1s}^{(i-1)}(\eta) \bar{Z}_{sN}^{(1)}(\eta). \qquad (5.48)$$

The nested graphs $X_{1N}^{(i)}$ will also contribute to each term in the cluster expansion.

From the current analogy, it is possible to generalize Eq. (5.46) to give a difference equation for the nested graphs of ith-order

$$\bar{X}_{1N}^{(i)}(\eta) = \Sigma \ \bar{Z}_{1i}^{(0)}(\eta)\bar{Z}_{jN}^{(0)}(\eta) \int \bar{h}(|\vec{\eta} - \vec{\xi}|)\bar{Z}_{ij}^{(i-1)}(\xi)d\vec{\xi} \qquad (5.49)$$

[sum over $1 \leq i \leq (j - 2)$, $j \leq N$]

It is obvious that the general terms $Z_{1N}^{(i)}$ in the cluster expansion will contain an enormous number of graphs of various topology. The isolated and nested graphs discussed are only two of many different types of graphs present. It does not seem practical or possible to classify and evaluate all the possible graphs. This will not be attempted here. Instead I will successively evaluate the isolated graphs only. This will demonstrate the behavior of the higher-order graphs $W_{1N}^{(i)}$ as a function of chain length.

Rather than evaluating $W_{1N}^{(i)}$ or $\bar{W}_{1N}^{(i)}$ directly, it is more convenient to compute the first two coefficients in the power series expansion of $\bar{W}_{1N}^{(i)}(k)$. The expansion of $\bar{Z}_{1N}^{(i)}(k)$ was given by Eq. (5.7)

with coefficients $z_{ij}(N)$. Let the coefficients in the expansion of $\bar{W}_{1N}^{(i)}(k)$ be denoted by $w_{ij}(N)$.

$$\bar{W}_{1N}^{(i)}(k) = \sum_{j} w_{ij}(N)k^{2j} \tag{5.50}$$

Obviously $z_{ij}(N)$ and $w_{ij}(N)$ are related by

$$z_{ij}(N) = w_{ij}(N) + [\text{terms of other topology}]. \tag{5.51}$$

We now substitute Eqs. (5.50) and (5.7) into Eq. (5.48) to obtain

$$\bar{W}_{1N}^{(i)}(k) = \sum_{s=2i-1}^{N-2} \{w_{i-10}(s)z_{10}(N-s). \tag{5.52}$$

$$+ [w_{i-10}(s)z_{11}(N-s) + w_{i-11}(s)z_{10}(N-s)]k + \ldots\}.$$

Comparison of the coefficients of k^{2j} in Eqs. (5.50) and (5.52) leads to the difference equations,

$$w_{i0}(N) = \sum_{s=2i-1}^{N-2} w_{i-10}(s)z_{10}(N-s), \tag{5.53a}$$

$$w_{i1}(N) = \sum_{s=2i-1}^{N-2} [w_{i-10}(s)z_{11}(N-s) + w_{i-11}(s)z_{10}(N-s)]. \tag{5.53b}$$

These difference equations were solved successively starting with $i = 2$ on an IBM 7094 computer. The initial conditions $z_{10}(N)$ and $z_{11}(N)$ were taken from Figs. (5.2) and (5.3) of this chapter. The hard core parameter b, was taken to be 0.25 and the calculation of $w_{i0}(N)$ and $w_{i1}(N)$ were performed as a function of chain length N. The results of these numerical computations are shown in Figs. (5.5) and (5.6).

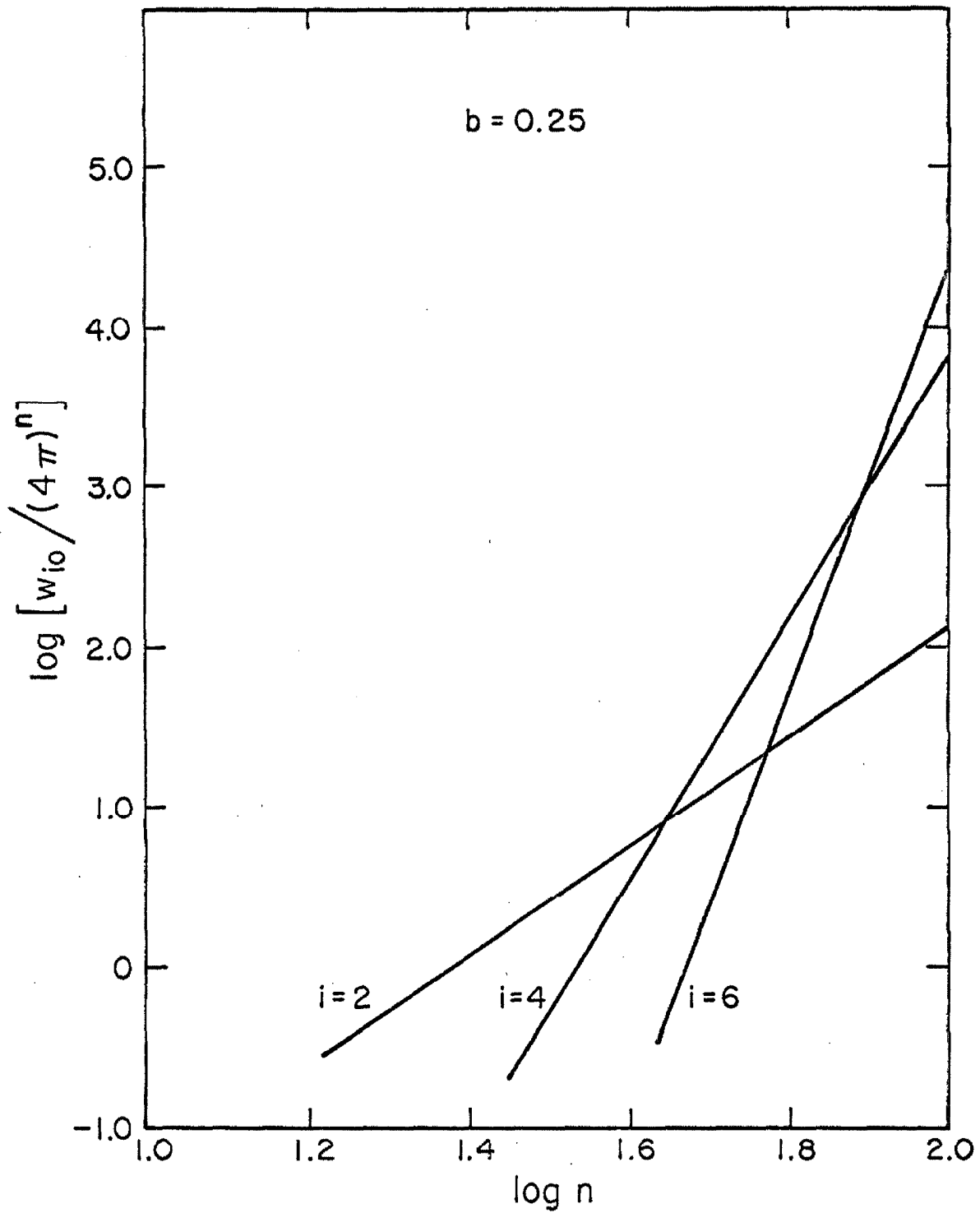These results can now be used to compute the mean square end-to-

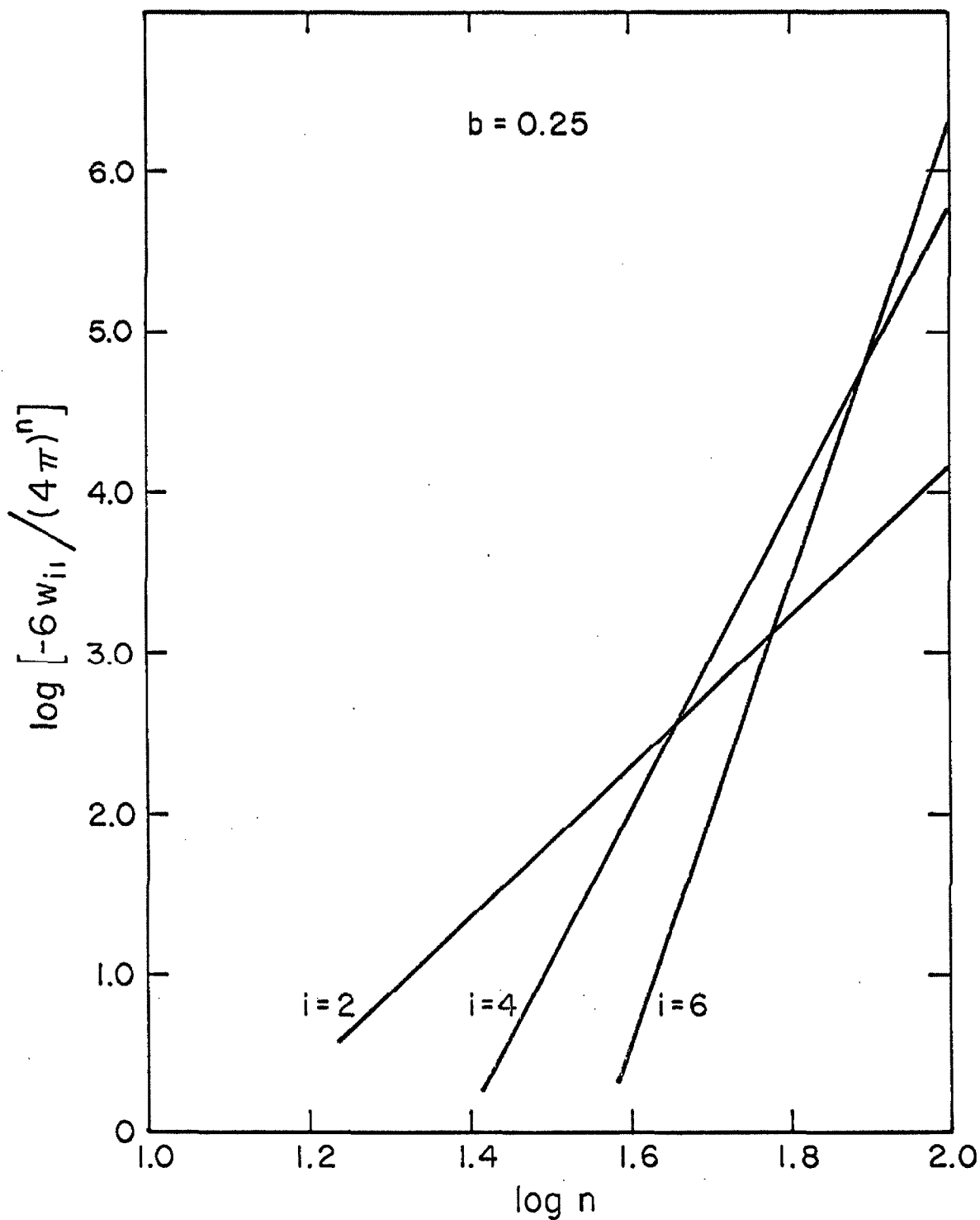Fig. (5.5) – CONTRIBUTIONS DUE TO NON-OVERLAPPING TOPOLOGIES

Fig.(5.6) – CONTRIBUTIONS DUE TO NON-OVERLAPPING TOPOLOGIES

end distance $<\rho^2_{1N}>$, assuming that all graphs other than "isolated

graphs" are negligible. Make the very crude assumption that

$$z_{i0}(N) \simeq w_{i0}(N)$$

$$\text{for } 1 \leq i \leq [(N - 1)/2],$$

$$z_{i1}(N) \simeq w_{i1}(N)$$

$$z_{i0}(N) \simeq 0$$

$$\text{for } [(N - 1)/2] < i \leq (N - 1)/2.$$

$$z_{i1}(N) \simeq 0$$

In words this means that all graphs except the "isolated" graphs are

omitted. For a given chain length N, the maximum number of "isolated"

h loops that is possible is $[(N - 1)/2]$ where the bracket denotes the

smallest integer less than or equal to $(N - 1)/2$. With this approxima-

tion, Eq. (5.9) becomes

$$<\rho^2_{1N}> \simeq \frac{-6 \sum_i (-1)^i w_{i1}(N)}{\sum_i (-1)^i w_{i0}(N)} . \qquad (5.54)$$

The mean square end-to-end distance was calculated from Eq. (5.54) using

the numerical results obtained from Eqs. (5.53). The results are shown

in Fig. (5.7). The erratic behavior of the mean square end-to-end dis-

tance for n > 40 indicates that inclusion of "isolated" graphs only,

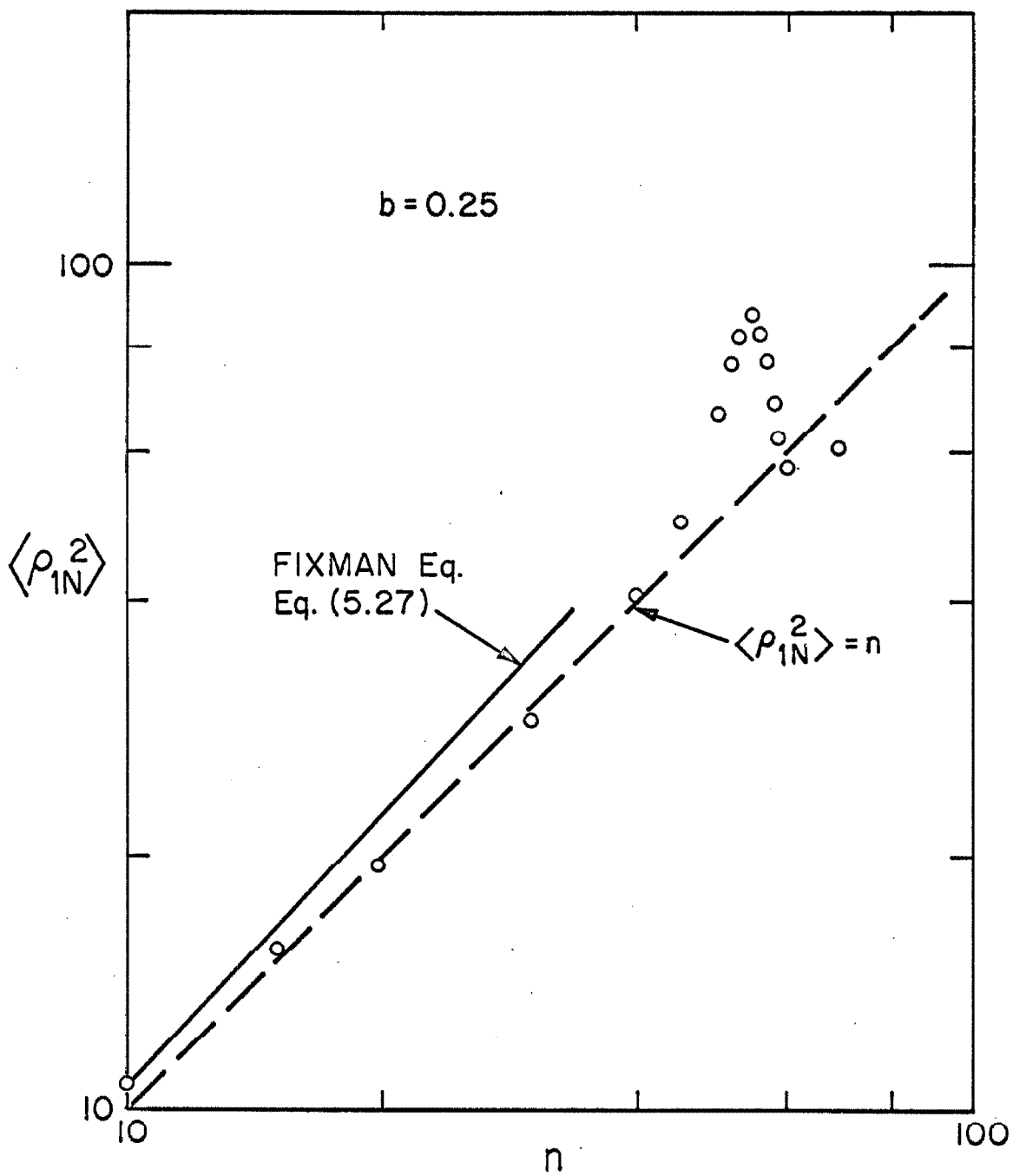results in incorrect weighting of the terms z_{i1} and z_{i0} for large n.

Fig. (5.7) — $\langle \rho_{1N}^2 \rangle$ vs. n CALC. FROM NON–OVERLAPPING TOPOLOGIES

6.   SELF-CONSISTENT CENTRAL FIELD APPROACH

It was seen in the previous chapter that contributions of higher-order graphs to the configurational partition function become important for long chain lengths. Since long chains are of interest from a practical standpoint, it is clear that some approach other than the cluster expansion is needed.

In this chapter I will describe the self-consistent field theory approach to the excluded volume problem. The major contributors to this theory are Edwards (9), Reiss (10) and Yamakawa (12). Edwards was the first to approximate the pair interactions by a central field. Reiss later attempted to show that this field satisfies a variational principle. The present author (30) has pointed out an error in Reiss' treatment, which indicates that Reiss' field does not satisfy that variational principle.

Reiss (10) has presented a method for finding the best central field approximation. The method consists of using those functions ϕ_s which minimize the Helmholtz free energy. In chapter 3 it was shown that the probability of observing a polymer chain in a particular configurational state for a canonical ensemble of chains was

$$P d\vec{\rho}_1 \ldots d\vec{\rho}_N = Z^{-1} \exp(-\beta V) d\vec{\rho}_1 \ldots d\vec{\rho}_N, \qquad (6.1)$$

where

$$V = \sum_i u_{ii+1} + (1/2) \sum_{i \neq j} v_{ij},$$

and

$$\exp(-\beta \sum_i u_{ii+1}) = \overset{N-1}{\underset{i=1}{\Pi\delta}} \ (\rho_{ii+1}-1) \equiv \Gamma_N.$$

Note that it makes no difference if adjacent interactions v_{ii+1} are included in the second sum because of the δ-function ordering potentials. Z is the unrestricted partition function defined by Eq. (3.5). The term Γ_N involving the δ-functions is of course due to the ordering of the adjacent segments. From statistical thermodynamics we can write the entropy of the polymer chain as

$$S = -k \int \ldots \int P \ln P \ d\vec{\rho}_1 \ldots d\vec{\rho}_N. \tag{6.2}$$

The macroscopic internal energy of the system is

$$E = \int \ldots \int V \ P \ d\vec{\rho}_1 \ldots d\vec{\rho}_N. \tag{6.3}$$

The Helmholtz free energy is defined to be

$$A = E - TS. \tag{6.4}$$

Thus for a polymer chain we have

$$A = \int \ldots \int [V + kT \ln P] P \ d\vec{\rho}_1 \ldots d\vec{\rho}_N \tag{6.5}$$

We now make the central field approximation, which decouples the many-body problem.

$$(1/2) \underset{m \neq n}{\sum} v_{mn} \simeq \underset{s}{\sum} \phi_s \tag{6.6}$$

This leads to an approximate probability distribution $\hat{P}$ and partition function $\hat{Z}$.

$$\hat{P} \, d\vec{\rho}_1 \ldots d\vec{\rho}_N = \hat{Z}^{-1} \, \Gamma_N \, \exp(-\beta \sum_s \phi_s) d\vec{\rho}_1 \ldots d\vec{\rho}_N \; , \qquad (6.7a)$$

where

$$\hat{Z} = \int \ldots \int \Gamma_N \, \exp(-\beta \sum_s \phi_s) d\vec{\rho}_1 \ldots d\vec{\rho}_N. \qquad (6.7b)$$

Let us now introduce a convenient notation for certain integrals that will arise. Let

$$\langle X \rangle_i = \hat{Z}_i^{-1} \int \ldots \int X \, \Gamma_N \, \exp(-\beta \sum_s \phi_s) \prod_{k \neq i} d\vec{\rho}_k, \qquad (6.8)$$

with

$$\hat{Z}_i = \int \ldots \int \Gamma_N \, \exp(-\beta \sum_s \phi_s) \prod_{k \neq i} d\vec{\rho}_k.$$

The subscripts refer to the segments that are held fixed in the integrations. The approximate Helmholtz free energy resulting from Eq. (6.6) is thus

$$\hat{A} = \langle V + kT \ln \hat{P} \rangle. \qquad (6.9)$$

It remains to determine the best possible set of ϕ_s. The criterion that Reiss used was minimization of the Helmholtz free energy in Eq. (6.9). Using Eqs. (6.7a) and (6.1), Eq. (6.9) can be written as

$$\hat{A} = \langle (1/2) \sum_{i \neq j} v_{ij} - \sum_s \phi_s - \beta^{-1} \ln \hat{Z} \rangle. \qquad (6.10)$$

Since $\hat{Z}$ is not a function of the coordinates, $\beta^{-1}\ell n \ \hat{Z}$ can be removed from under the integral signs in Eq. (6.10). Furthermore, since $\hat{P}$ is normalized, these integrations give unity.

$$\hat{A} = <(1/2) \sum_{i \neq j} v_{ij} - \sum_{s} \phi_s > -\beta^{-1}\ell n \ \hat{Z} \qquad (6.11)$$

We now take the variation of $\hat{A}$ by allowing each of the ϕ_k to vary independently.

$$\delta \hat{A} = -\beta <[(1/2) \sum_{i \neq j} v_{ij} - \sum_{s} \phi_s]\delta\phi_k>$$

$$+\beta <(1/2) \sum_{i \neq j} v_{ij} - \sum_{s} \phi_s > \cdot <\delta\phi_k>,$$

$$k = 1, \ldots N$$

This expression can be rewritten in the form

$$\beta^{-1}\delta\hat{A} = \qquad (6.12)$$

$$\int \hat{Z}_k \hat{Z}^{-1} [<(1/2) \sum_{i \neq j} v_{ij} - \sum_{s} \phi_s > - <(1/2) \sum_{i \neq j} v_{ij} - \sum_{s} \phi_s >_k]\delta\phi_k d\vec{\rho}_k$$

$$k = 1, \ldots N .$$

Since an extremal of $\hat{A}$ is desired, we set

$$\delta\hat{A} = 0.$$

Because the variation $\delta\phi_k$ is arbitrary, the kernel of the integral in Eq. (6.12) must vanish. The restricted partition function $\hat{Z}_k$ in general does not vanish, thus we are led to the set of equations,

$$<(1/2) \sum_{i \neq j} v_{ij} - \sum_s \phi_s> - <(1/2) \sum_{i \neq j} v_{ij} - \sum_s \phi_s>_k = 0 \qquad (6.13)$$

$$k = 1, 2, \ldots N.$$

If Eq. (6.13) is multiplied through by the factor $\hat{z}_k \hat{z}^{-1}$ the equation can be rewritten in the form,

$$\hat{z}_k \hat{z}^{-1} [<(1/2) \sum_{i \neq j} v_{ij} - \sum_s \phi_s>] - [\hat{z}_k \hat{z}^{-1} <(1/2) \sum_{i \neq j} v_{ij} - \sum_s \phi_s>_k] = 0. (6.14)$$

The method used in obtaining Eq. (6.14) is based on Reiss' paper (10). Eq. (6.14) is identical to Eq. (25) of Reiss' paper, only it is written in our notation. Observe that if the second bracketed term is integrated over the coordinates of k, the first term results.

$$\hat{z}^{-1} \int \hat{z}_k <(1/2) \sum_{i \neq j} v_{ij} - \sum_s \phi_s>_k d\vec{\rho}_k = <(1/2) \sum_{i \neq j} v_{ij} - \sum_s \phi_s> \qquad (6.15)$$

If one chooses,

$$\phi_i = (1/2) \sum_{\substack{j \neq i \\ i \text{ fixed}}} <v_{ij}>_i, \qquad (6.16)$$

then the first bracketed term in Eq. (6.14) is made equal to zero. This can easily be proven by direct substitution.

$$<(1/2) \sum_{i \neq j} v_{ij} - \sum_s \phi_s> = <(1/2) \sum_{i \neq j} (v_{ij} - <v_{ij}>_i)>$$

$$= (1/2) \sum_{i \neq j} (<v_{ij}> - <<v_{ij}>_i>)$$

$$<<v_{ij}>_i> = \hat{z}^{-1} \int \hat{z}_i [\hat{z}_i^{-1} \int \ldots \int v_{ij} \Gamma_N \exp(-\beta \sum_s \phi_s) \prod_{k \neq i} d\vec{\rho}_k] d\vec{\rho}_i$$

$$<<v_{ij}>_i> = <v_{ij}>$$

Therefore,

$$<(1/2) \sum_{i \neq j} (v_{ij} - <v_{ij}>_i)> = 0 .$$

Reiss contends that since Eq. (6.16)[*]makes the first bracketed term of Eq. (6.14) vanish, and since the integral of the second bracketed term is precisely the first bracketed term, then Eq. (6.16) is a solution to Eq. (6.14). This of course is not necessarily true as I have pointed out in (30). The fact that the integral

$$\int \hat{Z}_k <(1/2) \sum_{i \neq j} (v_{ij} - <v_{ij}>_i)>_k d\vec{\rho}_k = 0$$

vanishes does not imply that the integrand necessarily vanishes identically. Thus the second bracketed term of Eq. (6.14) is not necessarily zero when Eq. (6.16) is substituted for ϕ_i. Direct substitution of Eq. (6.16) into Eq. (6.14) leads to the condition

$$(1/2) \sum_{i \neq j} \hat{Z}_k \hat{Z}^{-1} (<v_{ij}>_k - <<v_{ij}>_i>_k) \overset{?}{=} 0 . \tag{6.17}$$

Proceeding as before, it is possible to show that

$$<<v_{ij}>_i>_k = \hat{Z}_k^{-1} \int \hat{Z}_{ik} [\hat{Z}_i^{-1} \int \ldots \int v_{ij} \Gamma_N \exp(-\beta \sum_s \phi_s) \prod_{k \neq i} d\vec{\rho}_k] d\vec{\rho}_i$$

$$<<v_{ij}>_i>_k \neq <v_{ij}>_k \text{ for arbitrary } v_{ij} .$$

Thus unless it can be shown that the sum of non-zero terms in Eq. (6.17)

---

[*]
 Actually, Reiss erroneously omitted the factor of 1/2 in Eq. (6.16).

add up to zero, then Reiss' solution in Eq. (6.16) does not satisfy this particular variational principle.

This does not mean that Reiss' solution for ϕ_i in Eq. (6.16) is not useful. It possesses the same form as the Hartree-Fock potential used in multi-electron atoms. Furthermore, it is a physically reasonable approximation to make since it effectively averages over all the interactions of a given segment of the chain.

Eq. (6.16) is an integral equation for ϕ_i. Reiss used the method of successive approximations to approximate the solution. A first-order approximation $\phi_i^{(1)}$ can be obtained by substituting an approximate $\phi_i^{(0)}$ in the right hand side of Eq. (6.16). This procedure could presumably be repeated to obtain higher-order approximations, although nothing is said about convergence in Reiss' paper. Reiss made the logical choice of $\phi_i^{(0)} = 0$ which represents the non-excluded volume problem discussed in chapter 4.

$$\phi_i^{(1)}(\vec{\rho}_i) = (1/2) \sum_{\substack{j \neq i \\ i \text{ fixed}}} \langle v_{ij} \rangle_i^{(0)}$$

$$= (1/2) \int_{\substack{i \text{ fixed}}} [\sum_{j \neq i} v_{ij} \, z_{ij}^{(0)} (z_i^{(0)})^{-1}] d\vec{\rho}_j$$

By making the Gaussian approximation for $z_{ij}^{(0)}$ and $z_i^{(0)}$, replacing the summation by an integration, and integrating over the angular parts of $\vec{\rho}_j$ above, it is possible to show that,

$$\rho_i \phi_i^{(1)} = 3 \int_0^\infty v(r) dr \int_{|r-\rho_i|}^{r+\rho_i} (r + x) \exp\{-(3/2i)[(x + r)^2 - \rho_i^2]\} dx,$$

which can be simplified to

$$\rho_i \phi_i^{(1)} = i \int_0^\infty v(x)\{1 - \exp[-6x(x + \rho_i)/i]\}dx. \tag{6.18}$$

Eq. (6.18) cannot be simplified any further without specifying the nature of the potential $v(r)$. It should be noted that because $v(r)$ appears as a factor in the integrand of Eq. (6.18), difficulty arises when the hard sphere potential is used for $v(r)$. This is because the zero-order approximation was taken to be the noninteracting chain probability distribution. To avoid this difficulty, Reiss used a finite repulsive potential

$$v(\rho) = \epsilon \text{ for } 0 \leq \rho \leq \lambda \tag{6.19}$$

$$= 0 \text{ for } \rho > \lambda.$$

Eq. (6.18) was then integrated to give

$$\rho \phi_i^{(1)}(\rho) = i\epsilon\{\lambda - (i\pi/24)^{1/2}\exp(3\rho^2/2i) \tag{6.20}$$

$$\times [\text{erf}[(\lambda + \rho/2)(6/i)^{1/2}] - \text{erf}(6\rho^2/4i)^{1/2}]\}.$$

Yamakawa in a later paper (12) used a potential similar to that used by Fixman (8)

$$v(\rho) = kT \ X \ \delta(\vec{\rho}). \tag{6.21}$$

where X is the binary cluster integral and $\delta(\vec{\rho})$ is a three dimensional δ-function. Inserting this potential into Eq. (6.18), Yamakawa obtained the result

$$\phi_i(\rho) = (2\pi/3)^{1/2} \xi [(\alpha^2 \rho) - (3\rho/i\alpha^4)] \tag{6.22}$$

with
$$\xi = (3/2\pi)^{3/2} X.$$

Now that the central field has been obtained, the probability

distribution $\hat{P}$ in Eq. (6.7a) can be written as

$$\hat{P} = \hat{Z}^{-1} \prod_{i=1}^{N-1} [\delta(\rho_{ii+1}-1)\exp(-\beta\phi_i)].$$

The singlet distribution function

$$\hat{P}_1[\rho_j] = \int \hat{P}[\rho_1 \cdots \rho_N] \prod_{i \neq j} d\vec{\rho}_i$$

can be written in Markoffian form.

$$\vec{P}_1[\rho_{j+1}] = \int \vec{P}_1[\rho_j] \, \psi(\rho_j \rho_{j+1}) d\vec{\rho}_j \tag{6.23}$$

$\psi(\rho_j \rho_{j+1})$ is the conditional probability. The details of these calcu-

lations can be found in the papers by Reiss and Yamakawa. Both authors

found an equation of the form of Eq. (6.23), although they differ on the

form of ψ. Both authors passed to a differential equation of the

Fokker-Planck type. The probability distributions were obtained and

Reiss found the result,

$$<\rho^2_{1N}> \propto n^{4/3} \tag{6.24}$$

whereas Yamakawa found

$$<\rho^2_{1N}> \propto n^{6/5}. \tag{6.25}$$

It should be noted that Reiss' solution was obtained in the limit as the

magnitude of the repulsive potential approaches zero. Yamakawa's solu-

tion was derived from the three dimensional δ-function potential of

Eq. (6.21) in the limit of large n. In both cases the parameter describ-

ing the strength of the interactions has been suppressed.

7. INTEGRAL EQUATIONS FOR Z_{1N}

Various integral equations for the radial distribution function have been derived in the theory of liquids. These equations give results that agree reasonably well with experiment. There are two general methods by which these integral equations have been derived:

1. The Yvon-Born-Green-Kirkwood type of equation (14,15) is obtained by differentiating the phase integral representation of the radial distribution function for a fluid. This leads to an equation for the pair distribution function in terms of the triplet distribution function. The Kirkwood superposition approximation (16), which relates the triplet and pair distribution functions, is usually made. These two relations lead to an integro-differential equation for the pair distribution function.

2. Other types of integral equations for the radial distribution function have been obtained for fluids by use of graph theory. The Percus-Yevick (31,32) and Hypernetted Chain (26,27) equations are familiar examples.

The excluded volume problem is very similar to the problem of the classical fluid. The form of the restricted partition function in Eq. (3.12) for a polymer chain is very similar in form to the phase integral representation for the radial distribution function of liquids. The essential difference between the two is the constraint that the adjacent subsystems in the polymer system be fixed relative to each other. This

gives rise to the δ-function ordering potentials discussed in chapter 3. In this chapter I will derive several integral equations for the restricted partition function Z_{1N} of a polymer chain. This approach has not been used by anyone on the excluded volume problem until now, with the exception of Naghizadeh (13), who recently derived a Kirkwood type of equation.

A. Yvon-Born-Green Type Equation

An integral equation can be obtained for Z_{1N} by following a procedure analogous to that used by Yvon, Born and Green (14) for liquids. In chapter 3 we found

$$Z_{1N} = \int \ldots \int \Gamma_N \exp(-\beta \sum_{ij} v_{ij}) d\vec{\rho}_2 \ldots d\vec{\rho}_{N-1} \tag{3.12}$$

We now take the gradient ∇_N with respect to the coordinates of the Nth subsystem.

$$\nabla_N Z_{1N} = -\beta \int \ldots \int \Gamma_N \prod_{ij} \exp(-\beta v_{ij}) \sum_{i=1}^{N-2} \nabla_N v_{iN} d\vec{\rho}_2 \ldots d\vec{\rho}_{N-1} \tag{7.1}$$

$$+ \int \ldots \int \Gamma_{N-1} \prod_{ij} \exp(-\beta v_{ij}) \nabla_N \delta(\rho_{N-1N}-1) d\vec{\rho}_2 \ldots d\vec{\rho}_{N-1}$$

This equation can be rewritten in terms of the restricted partition function Z_{1iN}, where 1, i, and N are held fixed.

$$\nabla_N Z_{1N} = -\beta Z_{1N} \nabla_N v_{1N} - \beta \sum_{i=2}^{N-2} \int Z_{1iN} \nabla_N v_{iN} d\vec{\rho}_i$$

$$+ \int [Z_{1N-1N}/\delta(\rho_{N-1N}-1)] \nabla_N \delta(\rho_{N-1N}-1) d\vec{\rho}_{N-1} \tag{7.2}$$

$[Z_{1N-1N}/\delta(\rho_{N-1N}-1)]$ simply means that $\delta(\rho_{N-1N}-1)$ is to be omitted in

Z_{1N-1N}. In order to solve for the function Z_{1N}, the triply restricted Z_{11N} must be determined. This can be accomplished by making the analog of the Kirkwood Superposition approximation, which is well-known in the theory of the liquid state (16). In our case this becomes,

$$Z_{11N}(\vec{\rho}_1\vec{\rho}_1\vec{\rho}_N) \approx Z_{1N}(\rho_{1N})Z_{11}(\rho_{11})Z_{1N}(\rho_{1N}). \qquad (7.3)$$

Eq. (7.2) then can be written as

$$\nabla_N(\ln Z_{1N} + \beta v_{1N}) = \int Z_{1N-1}\nabla_N \delta(\rho_{N-1N}-1)d\vec{\rho}_{N-1} \qquad (7.4)$$

$$-\beta \sum_{i=2}^{N-2} \int Z_{1i}Z_{iN}\nabla_N v_{iN}d\vec{\rho}_i .$$

In taking the gradient, ∇_N, all subsystems except the Nth sybsystem are to be considered fixed. As a consequence, we can write,

$$\nabla_N(\ln Z_{1N} + \beta v_{1N}) = \int Z_{1N-1}\nabla_{N-1N}\delta(\rho_{N-1N}-1)d\vec{\rho}_{N-1} \qquad (7.5)$$

$$-\beta \sum_{i=2}^{N-2} \int Z_{1i}Z_{iN}\nabla_{iN}v_{iN}d\vec{\rho}_i ,$$

where ∇_{1N} signifies the gradient with respect to a coordinate system with the origin at subsystem i. Eq. (7.5) is now dotted with a unit vector in the $\vec{\rho}_{1N}$ direction to give,

$$\frac{\partial}{\partial \rho_{1N}} (\ln Z_{1N} + \beta v_{1N}) = \int Z_{1N-1}\delta'(\rho_{N-1N}-1)\cos \theta_{N-1}d\vec{\rho}_{N-1} \qquad (7.6)$$

$$-\beta \sum_{i=2}^{N-2} \int Z_{1i}Z_{iN}v'_{iN}\cos \theta_i d\vec{\rho}_i ,$$

where θ_i is the angle between the vectors $\vec{\rho}_{1N}$ and $\vec{\rho}_{iN}$. From the law of cosines, $\cos \theta_i$ can be written as

$$\cos \theta_i = (\rho^2_{1i} - \rho^2_{1N} - \rho^2_{1N})/2\rho_{1N}\rho_{1N} \, . \qquad (7.7)$$

Using Eq. (7.7) and introducing bipolar coordinates into Eq. (7.6), we are led finally to,

$$\rho^2_{1N} \frac{\partial}{\partial \rho_{1N}}(\ell n \ Z_{1N} + \beta v_{1N}) = \pi \int_{|1+\rho_{1N}|}^{|1-\rho_{1N}|} Z_{1N-1}(x)(\rho^2_{1N} + 3 + x^2)dx \qquad (7.8)$$

$$+ \beta\pi \sum_{i=2}^{N-2} \int v'(x)Z_{1N}(x)dx \int_{|\rho_{1N}-x|}^{\rho_{1N}+x} yZ_{1i}(y)(\rho^2_{1N} + x^2 - y^2)dy \, .$$

Eq. (7.8) is a nonlinear, integro-differential equation for the restricted partition function Z_{1N}. It is analogous to the Yvon-Born-Green equation for the radial distribution function of a liquid. Eq. (7.8) is an approximate equation because of the utilization of the Kirkwood superposition approximation.

B. Kirkwood Type Equation

Kirkwood (15) used a method somewhat similar to that of Yvon, Born and Green. I will extend Kirkwood's method to obtain an equation for Z_{1N}.

Define a coupling parameter   by

$$V = \sum_{i=1}^{N-1} u_{ii+1} + \eta \sum_{i=1}^{N-2} v_{iN} + \sum_{i=1}^{N-3} \sum_{j=i+2}^{N-1} v_{ij} \qquad (7.9)$$

The coupling parameter η can vary between zero and one. It effectively "turns on" the interaction potential between subsystem N and the rest of the system. With this notation the restricted partition function Z_{1N} becomes

$$Z_{1N} = \int \cdots \int \Gamma_N \exp[-\beta(\eta \sum_i v_{iN} + \sum_{ij} v_{ij})] d\vec{\rho}_2 \cdots d\vec{\rho}_{N-1} . \qquad (7.10)$$

Now differentiate Eq. (7.10) with respect to the parameter η.

$$-\frac{\partial Z_{1N}}{\partial \eta} = \int \cdots \int \sum_{i=1}^{N-2} \beta v_{iN} \Gamma_N \exp[-\beta(\eta \sum_i v_{iN} + \sum_{ij} v_{ij})] d\vec{\rho}_2 \cdots d\vec{\rho}_{N-1}$$

Integration over all variables except $\vec{\rho}_i$ leads to

$$-\beta^{-1} \partial Z_{1N}/\partial \eta = Z_{1N}(\rho_{1N};\eta) v_{1N} + \sum_{i=2}^{N-2} \int Z_{1iN} v_{iN} d\vec{\rho}_i . \qquad (7.11)$$

We again apply the Kirkwood superposition approximation in order to express the triply restricted partition function Z_{1iN} in terms of the doubly restricted functions. Using Eq. (7.3) in Eq. (7.11), we obtain

$$-\beta^{-1} \partial \ell n \, Z_{1N}/\partial \eta = v_{1N} + \sum_{i=2}^{N-2} \int Z_{1i} Z_{iN} v_{iN} d\vec{\rho}_i . \qquad (7.12)$$

Eq. (7.12) is another nonlinear, approximate integro-differential equation for Z_{1N}.

Let us employ the method of successive approximations used by Reiss (chapter 6). Assume a zero-order solution of $Z_{1N}(\rho_{1N};\eta)$ is given by $Z_{1N}^{(0)}(\rho_{1N})$, the result obtained from the non-excluded volume problem. If this zero-order solution is inserted in the right hand side of Eq. (7.12), then the equation can be integrated immediately.

$$-\beta^{-1} \ell n[Z_{1N}(\rho_{1N};\eta)/Z_{1N}(\rho_{1N};0)] = \eta[v_{1N} + \sum_{i=2}^{N-2} \int z_{1i}^{(0)} z_{iN}^{(0)} v_{iN} d\vec{\rho}_i] \qquad (7.13)$$

η is now put equal to one since this corresponds to "turning on" the potential between subsystem N and the remaining system. The result is

$$Z_{1N}(\rho_{1N}) \approx Z_{1N}(\rho_{1N};0) \exp(-\beta v_{eff}) \qquad (7.14)$$

where,

$$v_{eff} = v_{1N} + \sum_{i=2}^{N-2} \int z_{11}^{(0)} z_{1N}^{(0)} v_{1N} d\vec{\phi}_i.$$

The appropriate initial condition is

$$z_{1N}(\rho_{1N};0) = z_{1N-1}(\rho_{1N-1})\delta(\rho_{N-1N}-1). \tag{7.15}$$

Eq. (7.14) now becomes

$$z_{1N}(\rho_{1N}) \simeq z_{1N-1}(\rho_{1N-1})\delta(\rho_{N-1N}-1)\exp(-\beta v_{eff}) \tag{7.16}$$

which is a difference equation for Z_{1N}.

This result is analogous to the central field approach of Reiss discussed in chapter 6. Reiss used an equivalent field potential ϕ_i which essentially is an average over all interactions v_{iN} (see Eq. (6.16)). In this treatment we found a v_{eff} which is essentially the same as Reiss' central field.

Naghizadeh (13) used a similar approach to obtain a different integro-differential equation. Naghizadeh solved this equation for the case of ring polymers.

C. Percus-Yevick Approach (33)

The Percus-Yevick (PY) equation for the radial distribution function of fluids was originally derived by Percus and Yevick by using a method based on "collective coordinates" (31). A much simpler derivation based on graph theory was presented by Stell (32). Recently, Percus (41) has shown that the PY equation can be obtained from a function-

al Taylor expansion by keeping only first-order terms, provided the proper functionals are chosen. The PY equation is generally considered to give results which agree with experiment better than any of the other integral equations available at the present time.

In this chapter I will derive the analog of the Percus-Yevick equation for a polymer chain (33). The method which I will employ will be analogous to that used by Stell.

In chapter 5 a cluster expansion for Z_{1N} was given in Eq. (5.2). A graph representation of this equation was presented in Eq. (5.3). It is convenient to introduce a parameter λ by

$$Z_{1N}(\rho_{1N};\lambda) = \sum_{i=0}^{\binom{N-1}{2}} \lambda^i Z_{1N}^{(i)}(\rho_{1N}).$$ (7.17)

This equation can be written in terms of graphs to give

$$Z_{1N}(\rho_{1N};\lambda) = \text{O—O—O} \cdots \text{O—O} + \lambda \sum_{\text{pairs}} \text{O—O—O} \cdots \text{O—O} \cdots \text{O—O}$$ (7.18)

$$+ \lambda^2 \sum_{\text{fours}} \text{O—O—O—O} \cdots \text{O—O—O—O} \cdots \text{O—O} + \cdots$$

These graphs represent the integrals $Z_{1N}^{(i)}$ as discussed in chapter 5. λ is merely a convenient expansion parameter whose exponent corresponds to the number of loops or h-bonds appearing in the graphs of its coefficient. When λ is set equal to -1, $Z_{1N}(\rho_{1N};\lambda)$ reduces to the conventional restricted partition function $Z_{1N}(\rho_{1N})$ previously used.

Furthermore, Eqs. (7.17) and (7.18) reduce to Eqs. (5.2) and (5.3)

respectively when $\lambda = -1$.

In the restricted partition function $Z_{1N}(\rho_{1N};\lambda)$ subsystems

with coordinates 1 and N are held fixed in the integration. This is

also true of the terms $Z_{1N}^{(i)}(\rho_{1N})$ in the cluster expansion. As a result,

the bond h_{1N} can be factored out of some of the graphs appearing in

Eqs. (7.17) or (7.18). Eq. (7.17) can then be written as

$$Z_{1N}(\rho_{1N};\lambda) = (1 + \lambda h_{1N}) \sum_{i=0}^{\binom{N-1}{2}-1} \zeta_i(\rho_{1N})\lambda^i \qquad (7.19)$$

where $\zeta_i(\rho_{1N})$ is the sum of all graphs of i loops or h-bonds, except

those with an h_{1N} bond, in a chain of N subsystems. Eq. (7.19) is ana-

logous to the density expansion of the radial distribution function of

a fluid. The parameter λ is analogous to the fluid density. We saw

in chapter 5 that the integrals ζ_i, for $i \geq 3$, become extremely diffi-

cult to evaluate and that the cluster expansion does not converge rapid-

ly (i.e. higher-order graphs are important). Complete summation of the

cluster expansion in Eq. (7.19) can in principle be achieved if certain

classes of graphs are omitted. This can be accomplished by expressing

Z_{1N} in an integral equation by using some topological arguments.

I am now going to make a distinction between two different types

of graphs in $Z_{1N}(\rho_{1N};\lambda)$. Nodal graphs are defined as those graphs which

contain a field point through which all paths from one end of the graph

to the other must pass. These points are called nodes (see Fig. 7.1).

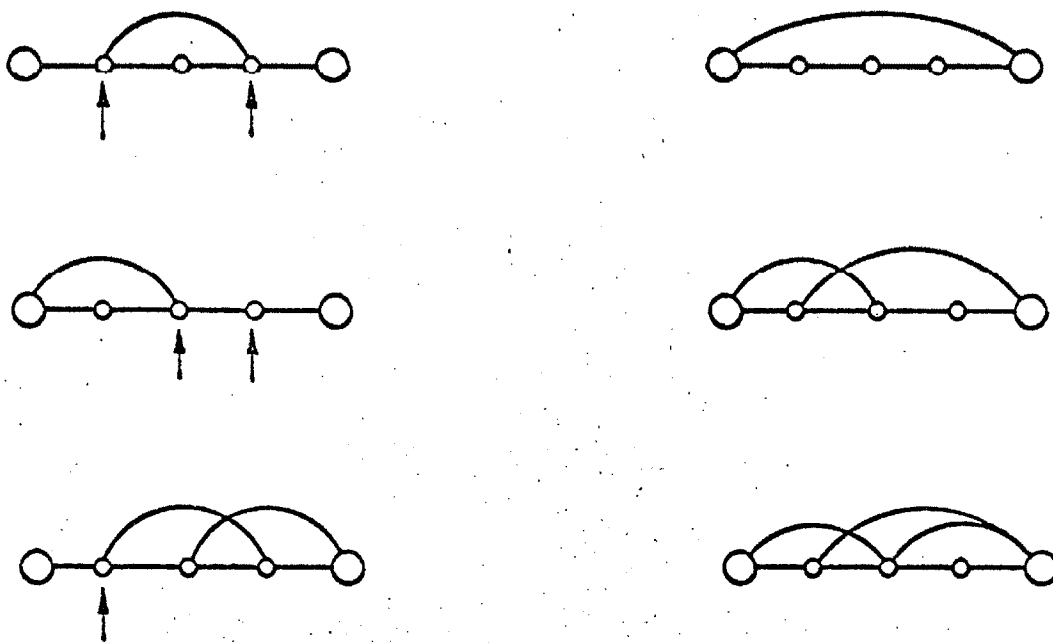Alternatively, a node is a point which cuts the graph into two parts.

Fig. (7.1)
Examples of nodal and elementary graphs
Nodes are marked by arrows.

Graphs which are not nodal are defined to be elementary.

The function $Z_{1N}(\rho_{1N};\lambda)$ is the sum of the nodal graphs $N_{1N}(\rho_{1N};\lambda)$ and the elementary graphs $E_{1N}(\rho_{1N};\lambda)$.

$$Z_{1N}(\rho_{1N};\lambda) = N_{1N}(\rho_{1N};\lambda) + E_{1N}(\rho_{1N};\lambda) \qquad (7.20)$$

The nodal and elementary graphs are given by the expansions

$$N_{1N}(\rho_{1N};\lambda) = \sum_{i=0}^{\binom{N-1}{2}} \nu_i(\rho_{1N})\lambda^i \qquad (7.21a)$$

$$E_{1N}(\rho_{1N};\lambda) = \sum_{i=0}^{\binom{N-1}{2}} \varepsilon_i(\rho_{1N})\lambda^i \qquad (7.21b)$$

where $\nu_i(\rho_{1N})$ and $\varepsilon_i(\rho_{1N})$ are the sums of nodal graphs and elementary graphs respectively with i h-bonds or loops in a chain of N subsystems.

Nodal graphs have the property that they can be synthesized from other graphs. In effect, two graphs can be joined at a point which becomes a node of the new graph. For example, the graphs $f_1(\rho_{13})$ and $f_2(\rho_{14})$ defined by

$$f_1(\rho_{13}) = \quad \underset{1 \qquad 3}{\text{⌒⌒}}$$

$$f_2(\rho_{14}) = \quad \underset{1 \qquad\quad 4}{\text{⌒⌒}}$$
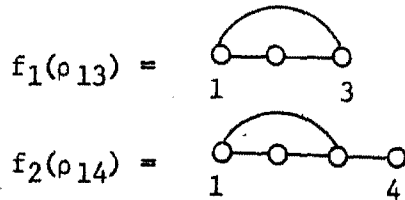
can be jointed to form a new nodal graph $f_3(\rho_{16})$.

$$f_3(\rho_{16}) = \quad \underset{1 \qquad\qquad\qquad 6}{\text{⌒⌒⌒⌒}}$$

$$= \int f_1(\rho_{13}) f_2(\rho_{36}) d\vec{\rho}_3$$

This property of nodal graphs is very useful. In fact, all the nodal

graphs in $N_{1N}(\rho_{1N};\lambda)$ can be constructed from simpler graphs. Consider

the graphs in $N_{1N}(\rho_{1N};\lambda)$ which possess a node at point i, but which have

no nodes to the left of point i. Then all graphs with this property

are given by

$$\int E_{1i}(\rho_{1i};\lambda)Z_{iN}(\rho_{iN};\lambda)d\vec{\rho}_i.$$

In words, the elementary graphs of chain length i are joined with both

nodal and elementary graphs of chain length $N + 1 - i$, to give a nodal

graph of length N whose left-most node is at point i. By summing over

i, all graphs in $N_{1N}(\rho_{1N};\lambda)$ are accounted for. Thus

$$N_{1N}(\rho_{1N};\lambda) = \sum_{i=2}^{N-1} \int E_{1i}(\rho_{1i};\lambda)Z_{iN}(\rho_{iN};\lambda)d\vec{\rho}_i. \qquad (7.22)$$

Since $E_{12}(\rho_{12};\lambda)$ and $Z_{N-1N}(\rho_{N-1N};\lambda)$ are simply δ-functions, these terms

will be removed from the summation in Eq. (7.22).

$$N_{1N}(\rho_{1N};\lambda) = \int E_{1N-1}(\rho_{1N-1};\lambda)\delta(\rho_{N-1N}-1)d\vec{\rho}_{N-1} \qquad (7.23)$$

$$+ \int Z_{2N}(\rho_{2N};\lambda)\delta(\rho_{12}-1)d\vec{\rho}_2 + \sum_{i=3}^{N-2} \int E_{1i}(\rho_{1i};\lambda)Z_{iN}(\rho_{iN};\lambda)d\vec{\rho}_i$$

Eq. (7.23) is the relation between the nodal and elementary graphs in

Z_{1N}. It is analogous to the well-known Ornstein-Zernike equation (26,27)

in the theory of fluids.

If it were possible to obtain another independent relation be-

tween the nodal and elementary graphs, then this relation together with

Eqs. (7.20) and (7.23) would uniquely determine $Z_{1N}(\rho_{1N};\lambda)$. In order to

obtain this second relation I will employ an approximation analogous to

the Percus-Yevick approximation given by Stell (32) in the theory of fluids. For the excluded volume problem this approximation is

$$\varepsilon_i(\rho_{1N}) \simeq h_{1N}\zeta_{i-1}(\rho_{1N}) \text{ for } i \geq 1. \tag{7.24}$$

By definition we have

$$\varepsilon_o(\rho_{1N}) = \zeta_o(\rho_{1N}) \text{ for } N = 2 \tag{7.25}$$

$$\varepsilon_o(\rho_{1N}) = 0 \text{ for } N \geq 3.$$

For $N = 3$, approximation Eq. (7.24) is exact. For $N = 4$, all graphs are accounted for except the graph (see Appendix X). In general, this approximation fails to account for those elementary graphs which do not contain an h_{1N}-bond. If it is used successively (starting from $N = 3$), only those elementary graphs which are formed by adding an h-bond to nodal graphs are counted.

Eq. (7.24) can be put in a more useful form by multiplying both sides by λ^i and then summing on i.

$$\sum_{i=1}^{\binom{N-1}{2}} \varepsilon_i(\rho_{1N})\lambda^i \simeq \lambda h_{1N} \sum_{i=0}^{\binom{N-1}{2}-1} \zeta_i \lambda^i \tag{7.26}$$

Using Eqs. (7.19) and (7.21b), Eq. (7.26) becomes,

$$E_{1N}(\rho_{1N};\lambda) \simeq [\lambda h_{1N}/(1 + \lambda h_{1N})]Z_{1N}(\rho_{1N};\lambda). \tag{7.27}$$

If λ is put equal to -1, we obtain

$$E_{1N}(\rho_{1N}) \simeq (-h_{1N}/H_{1N})Z_{1N}(\rho_{1N}). \tag{7.28}$$

where $H_{1N} = 1 - h_{1N}$. Substitution of Eq. (7.28) into Eq. (7.23), putting $\lambda = -1$ leads to,

$$Z_{1N} = H_{1N}[\int \delta(\rho_{12}-1)Z_{2N}d\vec{\rho}_2 - \int (h_{1N-1}/H_{1N-1})Z_{1N-1}\delta(\rho_{N-1N}-1)d\vec{\rho}_{N-1}$$
$$- \sum_{i=3}^{N-2} \int (h_{1i}/H_{1N})Z_{1i}Z_{iN}d\vec{\rho}_i] , \tag{7.29}$$

Eq. (7.29) is analogous to the Percus-Yevick equation for fluids. The PY equation is an integral equation only, but Eq. (7.29) is an $(N - 1)$th-order integro-difference equation. This additional complication arises because we are dealing with a chain rather than a uniform fluid.

8. SOLUTION OF THE PERCUS-YEVICK TYPE OF EQUATION (33)

In chapter 7, three different approximate integral equations were derived for the restricted partition function $Z_{1N}(\rho_{1N})$. The Yvon-Born-Green and Kirkwood types were obtained by invoking the analog of the Kirkwood superposition approximation. The Percus-Yevick type employed another type of approximation. It is known from the theory of liquids that the Kirkwood superposition approximation is a rather crude assumption. Furthermore, the Percus-Yevick approximation is known to give much better results than the Kirkwood superposition approximation. In fact, the Percus-Yevick equation is considered to be the best available integral equation for the radial distribution function. For this reason it is hoped that the Percus-Yevick type of equation presented in chapter 7 will provide a satisfactory solution to the excluded volume problem. This equation will now be solved for the case of a hard core potential.

The exact solution to the Percus-Yevick integral equation for fluids has been obtained for hard spheres by Wertheim (34) and Thiele (35). Since Eq. (6.29) is an $(N - 1)$th-order difference equation as well as an integral equation, an analytical solution for the polymer chain problem is much more difficult to obtain than with the Percus-Yevick equation. Even if it were possible to solve this nonlinear equation, a large number of conditions would be necessary to determine the resulting arbitrary constants. Fortunately, for a hard core potential and the special case when the hard core diameter is equal to the

segment length of the chain (i.e. $b = 1$), this $(N - 1)$th-order difference equation reduces to a second-order difference equation.

A. Analytical Result When $b = 1$

Introduce the variable $t_{ij}(\rho_{ij})$ defined by

$$t_{ij}(\rho_{ij}) = \exp(\beta v_{ij}) Z_{ij}(\rho_{ij}) \tag{8.1}$$

$$= Z_{ij}(\rho_{ij}) / H_{ij}.$$

In terms of t_{ij}, Eq. (7.29) becomes

$$t_{1N}(\rho_{1N}) = \int \delta(\rho_{12}-1) t_{2N}(\rho_{2N}) H_{2N} d\vec{\rho}_2$$

$$- \int h_{1N-1} t_{1N-1}(\rho_{1N-1}) \delta(\rho_{N-1N}-1) d\vec{\rho}_{N-1} \tag{8.2}$$

$$- \sum_{i=3}^{N-2} \int h_{1i} t_{1i}(\rho_{1i}) H_{iN} t_{iN}(\rho_{iN}) d\vec{\rho}_i \; .$$

We now introduce the hard core potential.

$$h_{ij} = 1 \text{ for } \rho_{ij} < b \tag{8.3}$$

$$h_{ij} = 0 \text{ for } \rho_{ij} > b$$

The parameter b is the radio of the hard core diameter to the segment length (a), hence our model is a "pearl necklace" model. Consider now the special case of $b = 1$. After introducing bipolar coordinates into Eq. (8.2) and simplifying, we obtain a set of two equations.

$$u_{1N}(\rho_{1N}) = \int_{1}^{1+\rho_{1N}} u_{2N}(\rho_{2N})d\rho_{2N} - \int_{|1-\rho_{1N}|}^{1} u_{1N-1}(\rho_{1N-1})d\rho_{1N-1}$$

$$\qquad\qquad (8.4a)$$

$$- \sum_{i=3}^{N-2} \int_{1}^{1+\rho_{1N}} u_{iN}(\rho_{iN})d\rho_{iN} \int_{|\rho_{1N}-\rho_{iN}|}^{1} u_{1i}(\rho_{1i})d\rho_{1i}$$

when $0 \leq \rho_{1N} \leq 2$ and,

$$u_{1N}(\rho_{1N}) = \int_{\rho_{1N}-1}^{\rho_{1N}+1} u_{2N}(\rho_{2N})d\rho_{2N}$$

$$\qquad\qquad (8.4b)$$

$$- \sum_{i=3}^{N-2} \int_{\rho_{1N}-1}^{\rho_{1N}+1} u_{iN}(\rho_{iN})d\rho_{iN} \int_{|\rho_{1N}-\rho_{iN}|}^{1} u_{1i}(\rho_{1i})d\rho_{1i}$$

when $2 \leq \rho_{1N} < \infty$.

The function $u_{ij}(\rho_{ij})$ is related to $t_{ij}(\rho_{ij})$ by,

$$u_{ij}(\rho_{ij}) = \rho_{ij}t_{ij}(\rho_{ij})/(2\pi)^{j-i-1}. \qquad\qquad (8.5)$$

By starting with $u_{12} = \delta(\rho_{12}-1)$ it is possible to successively calculate the u_{1N} for small N using Eqs. (8.4). u_{12} through u_{15} are shown in Table 8.1.

Three observations can be made from Table 8.1:

1. u_{1N} is a piecewise analytic function, analytic between integer values of ρ_{1N}.

2. u_{1N} is continuous at integer values of ρ_{1N}.

3. $u_{1N} = 0$ in the region $0 \leq \rho_{1N} \leq 1$, N = 4, 5.

If we assume that condition (3) holds for u $(4 \leq k \leq N - 1)$, then Eqs. (8.4) simplify to linear, second-order difference equations.

Table 8.1

u_{1N} calculated from Eqs. (8.4)

N	$u_{1N}(\rho_{1N})$	Range of ρ_{1N}
2	$\delta(\rho_{12}-1)$	
3	1	$0 \leq \rho_{13} \leq 2$
	0	$2 \leq \rho_{13} < \infty$
4	0	$0 \leq \rho_{14} \leq 1$
	$\rho_{14}-1$	$1 \leq \rho_{14} \leq 2$
	$3-\rho_{14}$	$2 \leq \rho_{14} \leq 3$
	0	$3 \leq \rho_{14} < \infty$
5	0	$0 \leq \rho_{15} \leq 1$
	$(1/2)(\rho_{15}-1)^2$	$1 \leq \rho_{15} \leq 2$
	$(1/2)(10\rho_{15}-2\rho_{15}^2-11)$	$2 \leq \rho_{15} \leq 3$
	$(1/2)(4-\rho_{15})^2$	$3 \leq \rho_{15} \leq 4$
	0	$4 \leq \rho_{15} < \infty$

$$u_{1N}(\rho_{1N}) = \int\limits_{1}^{1+\rho_{1N}} u_{2N}(\rho_{2N})\,d\rho_{2N} - \int\limits_{1}^{1+\rho_{1N}} u_{3N}(\rho_{3N})\,[1 - |\rho_{1N} - \rho_{3N}|]\,d\rho_{3N}$$

$$\text{when } 0 \le \rho_{1N} \le 2 \qquad\qquad (8.6a)$$

$$u_{1N}(\rho_{1N}) = \int\limits_{\rho_{1N}-1}^{\rho_{1N}+1} u_{2N}(\rho_{2N})\,d\rho_{2N} - \int\limits_{\rho_{1N}-1}^{1+\rho_{1N}} u_{3N}(\rho_{3N})\,[1 - |\rho_{1N} - \rho_{3N}|]\,d\rho_{3N}$$

$$\text{when } 2 \le \rho_{1N} \le \infty \qquad\qquad (8.6b)$$

The solution to these equations is piecewise analytic. After some manipulation, this solution is found to be (see Appendix XI)

$$u_{1N}^{(j)}(\rho_{1N}) = \sum_{s=0}^{j-1} (-1)^s \binom{N-2}{s}(\rho_{1N} - s - 1)^{N-3}/(N - 3)!\qquad (8.7)$$

$$\text{for } b = 1,\ j \le \rho_{1N} \le j + 1,\ j \ge 1.$$

Using Eq. (8.7) it can be shown by induction that condition (3) $(u_{1N}^{(0)} = 0)$ holds for all $N \ge 4$. Thus Eq. (8.7) is also a solution to Eqs. (8.4).

Let us now compute the mean square end-to-end distance $<\rho^2_{1N}>$. Using Eqs. (8.5) and (8.7) we obtain,

$$<\rho^2_{1N}> = \frac{\sum\limits_{j=1}^{N-2}\sum\limits_{s=0}^{j-1} (-1)^s \binom{N-2}{s} \int\limits_{j}^{j+1} \rho^3_{1N}(\rho_{1N} - s - 1)^{N-3}d\rho_{1N}}{\sum\limits_{j=1}^{N-2}\sum\limits_{s=0}^{j-1} (-1)^s \binom{N-2}{s} \int\limits_{j}^{j+1} \rho_{1N}(\rho_{1N} - s - 1)^{N-3}d\rho_{1N}} \cdot (8.8)$$

We now expand $\rho^3_{1N} = [(\rho_{1N} - s - 1) + (s + 1)]^3$ in powers of $(\rho_{1N} - s - 1)$ and integrate. After interchanging the jth and the sth summation operations and summing on j we obtain

$$<\rho^2_{1N}> = \{\phi(N + 1)[1/(N + 1) -3/N + 3/(N - 1) -1/(N - 2)]$$

$$+ 3\phi(N)[(N - 1)/(N - 2) - 2 + (N - 1)/N] \tag{8.9}$$

$$+ 3\phi(N - 1)[N - 1 - (N - 1)^2/(N - 2)] + \phi(N - 2)(N - 1)^3/(N - 2)\}$$

$$\times \{\phi(N - 1)[1/(N - 1) -1/(N - 2)] + \phi(N - 2)(N - 1)/(N - 2)\}^{-1}$$

where

$$\phi(\ell) = \lim_{z \to 1} \phi_z(\ell) = \lim_{z \to 1} \sum_{k=0}^{N-2} \binom{N-2}{k} z^k (-1)^k k^\ell.$$

After considerable manipulation, it is possible to perform the summations in Eq. (8.9) (see Appendix XII). The final result reduces to the simple form,

$$<\rho^2_{1N}> = (N - 1)(N + 2)/4. \tag{8.10}$$

This result can also be obtained by examining the coefficients in the power series of the Fourier transform of $t_{1N}(\rho_{1N})$. This will be shown later in this chapter.

Eq. (8.10) represents the mean square end-to-end distance when the diameter of the hard core potential is exactly equal to the segment length (i.e. $b = 1$). For long chains (large N) it can be seen that the mean square end-to-end distance is proportional to $n^2 (n = N - 1)$. When there is no excluded volume effect (i.e. $b = 0$), we know that the mean square end-to-end distance is proportional to n. It would be extremely interesting to examine the solutions to Eq. (8.2) for intermediate values of b. Unfortunately the equation does not simplify as before, and an

analytical result has not been obtained. We have computed the mean square end-to-end distances numerically for some intermediate values of b; this is discussed in a later section.

B. The Transformed Equation

For numerical computations it is convenient to transform Eq. (8.2) into Fourier space. Whereas t_{1N} is piecewise analytic, the Fourier transform $\bar{t}_{1N}(k)$ is analytic for all k; furthermore, the moments of t_{1N} can be found by examining the coefficients in the power series for $\bar{t}_{1N}(k)$. Define the following transform pairs:

$$\bar{t}_{1N}(k) = \int_{-\infty}^{\infty} t_{1N}(\rho_{1N})\exp(-i\vec{k}\cdot\vec{\rho}_{1N})d\vec{\rho}_{1N} \tag{8.11}$$

$$8\pi^3 t_{1N}(\rho_{1N}) = \int_{-\infty}^{\infty} \bar{t}_{1N}(k)\exp(i\vec{k}\cdot\vec{\rho}_{1N})d\vec{k}$$

$$\bar{F}_{1N}(k) = \int_{-\infty}^{\infty} h_{1N}t_{1N}(\rho_{1N})\exp(-i\vec{k}\cdot\vec{\rho}_{1N})d\vec{\rho}_{1N} \tag{8.12}$$

$$8\pi^3 h_{1N}t_{1N}(\rho_{1N}) = \int_{-\infty}^{\infty} \bar{F}_{1N}(k)\exp(i\vec{k}\cdot\vec{\rho}_{1N})d\vec{k}$$

$$\bar{h}(k) = \int_{-\infty}^{\infty} h(\rho_{1N})\exp(-i\vec{k}\cdot\vec{\rho}_{1N})d\vec{\rho}_{1N} \tag{8.13}$$

$$8\pi^3 h(\rho_{1N}) = \int_{-\infty}^{\infty} \bar{h}(k)\exp(i\vec{k}\cdot\vec{\rho}_{1N})d\vec{k}.$$

If we multiply Eq. (8.2) through by $\exp(-i\vec{k}\cdot\vec{\rho}_{1N})$ and integrate over $d\vec{\rho}_{1N}$ using the properties of convolution integrals, we obtain,

$$\bar{t}_{1N}(k) = 4\pi k^{-1}\sin k[\bar{t}_{2N}(k) - 2\bar{F}_{2N}(k)] \tag{8.14}$$

$$+ \sum_{i=3}^{N-2} [\bar{F}_{1i}(k)\bar{F}_{iN}(k) - \bar{F}_{1i}(k)\bar{t}_{iN}(k)].$$

For the hard core potential Eq. (8.3), $\bar{h}(k)$ becomes,

$$\bar{h}(k) = 4\pi[\sin(bk) - bk\cos(bk)]/k^3 . \qquad (8.15)$$

The function $\bar{F}_{1N}(k)$ can be expressed in terms of $\bar{t}_{1N}(k)$. Substitution of the Fourier integral representation of $t_{1N}(\rho_{1N})$ into Eq. (8.12) for $\bar{F}_{1N}(k)$ leads to the relation

$$8\pi^3\bar{F}_{1N}(k) = \int h(|\vec{k} - \vec{\ell}|)\bar{t}_{1N}(\ell)d\vec{\ell}. \qquad (8.16)$$

If Eq. (8.15) is now used for $\bar{h}(|\vec{k} - \vec{\ell}|)$, the angular integrations in Eq. (8.16) can be performed using the technique discussed in Appendix I.

$$\pi k\bar{F}_{1N}(k) = \int_{-\infty}^{\infty} \ell\bar{t}_{1N}(\ell)\sin[(k - \ell)b]/(k - \ell)bd\ell \qquad (8.17)$$

Eqs. (8.14) and (8.17) now provide an integro difference equation for the analytic function $\bar{t}_{1N}(k)$. The mean square end-to-end distance can be found from the first two coefficients in $\bar{Z}_{1N}(k)$. From Eqs. (8.1), (8.11) and (8.12) it can easily be shown that

$$\bar{Z}_{1N}(k) = \bar{t}_{1N}(k) - \bar{F}_{1N}(k). \qquad (8.18)$$

From Appendix II we find that the mean square end-to-end distance is given by

$$\langle\rho^2_{1N}\rangle = \frac{\text{coeff}(-k^2/6)\text{in}[\bar{t}_{1N}(k) - \bar{F}_{1N}(k)]}{\text{coeff}(1)\text{in}[\bar{t}_{1N}(k) - \bar{F}_{1N}(k)]} . \qquad (8.19)$$

Eqs. (8.14), (8.17) and (8.19) thus provide a method of calculating the mean square end-to-end distance for any hard core diameter $0 \leq b \leq 1$.

When b = 1 the above method should give the same mean square end-to-end distance as was obtained in the previous section by calculating $Z_{1N}(\rho_{1N})$ directly. This would provide a valuable consistency check on both procedures. From the previous section we know that when b = 1

$$t_{1N}(\rho_{1N}) = 0 \text{ for } 0 \leq \rho_{1N} \leq 1, \ N \geq 4 \qquad (8.20)$$

$$t_{1N}(\rho_{1N}) = 2\pi/\rho_{1N} \text{ for } 0 \leq \rho_{1N} \leq 1, \ N = 3.$$

From Eq. (8.12) it can be seen that

$$\overline{F}_{1N}(k) = 0 \text{ for } N \geq 4, \ b = 1 \qquad (8.21)$$

$$k^2\overline{F}_{1N}(k) = 8\pi^2(1 - \cos kb) \text{ for } N = 3, \ b = 1.$$

Thus Eq. (8.14) can be greatly simplified. The result for $N \geq 6$ is

$$\overline{t}_{1N}(k) = (4\pi \sin k/k)\overline{t}_{1N-1}(k) - 8\pi^2 k^{-2}(1 - \cos k)\overline{t}_{1N-2}(k) \qquad (8.22)$$

when $N \geq 6, \ b = 1.$

The results for $2 \leq N \leq 5$ are given in Table 8.2.

Since we are mainly interested in the coefficients in the power series of $\overline{t}_{1N}(k)$, let us introduce

$$\overline{t}_{1N}(k) = (4\pi)^{N-1} \sum_{i=0}^{\infty} \tau_{iN} k^{2i}. \qquad (8.23)$$

If Eq. (8.23) is introduced into Eq. (8.22) and the sum of the coefficients of like powers of k set equal to zero, the following two difference equations are obtained,

Table 8.2

Results of Eq. (8.14) when $b = 1$

$\underline{N}$	$\bar{t}_{1N}(k)$	τ_{ON}	τ_{1N}
2	$4\pi\,(\sin k/k)$	1	$-1/6$
3	$4\pi(\sin k/k)\,\bar{t}_{12}$	1	$-1/3$
4	$4\pi(\sin k/k)[\bar{t}_{13} - 16\pi^2(1 - \cos k)/k^2]$	$1/2$	$-3/8$
5	$4\,(\sin k/k)\,\bar{t}_{14}$ $-\dfrac{8\pi^2}{k^2}(1 - \cos k)[\bar{t}_{35} - 8\pi^2(1 - \cos k)/k^2]$	$5/16$	$-35/96$
6	Eq. (8.22)	$3/16$	$-5/16$
7	Eq. (8.22)	$7/64$	$-65/256$

$$\tau_{ON} = \tau_{ON-1} - (1/4)\tau_{ON-2} \qquad (8.24a)$$

$$\tau_{1N} = \tau_{1N-1} - (1/4)\tau_{1N-2} - (1/6)\tau_{ON-1} + (1/48)\tau_{ON-2} \qquad (8.24b)$$

which are valid for $N \geq 6$. The coefficients for $2 \leq N \leq 5$ can be found, starting with $t_{12}(\rho_{12}) = \delta(\rho_{12} - 1)$ and successively calculating the higher-order terms. These are also shown in Table 8.2. The τ_{ON} and τ_{1N} when $N = 6, 7$ will serve as initial conditions for the difference equations (8.24). Let E_1 represent the operator which converts τ_{ON-1} into τ_{ON}.

$$\tau_{ON} = E_1 \tau_{ON-1}$$

Eq. (8.24a) becomes

$$(E_1{}^2 - E_1 + 1/4)\tau_{ON-2} = 0.$$

This linear, homogeneous equation has a solution,

$$\tau_{ON} = C_1(1/2)^N + C_2(1/2)^N N \qquad (8.25)$$

The initial conditions τ_{06} and τ_{07} of Table 8.2 determine the constants C_1 and C_2. The final result which satisfies the initial conditions is,

$$\tau_{ON} = 2N(1/2)^N \quad \text{for} \quad N \geq 6. \qquad (8.26)$$

If Eq. (8.26) is substituted into Eq. (8.24b), a nonhomogeneous difference equation for τ_{1N} results

$$(E^2{}_2 - E_2 + 1/4)\tau_{1N} = (1/2)^N(1/3 - N/2) \qquad (8.27)$$

where E_2 is the operator defined by,

$$\tau_{1N} = E_2 \tau_{1N-1}.$$

The solution to this nonhomogeneous equation (8.27) is given by

$$\tau_{1N-2} = (1/2)^N (C_3 + C_4 N) + \tau_{1N-2}^{(p)} \qquad (8.28)$$

where $\tau_{1N-2}^{(p)}$ is a particular solution to Eq. (8.27). A particular solution can be found by an operator method discussed in Appendix XIII. This particular solution is

$$\tau_{1N}^{(p)} = - (1/2)^N N(N - 1)(N - 4)/3. \qquad (8.29)$$

The general solution for τ_{1N-2} is finally

$$\tau_{1N-2} = (1/2)^N [C_3 + C_4 N - N(N - 1)(N - 4)/3]. \qquad (8.30)$$

Using the initial conditions τ_{16} and τ_{17} of Table 8.2 leads to the results

$$\tau_{1N} = - (1/2)^{N+2} N(N - 1)(N + 2)/3. \qquad (8.31)$$

From Eq. (8.19) the mean square end-to-end distance is given by

$$<\rho^2_{1N}> = -6\tau_{1N}/\tau_{0N} \qquad (8.10)$$

$$= (N - 1)(N + 2)/4$$

which agrees with previously obtained results of Eq. (8.10) for $b = 1$.

C. Intermediate Values of b

An analytical solution to Eq. (8.14) has not been found when the hard core diameter b is intermediate between zero and one. The system of equations (8.14) and (8.17) are suitable, however, for numerical solution. Fortunately the right hand side of the difference equation (8.14) involves the functions $\bar{t}_{ij}(k)$ which are of lower-order than $\bar{t}_{1N}$ on the left hand side. Starting with the initial condition

$$\tau_{12}(\rho_{12}) = \delta(\rho_{12} - 1)$$

$$\bar{\tau}_{12}(k) = 4\pi \sin k/k,$$

higher-order t_{1N} were successively calculated numerically using Eqs. (8.14) and (8.17). These computations were done on an IBM 7094 digital computer. The integrations involved in Eq. (8.17) were performed using a Simpson rule subroutine. The calculations were done as a function of the variable k with b as a parameter. For practical reasons the number of iterations was not allowed to exceed 64. The results were used to find the first two coefficients in the power series expansion of $[\bar{t}_{1N}(k) - \bar{F}_{1N}(k)]$. These coefficients were found by curve fitting numerically using a least-square procedure. The mean square end-to-end distance was then computed using Eq. (8.19). The results of these numerical computations are shown for four intermediate values of b in Fig. (8.1).

It can be seen from the log-log plot in Fig. (8.1) that for long chains,
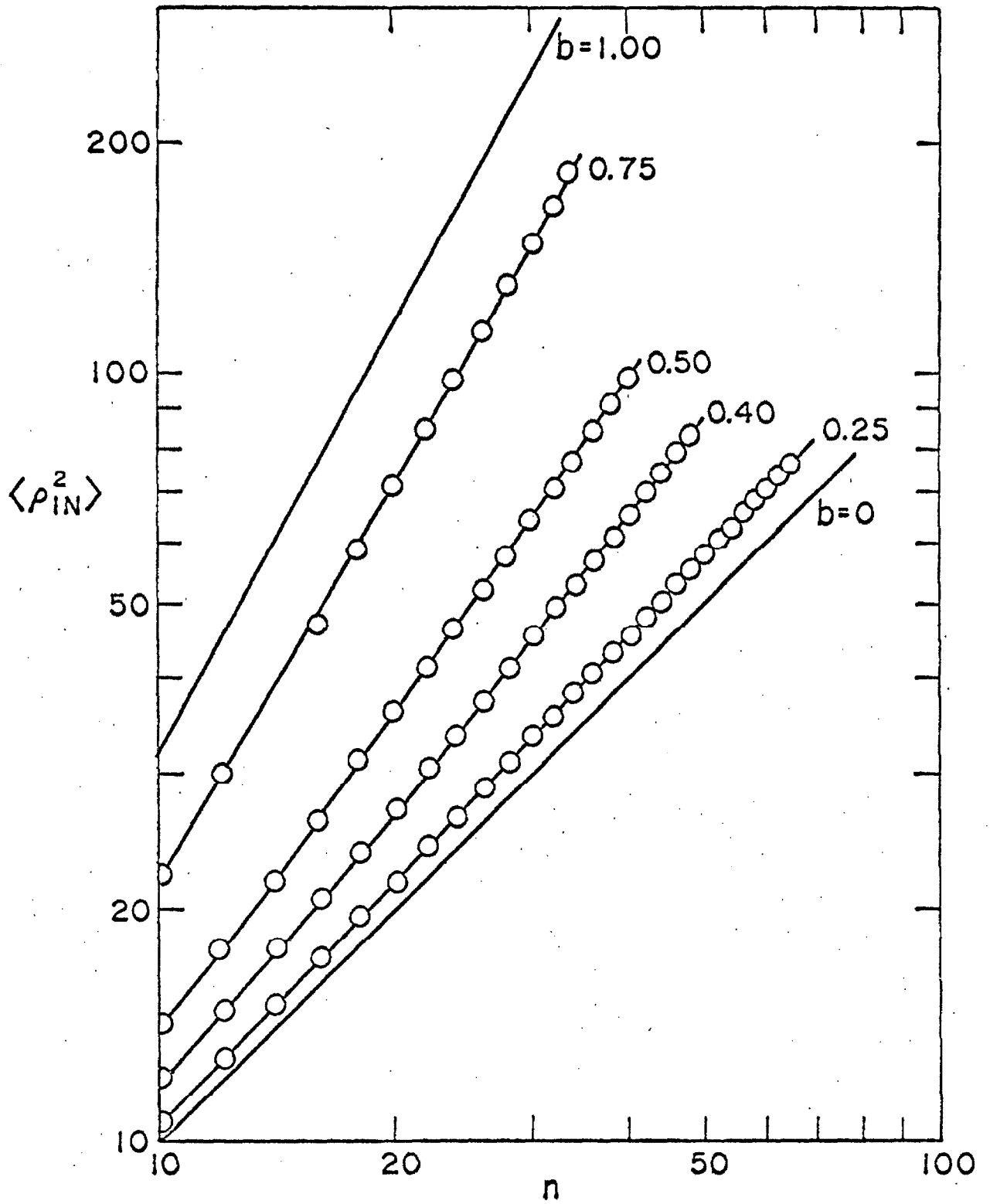
Fig. (8.1)
Numerical results for intermediate b.

$$\langle \rho^2_{1N} \rangle = C(b)n^{\gamma(b)}$$

where n is the number of segments in the chain (i.e. $n = N - 1$). The exponent γ was computed from the slopes of the curves in Fig. (8.1). These are shown plotted against b in Fig. (8.2). Unfortunately, the error in solving the system of equations (8.14) and (8.17) is cumulative. The points in Fig. (8.2) are drawn to depict the maximum estimated uncertainty. The coefficient C was determined from Fig. (8.1) and is plotted in Fig. (8.3) as a function of the hard core diameter b.

D. Mean Square Radius of Gyration

The mean square radius of gyration $\langle R^2_G \rangle$ is a useful measure of the size of a polymer chain and can be found experimentally from light scattering measurement. In chapter 4 it was shown that the mean square radius of gyration was given by

$$\langle R^2_G \rangle = (a^2/2N^2) \sum_i \sum_j \langle \rho^2_{ij} \rangle . \qquad (4.15)$$

Thus, in order to find the mean square radius of gyration, it is necessary to know the mean square distance $\langle \rho^2_{ij} \rangle$ between any two points ij of the chain. Unfortunately, the equations developed in this chapter from the PY approximation are for the function $Z_{1N}(\rho_{1N})$, which leads naturally to the mean square end-to-end distance $\langle \rho^2_{1N} \rangle$. In order to calculate $\langle \rho^2_{ij} \rangle$, it is necessary to deal with the function $Z_{ij}(\rho_{ij})$, the restricted partition function for a chain of N subsystems with subsystems i and j held fixed. It is possible to generalize our previous
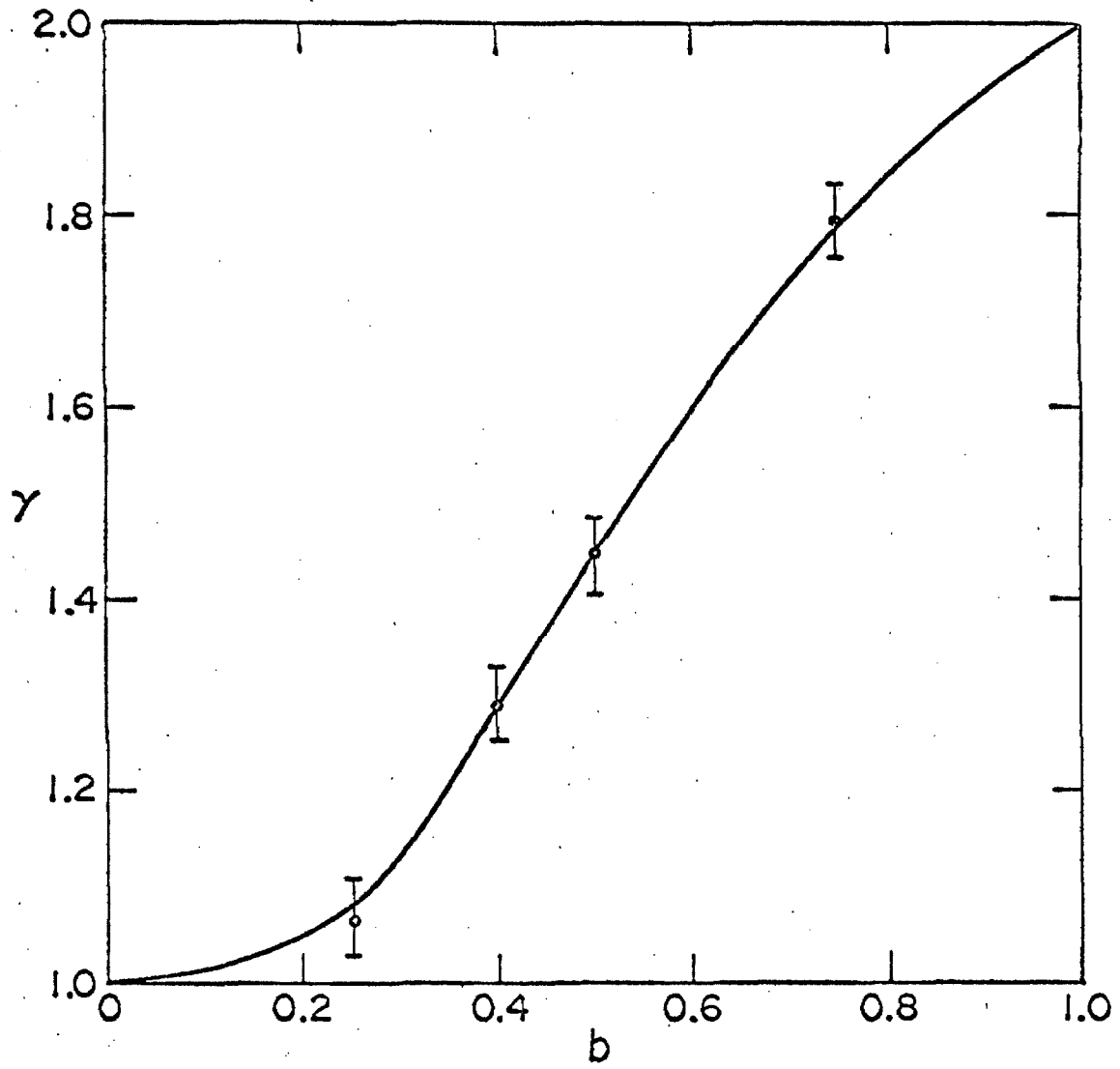
Fig. (8.2)
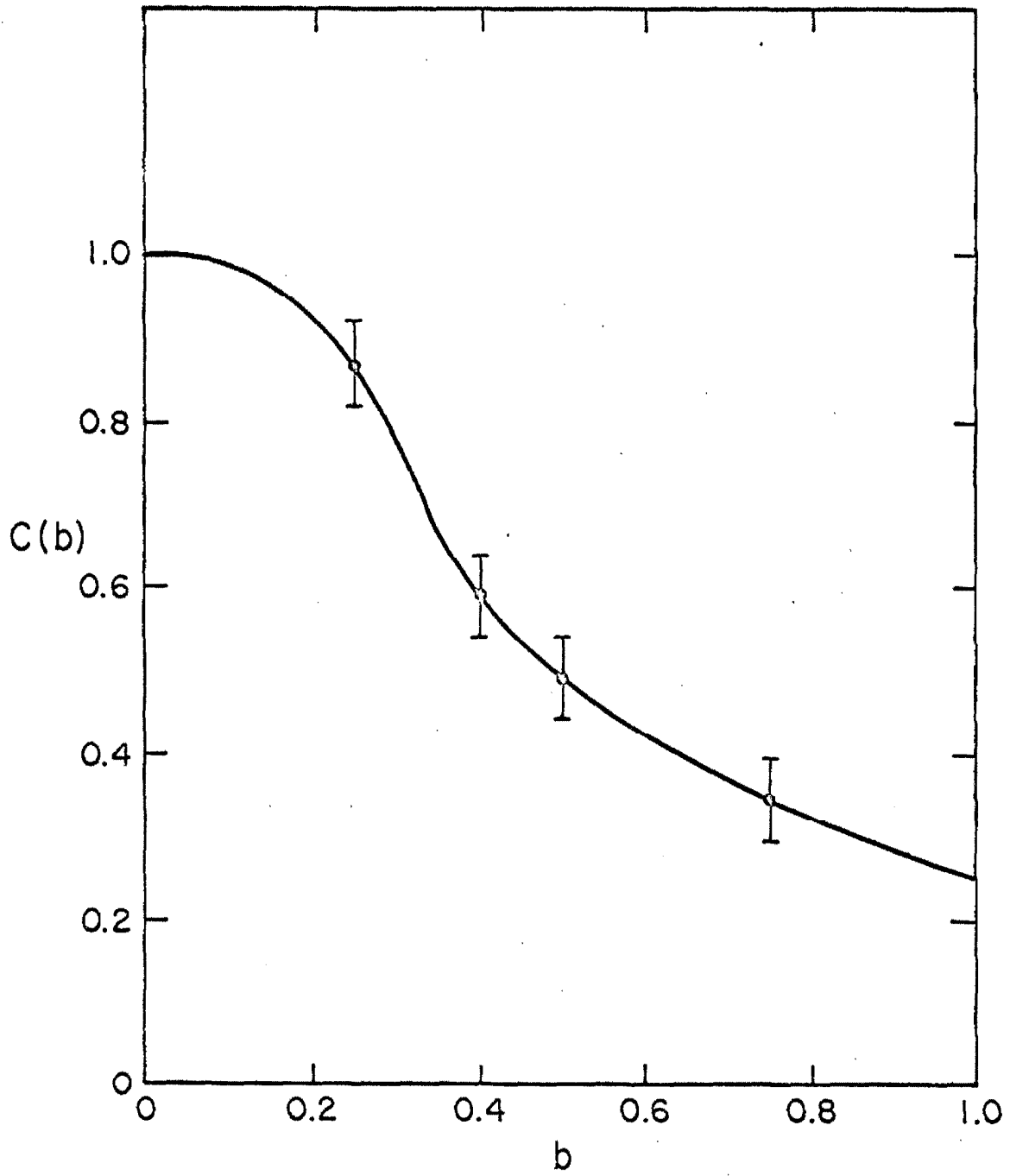Exponent in $\langle \rho^2_{1N} \rangle = Cn^{\gamma}$
as a function of b.

Fig. (8.3)
Coefficient in $\langle \rho^2_{1N} \rangle = Cn^{\gamma}$
as a function of b.

equations to this case. The generalizations of Eqs. (7.19), (7.21a) and (7.21b) are

$$Z_{ij}(N;\lambda) = (1 + \lambda h_{ij}) \sum_i \zeta_i(\rho_{ij},N)\lambda^i$$

$$N_{ij}(N;\lambda) = \sum_i \nu_i(\rho_{ij},N)\lambda^i$$

$$E_{ij}(N;\lambda) = \sum_i \epsilon_i(\rho_{ij},N)\lambda^i.$$

The symbols have the same meaning as before except that arbitrary sub-systems i and j rather than 1 and N are held fixed. The equivalent of Eq. (7.23) can be written and the PY approximation Eq. (7.24) can be made. This leads finally to an integro-difference equation for $Z_{ij}(N)$ of the same form as Eq. (7.29) for $Z_{1N}(\rho_{1N})$. Making the substitution

$$t_{ij}(N) = Z_{ij}(N)/H_{ij}, \tag{8.32}$$

leads to the generalization of Eq. (8.2)

$$t_{ij}(N) = \int t_{ii+1}(i + 1)t_{i+1j}(N - i)H_{i+1N}d\vec{\rho}_{i+1}$$

$$- \int h_{ij-1}t_{ij-1}(j - 1)t_{j-1j}(N - j + 2)d\vec{\rho}_{j-1}$$

$$- \sum_{k=i+2}^{j-2} \int h_{ik}t_{ij}(k)t_{kj}(N - k + 1)H_{kj}d\vec{\rho}_k. \tag{8.33}$$

When i = 1 and j = N, Eq. (8.33) reduces to Eq. (8.2). Eq. (8.33) is a partial integro-difference equation in the variables i, j, and N. Its solution will not be attempted here.

If the assumption is made that the ends of the chain (1 - i, j - N), do not interact with each other or the middle of the chain

(j - i), then the solution to Eq. (8.33) can be found by taking the
solution to Eq. (8.2) and replacing N by $|j - i|$. The accuracy of this
approximation obviously depends on the magnitude of $|j - i|$, becoming
exact as $|j - i|$ approaches N. With this assumption, $<\rho^2_{ij}>$ can be
written approximately as

$$<\rho^2_{ij}> \approx C(b)|j - i|^{\gamma(b)}, \qquad (8.34)$$

where $C(b)$ and $\gamma(b)$ are plotted in Figs. (8.2) and (8.3) respectively.

From Eq. (4.15), the mean square radius of gyration becomes,

$$<R^2_G> \approx (Ca^2/2N^2) \sum_i \sum_j |j - i|^\gamma \qquad (8.35)$$

The summations are now approximated by integrals

$$<R^2_G> = (Ca^2/N^2) \int_i^N \int_{j+1}^N (y - x)^\gamma dxdy.$$

The integrations are easily performed to give

$$<R^2_G> \approx Ca^2N^\gamma[(1 + \gamma)(2 + \gamma)]^{-1}. \qquad (8.36)$$

When b = 0, then C = γ = 1 and the mean square radius of gyration becomes

$$<R^2_G> = Na^2/6,$$

which agrees with the result obtained in chapter 4 for the non-excluded
volume chain. It is interesting to note that with the assumption made
here, the mean square end-to-end distance and radius of gyration are both
proportional to the chain length raised to the same power.

E. Graphs in the Percus-Yevick Type Approximation

In Appendix V it was shown that the number of graphs C_N in the restricted partition function $Z_{1N}(\rho_{1N})$ is given by

$$C = 2^{(N-1)(N-2)/2}. \tag{8.37}$$

The analog of the Percus-Yevick approximation Eq. (7.24), if used successively, accounts for all nodal graphs N_{1N} and those elementary graphs E_{1N} which are formed by adding an h_{1N}-bond to the nodal graphs of chain length N. In order to obtain some measure of the error involved when the Percus-Yevick type of approximation is applied to a polymer chain, it would be useful to determine the number of graphs P_N that are not accounted for. Let a_N and b_N be the number of nodal and elementary graphs respectively for a chain of N subsystems. The number of graphs that are not accounted for is then

$$P_N = C_N - 2a_N \tag{8.38}$$

$$= b_N - a_N.$$

Because of the property of nodal graphs discussed in chapter 7, it is possible to synthesize the nodal graphs from simpler graphs. Following a procedure analogous to that used in chapter 7 for writing nodal graphs in terms of elementary graphs, it is possible to show that

$$a_N = C_{N-1} + b_{N-1} + \sum_{i=3}^{N-2} b_i C_{N+1-i} \quad \text{for } N \geq 3. \tag{8.39}$$

This relation can be verified for small N by direct counting of graphs (see Table 8.3). Since the sum of the nodal and elementary graphs is the total number of graphs C_N,

$$a_N + b_N = C_N$$

we can rewrite Eq. (8.39) in terms of the number of elementary graphs b_N.

$$b_N = C_N - C_{N-1} - b_{N-1} - \sum_{i=3}^{N-2} b_i C_{N+1-i} \tag{8.40}$$

for $N \geq 3$

Table 8.3

Numbers of graphs for small N by direct counting.

N	a_N	b_N	C_N
0	0	0	0
1	0	1	1
2	0	1	1
3	1	1	2
4	3	5	8
3	15	49	64

Using the values of b_0, b_1 and b_2 from Table 8.3, it is possible to rewrite Eq. (8.40) in the form

$$\sum_{i=0}^{N} b_i C_{N+1-i} = 2C_N \text{ for } N \geq 2$$

$$= 1 \quad \text{for } N = 1 \tag{8.41}$$

$$= 0 \quad \text{for } N = 0.$$

Eq. (8.41) is a $(N-1)$th-order difference equation for the number of elementary graphs b_N. The left hand side of Eq. (8.41) is in the form of a convolution. For this reason a generating function approach or the Mikusinski calculus (36) approach might provide a solution for this difference equation. A solution has been obtained by this method, however it does not satisfy the required initial conditions.

An alternative approach is to view Eq. (8.41) as a system of N linear equations for the N unknowns b_i. From the theory of linear equations the solution b_N to Eq. (8.41) is given by

$$b_N = \Delta'_N / \Delta_N. \tag{8.42}$$

Δ is an infinite triangular determinant

$$\Delta_N = \begin{vmatrix} C_1, & 0, & 0, & 0, & \ldots \\ C_2, & C_1, & 0, & 0, & \ldots \\ C_3, & C_2, & C_1, & 0, & \ldots \\ & & \vdots & & \\ C_{N+1}, & C_N, & \ldots \end{vmatrix},$$

and Δ' is given by

$$\Delta'_N = \begin{vmatrix} c_1, & 0, & 0, & \ldots 1 \\ c_2, & c_1, & 0, & \ldots 2c_1 \\ c_3, & c_2, & c_1, & \ldots 2c_2 \\ & & \vdots & \\ c_{N+1}, & c_N, & \ldots & \end{vmatrix} .$$

The triangular determinant Δ_N collapses to the very simple form

$$\Delta_N = (c_1)^{N+1} = 1. \tag{8.43}$$

The $(N + 1)$st row of Δ'_N can be shifted to the first row by the standard rules for determinants. The number of elementary graphs b_N can finally be written as the infinite determinant

$$b_N = \Delta'_N$$

$$= (-1)^N \begin{vmatrix} 1, & c_1, & 0, & 0, & \ldots \\ 2c_1, & c_2, & c_1, & 0, & \ldots \\ 2c_2, & c_3, & c_2, & c_1, & \ldots \\ \vdots & & & & \\ 2c_N, & c_{N+1}, & \ldots & & \end{vmatrix} . \tag{8.44}$$

It does not appear that the infinite determinant of Eq. (8.44) can be evaluated easily. We can, however, obtain an approximate solution to Eq. (8.41) using a method of successive approximations. If Eq. (8.41) is solved for b_N in terms of the lower-order b_i we obtain

$$b_N = c_N - c_{N-1} - c_{N-2} - \sum_{i=4}^{N-1} b_i c_{N+1-i}, \tag{8.45}$$

where some of the values from Table 8.3 have been substituted. In order

to guess at the general form of the solution, it is instructive to successively calculate the b_N in terms of the C_i for small N. It can be demonstrated from the structure of Eq. (8.45) that in general b_N will be of the form

$$b_N = C_N - 2C_{N-1} + \text{terms in } C_i(i \leq N - 2). \qquad (8.46)$$

We will use these leading terms as a zero-order solution to Eq. (8.45).

$$b_N^{(0)} = C_N - 2C_{N-1} \qquad (8.47)$$

Define a sequence of functions $b_N^{(k)}$, k = 1, 2, ... by the equation

$$b_N^{(k)} = C_N - C_{N-1} - C_{N-2} - \sum_{i=4}^{N-1} b_i^{(k-1)} C_{N+1-i} . \qquad (8.48)$$

It will be assumed that the sequence $b_N^{(k)}$ converges to b_N, as N → ∞. No proof of this will be given here. The first-order approximation is then given by

$$b_N^{(1)} = C_N - C_{N-1} - C_{N-2} - \sum_{i=4}^{N-1} (C_i - 2C_{i-1})C_{N+1-i} . \qquad (8.49)$$

The values of b_N, $b_N^{(0)}$ and $b_N^{(1)}$ were calculated from Eqs. (8.45), (8.47) and (8.49) respectively for N = 1 to 8. These results appear in Table 8.4. It can be seen from the Table that $b_N^{(1)}$ is an excellent approximation to b_N and N becomes large. In fact, as N → ∞, b_N, $b_N^{(0)}$ and $b_N^{(1)}$ all approach C_N.

The number of graphs P_N that are not counted when the Percus-Yevick approximation is applied successively can now be computed.

Table 8.4

A comparison of approximations to b_N.

N	C_N	b_N	$b_N^{(0)}$	$b_N^{(1)}$
0	0	0	0	0
1	1	1	1	1
2	1	1	-	1
3	2	1	-	1
4	8	5	4	5
5	64	49	48	50
6	1,024	843	896	896
7	32,768	30,649	30,720	30,656
8	2,097,152	2,030,213	2,031,616	2,030,216

From Eqs. (8.38) and (8.49) we obtain

$$P_N = C_N - 2C_{N-1} - 2C_{N-2} - 2 \sum_{i=4}^{N-1} (C_i - 2C_{i-1})C_{N+1-i}. \qquad (8.50)$$

The fraction of graphs ξ that are not counted is thus

$$\xi = P_N/C_N \qquad (8.51)$$

$$= C_N^{-1} [C_N - 2C_{N-1} - 2C_{N-2} - 2 \sum_{i=4}^{N-1} (C_i - 2C_{i-1})C_{N+1-i}].$$

For large N this becomes

$$\xi = C_N^{-1} [C_N - 4C_{N-1} + 0(C_{N-2})].$$

Using the definition of C_N in Eq. (8.37) in the above equation leads to

$$\xi = 1 - 2^{-(N-4)} \text{ as } N \to \infty. \qquad (8.52)$$

Thus as the chain length N increases to infinity, the fraction of graphs not counted in the theory approaches unity. If all graphs contributed equally to Z_{1N}, then the Percus-Yevick type theory would not be valid as the polymer chain length approaches infinity. It is known from chapter 5 that all graphs do not contribute equally to Z_{1N}. In the theory of liquids the Percus-Yevick approximation appears to count the "right combination" of graphs. If attempts are made to improve the PY approximation by including more graphs, agreement with experiment becomes less satisfactory. It is probable that a similar situation exists when the Percus-Yevick approximation is applied to a polymer.

9. DISCUSSION

In the preceding chapters I have investigated various theoretical approaches for the calculation of the configurational statistics of a model, self-interacting polymer chain. I will now briefly discuss some experimental methods for studying the configuration of polymer chains . I will then discuss the theoretical results in more detail.

A. Experimental Techniques

Unfortunately, it is not possible to isolate a single polymer chain in order to measure its size. We can obtain information about the size of polymers by measuring the properties of dilute polymer solutions. In dilute solution intermolecular effects are usually small, but solvent-polymer interactions are important. The average dimensions of a polymer chain are markedly dependent on the particular solvent that is used. The solvent interactions tend to compress the size of the chain and the intramolecular (excluded volume) interactions tend to expand the chain. A solvent in which these opposing tendencies exactly balance each other is called a theta-solvent. More precisely, a theta-solvent for a particular polymer at a given temperature is one in which the polymer solute is governed by random walk (non-excluded volume) statistics. Some of the measurements on polymer solutions which lead to information about the average size of the polymer solute are osmotic pressure, intrinsic viscosity and light scattering measurements. For a thorough discussion of this topic the reader is referred to Tanford (37).

Osmotic pressure

Osmotic pressure is the most sensitive measurement available for determination of the chemical potential change of the solvent due to the solute. The osmotic pressure can be expressed as a virial expansion

$$\Pi C_1^{-1} = RT[M_2^{-2} + BC_2 + CC_2^2 + \ldots],\tag{9.1}$$

where Π is the osmotic pressure, C_1 the concentration of solvent, and M_2 the molecular weight and C_2 the concentration respectively of the solute. The second virial coefficient B is due to intermolecular effects. This second virial coefficient has been theoretically related to the average size of the polymer chains. The expansion coefficient α, is given by

$$\alpha^2 = <\rho^2_{1N}>/<\rho^2_{1N}>_0,$$

where $<\rho^2_{1N}>_0$ is the mean square end-to-end distance for a polymer in a theta-solvent. α can be obtained by measuring the second virial coefficient. Measurements of this type show that $\alpha = CM_2^{.05-.10}$ depending on the solvent.

Intrinsic viscosity

The specific viscosity is defined by

$$\eta_{sp} = (\eta - \eta_1)/\eta_1\tag{9.2}$$

where η is the viscosity of the solution and η_1, the viscosity of the

pure solvent. The intrinsic viscosity [η] is an important quantity of interest in macromolecular solutions. It is defined by

$$[\eta] = \lim_{C_2 \to 0} (\eta_{sp}/C_2) \qquad (9.3)$$

where C_2 is the concentration of solute. From theoretical considerations, the intrinsic viscosity can be related to the size of the polymer solute which depends on the expansion coefficient α, the molecular weight and the segment size (a). Intrinsic viscosity measurements on various polymers with different solvents give results similar to those obtained from osmotic pressure measurements.

Light scattering

In the light scattering technique the intensity of scattered radiation is measured as a function of the scattering angle θ. By extrapolation of the scattering function

$$P(\theta) = \frac{\text{Scattering intensity}}{\text{Scattered intensity without interference}}$$

to zero concentration and zero angle θ, it is possible to obtain the mean square radius of gyration $<R_G^2>$ of the solute molecules. This measurement is useful because it gives an absolute value of $<R_G^2>$ independent of any theoretical model. These measurementes show that for typical flexible polymers in solution (37),

$$<R_G^2> \propto M_2^{1.0-1.2}$$

where the exponent depends on the solvent used.

Computer generated chains

Many authors (38-49) have generated random walks on various

lattices with the aid of computers. Walks that cross back over them-

selves are discarded. In these computer experiments, measurement of

the intramolecular excluded volume effects, independent of intermole-

cular and solvent effects, can be achieved. There is some question,

however, whether these lattice results can be applied to a chain in

continuous space. Calculations on various lattices indicate that

$$<\rho^2_{1N}> \propto n^{1.2-1.33},$$

where n is the number of lattice steps.

B. Discussion of Theoretical Results

Short chains

In chapter 4, the configuration of two and three segment chains

was computed from Eq. (3.12) exactly, for the hard core potential. The

integrations were accomplished by introduction of bipolar coordinates

into Z_{13} and tripolar coordinates into Z_{14} . Although these calculations

are of no value in predicting the configuration of real polymer chains

which are much longer, these represent the only cases in which Eq. (3.12)

has been solved exactly for a nontrivial potential. The mean square

end-to-end distances computed from Z_{13} and Z_{14} are

$$<\rho^2_{13}> = (16 - b^4)/2(4 - b^2) \qquad (9.4a)$$
$$= n^{1.32} \text{ for } b = 1$$

$$<\rho^2_{14}> = n^{1.33} \text{ for } b = 1. \tag{9.4b}$$

These results provide a valuable check on approximate theories in the limit of short chains.

Cluster expansion

In chapter 5, a cluster expansion was developed for the restricted partition function $Z_{1N}(\rho_{1N})$. If terms higher than first-order in this expansion are neglected, the mean square end-to-end distance can be calculated analytically in the limit of small hard core diameter b. This result is identical to the well-known first-order perturbation theory obtained by many authors.

The first-order term in the cluster expansion was computed numerically by several methods. The results were used to build up higher-order terms of "isolated" topology. It was seen that for this particular topology, higher-order graphs become increasingly important for large chain lengths. If only these isolated graphs are included in the cluster expansion, it was seen that the resulting mean square end-to-end distance deviated greatly from linearity when $\log <\rho^2_{1N}>$ was plotted versus $\log n$. It is apparent then that graphs of more complicated topology are important in the higher-order terms of the cluster expansion for large N. It does not appear practical to insert integrals of more complicated topology into the cluster expansion of Z_{1N}, because both the variety of topologies and difficulty in the calculation of the integrals increase tremendously for long chains.

Percus-Yevick analog

In chapters 7 and 8, the analog of the Percus-Yevick equation was obtained for a polymer chain. An analytical solution was obtained for the hard core potential when b = 1 and numerical solutions were obtained for values of b intermediate between zero and one.

Small N: The mean square end-to-end distance predicted by the Percus-Yevick approximation for b = 1 is given by Eq. (8.10). For the two and three segment chains this equation gives

$$<\rho^2_{13}> = 2.50 \quad \text{(PY approximation)}$$

$$<\rho^2_{14}> = 4.50 \quad \text{(PY approximation)}.$$

These results compare very favorably with the exact results obtained in chapter 4.

$$<\rho^2_{13}> = 2.50 \quad \text{(exact)}$$

$$<\rho^2_{14}> = 4.31 \quad \text{(exact)}$$

This agreement is not surprising since the Percus-Yevick approximation counts all graphs for N = 3, and all but two when N = 4.

Small b: If b is put equal to zero into the Percus-Yevick type integral Eq. (8.2), a piecewise analytic solution is obtained which corresponds exactly to the exact solution of the random walk problem given in Treloar (41). Thus the Percus-Yevick solution correctly reduces

to the non-excluded volume solution when b = 0.

Many authors have obtained a so-called perturbation expansion for the mean square end-to-end distance, which is good for small values of the hard core potential (5-8). These expansions were discussed in chapters 2 and 5. Fixman's second-order theory gives

$$<\rho^2_{1N}> = n[1 + 4z/3 - (16/3 - 28\pi/3)z^2 + \ldots]$$ (5.27)

where $\quad z = (6n/\pi)^{1/2}b^3.$

If n and b are small enough, this expansion converges rapidly so that terms of $O(z^3)$ are negligible. Eq. (5.7) is plotted in Fig. (9.1) for b = .25 and .40 in the range of n where rapid convergence exists. Also plotted in this figure are the numerical results obtained by solving Eqs. (8.14) and (8.17) (see Fig. 8.1). It can be seen from Fig. (9,1) that there is excellent agreement between our results using the Percus-Yevick method and previously obtained results for small b.

Eq. (5.27) is exact in the limit as b → 0. Evaluation of the derivative of $<\rho^2_{1N}>$ with respect to b at b = 0 gives zero. This agrees with the observed zero slope γ and C versus b in Figs. (8.2) and (8.3).

Comparison with experiment: As was indicated in the first part of this chapter, experiments on polymer solutions and computer experiments on lattices show that

$$<\rho^2_{1N}> = Cn^\gamma$$
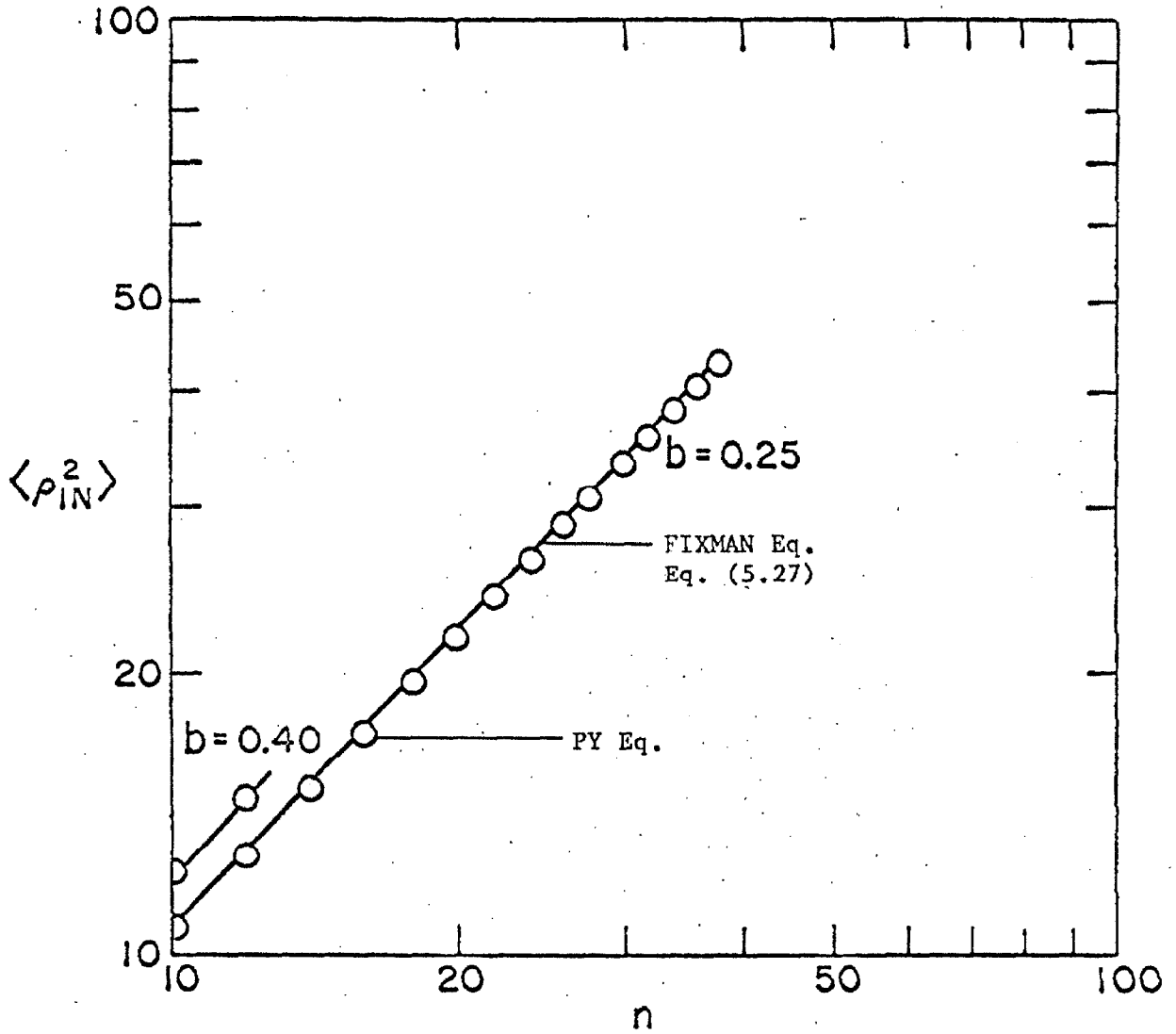
Fig. (9.1)
Comparison of the PY theory to the second-order
perturbation theory of Fixman in the
limit of small b.

where $\gamma \simeq 1.2$ to 1.3 and n is proportional to the molecular weight. Because our theory contains a parameter b, it is difficult to make an unambiguous comparison with experiment. By choosing our results from the Percus-Yevick equation to give the correct value for γ (see Fig. 8.2), one can see that $b \simeq .4.$ This means that the actual hard core diameter is .4 times the segment length a (see Fig. 9.2).
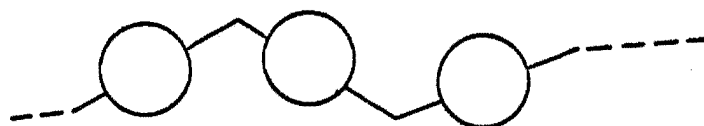
Fig. (9.2)
A portion of a chain with $b = .40$.

This value of b seems quite reasonable since the hard core diameter is obviously an oversimplification of the true repulsive potential between segments. An elliptically symetric type of potential would probably be a more realistic choice.

The results of the self-consistent field approach used by Edwards, Reiss and Yamakawa and discussed in chapter 6 gives

$$<\rho^2_{1N}> \propto n^{4/3} \quad \text{(Reiss)}$$

$$<\rho^2_{1N}> \propto n^{6/5} \quad \text{(Edwards, Yamakawa)}$$

In these treatments the hard sphere parameter was suppressed by taking limits. Unfortunately, the self-consistent field approach is not easily expressed in terms of graphs, so a comparison between our theory and the

self-consistent field theory is not possible on this basis.

C. Suggestions For Further Work

The Percus-Yevick approach is a promising new method for treatment of the excluded volume problem. It is a desirable alternative for the cluster expansion and, unlike the self-consistent field approach, is a well-defined approximation in terms of graphs. I think the following suggestions are worthwhile topics for future research in this field.

1. The Percus-Yevick integral equation (8.2) could possibly be simplified by passing to a Fokker-Planck type of differential equation.

2. Improvements on the Percus-Yevick approximation should be sought. For fluids, Percus has shown (41) that by expanding the proper functionals in a functional Taylor expansion, the Percus-Yevick integral equation can be obtained by truncating the expansion at the first term. The logical next higher-order approximation is obtained by including the next term in the expansion. This procedure could possibly be extended to the polymer problem.

3. Experimental determination of the intramolecular potential of a polymer chain would be worthwhile. This might be achieved by experimentally determinimg the complete Z_{1N}, rather than just the second moment $<\rho_{1N}^2>$. A possible method for this might be to chemically "tag" the ends of polymer chains with heavy atoms such as Ag atoms. A scat-

tering experiment on such a solution of polymer molecules would lead to a radial distribution function for the ends of the chains. This distribution function would be proportional to Z_{1N} . Krigbaum (42) has suggested a variation of this method for measuring the sizes of polymer chains in bulk.

APPENDIX I

SIMPLIFICATION OF EQ. (4.5)

Eq. (4.2a) is the Fourier transform of the δ-function.

$$f(k) = \int \delta(\rho - 1)\exp(-i\vec{k}\cdot\vec{\rho})\,d\vec{\rho} \qquad (4.2a)$$

Introduce spherical coordinates for $d\vec{\rho}$ and choose the z-axis to coincide with the $\vec{k}$ vector which is fixed in the integration (see Fig. A.1).
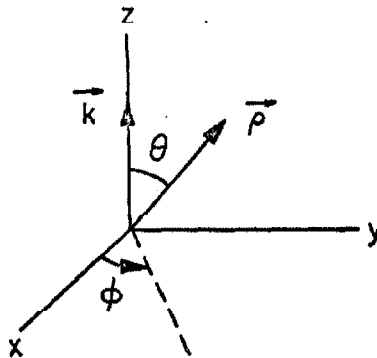
Fig. (A.1)
Orientation of the spherical coordinate system.

The scalar product in the equation can then be written as

$$\exp(-i\vec{k}\cdot\vec{\rho}) = \exp(-ik\rho \cos\theta). \qquad (A.1)$$

Making the substitution,

$$x = ik\rho \cos\theta$$

$$\qquad (A.2)$$

$$dx = -ik\rho \sin\theta \, d\theta,$$

Eq. (4.2a) now becomes,

$$kf(k) = 2\pi i \int_0^\infty \delta(\rho - 1)\rho d\rho \int_{-ik\rho}^{ik\rho} \exp(-x)dx. \qquad (A.3)$$

The integrations are easily performed to give

$$f(k) = 4\pi(\sin k/k). \qquad (A.4)$$

This result is now substituted into Eq. (4.5).

$$8\pi^3 Z_{1N} = (4\pi)^{N-1} \int (\sin k/k)^{N-1} \exp(i\vec{k}\cdot\vec{\rho}_{1N})d\vec{k}$$

A spherical coordinate system, oriented with the z-axis along $\vec{k}$ is introduced for $d\vec{k}$. By following a procedure similar to the above, it is possible to integrate over the angular variables. The result of this integration is,

$$2\pi^2 Z_{1N} = (4\pi)^{N-1} \int_0^\infty (\sin k/k)^{N-1} k^2 (\sin k\rho_{1N}/k\rho_{1N})dk. \qquad (4.6)$$

APPENDIX II

MEAN SQUARE END-TO-END DISTANCE FROM

THE FOURIER TRANSFORM OF $Z_{1N}(\rho_{1N})$

From Eq. (3.8) we have for the mean square end-to-end distance

$$<\rho^2_{1N}> = \int \rho^2 Z_{1N}(\rho)\,d\vec{\rho} / \int Z_{1N}(\rho)\,d\vec{\rho}.$$

Introducing spherical coordinates and integrating over angular variables gives,

$$<\rho^2_{1N}> = \int_0^\infty \rho^4 Z_{1N}(\rho)\,d\rho / \int_0^\infty \rho^2 Z_{1N}(\rho)\,d\rho. \qquad (A.5)$$

The Fourier transform of $Z_{1N}(\rho_{1N})$ is defined to be,

$$\bar{Z}_{1N}(k) = \int Z_{1N}(\rho)\exp(-i\vec{k}\cdot\vec{\rho})\,d\vec{\rho}.$$

If spherical coordinates are introduced for $\vec{\rho}$, the angular integrations above can be performed (see Appendix I) to give,

$$\bar{Z}_{1N}(k) = 4\pi \int_0^\infty Z_{1N}(\rho)(\sin k\rho/k\rho)\rho^2\,d\rho. \qquad (A.6)$$

$(\sin k\rho)$ in Eq. (A.6) is now expanded in a power series to yield

$$\bar{Z}_{1N}(k) = 4\pi \int_0^\infty Z_{1N}(\rho)[\rho^2 - (k\rho)^2/6 + \ldots]\,d\rho. \qquad (A.7)$$

If the function $Z_{1N}(\rho)$ is such that integrals of the form

$$\int_0^\infty \rho^m Z_{1N}(\rho)\,d\rho$$

converge for all m, then the summation and integration can be inter-changed in Eq. (A.7). Thus, for this case

$$\bar{Z}_{1N}(k) = 4\pi \int_0^\infty \rho^2 Z_{1N}(\rho)\,d\rho - 4\pi k^2/6 \int_0^\infty \rho^4 Z_{1N}(\rho)\,d\rho + \ldots . \qquad (A.8)$$

Comparison of Eqs. (A.8) and (A.5) indicates that

$$<\rho^2_{1N}> = \frac{\text{coeff}(-k^2/6) \text{ in } \bar{Z}_{1N}(k)}{\text{coeff}(1) \text{ in } \bar{Z}_{1N}(k)}$$

for sufficiently well-behaved functions $Z_{1N}(\rho_{1N})$.

As an example consider the case of no excluded volume (see chapter 4). From Eqs. (4.5) and (A.4), we have

$$\bar{Z}_{1N}(k) = [f(k)]^{N-1} = (4\pi \sin k/k)^{N-1}. \qquad (A.9)$$

This can be expanded in a Maclaurin series to give

$$\bar{Z}_{1M}(k) = (4\pi)^{N-1}[1 - (N - 1)k^2/6 + \ldots] .$$

The mean square end-to-end distance can now be computed from the above to give

$$<\rho^2_{1N}> = (N - 1) = n.$$

This is the same result that was obtained in chapter 4 by direct integration using the Gaussian approximation to $Z_{1N}(\rho_{1N})$.

APPENDIX III

JACOBIAN FOR BIPOLAR COORDINATES

The bipolar coordinate system is shown in Fig. (A.2).
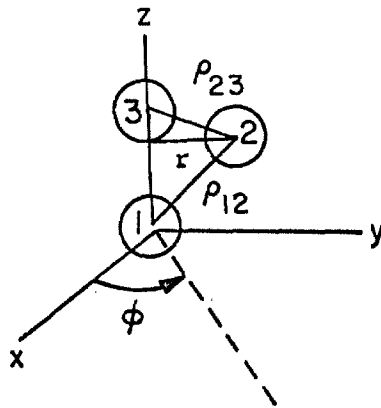
Fig. (A.2)
Bipolar Coordinates

Consider the spheres 1 and 3 to be fixed. Erect a cartesian coordinate system with its origin at sphere 1 and oriented with sphere 3 on the z-axis. We will permit ρ_{12}, ρ_{23} and the angle of rotation ϕ to locate the position of sphere 2 in space.

To find the Jacobian for the transformation it is convenient to introduce the cylindrical coordinates z, r, ϕ (see Fig. A.2). The derivatives of the cartesian coordinates with respect to the bipolar coordinates form a matrix whose determinant is the desired Jacobian. Thus,

$$(\partial \xi_i / \partial \beta_j) = \sum_{k=1}^{3} (\partial \xi_i / \partial \eta_k)(\partial \eta_k / \partial \beta_j)$$

where:

$$\xi_1 = x \quad \eta_1 = r \quad \beta_1 = \rho_{12}$$

$$\xi_2 = y \quad \eta_2 = z \quad \beta_2 = \rho_{23}$$

$$\xi_3 = z \quad \eta_3 = \phi \quad \beta_3 = \phi .$$

Since the determinant of the product of two matrices is given by the product of their determinants,

$$J_B = \partial(xyz)/\partial(\rho_{12}\rho_{23}\phi)$$

$$= \det(\partial\xi_i/\partial\eta_k)\det(\partial\eta_k/\partial\beta_j) .$$

(A.10)

In order to find the derivatives $\partial\eta_k/\partial\beta_j$, let us express the cylindrical coordinates in terms of the bipolar coordinates. From Fig. (A.2) we have,

$$(\rho_{13} - z)^2 = r^2 + \rho^2_{23}$$

$$z^2 = r^2 + \rho^2_{12} .$$

This pair of equations can be solved for z and r.

$$z = (\rho^2_{13} - \rho^2_{23} + \rho^2_{12})/2\rho_{13}$$

$$r^2 = \rho^2_{12} - [(\rho^2_{13} - \rho^2_{23} + \rho^2_{12})/2\rho_{13}]^2$$

The appropriate derivatives can be computed which leads to

$$\det(\partial \eta_k / \partial \beta_j) = \rho_{12}\rho_{23}/\rho_{13}r. \tag{A.11}$$

The cartesian coordinates can be easily expressed in terms of the cylindrical coordinates.

$$x = r \cos \phi \quad y = r \sin \phi \quad z = z$$

The other determinant then becomes,

$$\det(\partial \xi_i / \partial \eta_k) = r(\cos^2\phi + \sin^2\phi) = r. \tag{A.12}$$

The Jacobian for bipolar coordinates can be found from Eqs. (A.10), (A.11) and (A.12).

$$J_B = \rho_{12}\rho_{23}/\rho_{13} \tag{A.13}$$

APPENDIX IV

JACOBIAN FOR TRIPOLAR COORDINATES

The tripolar coordinate system is shown in Fig. (4.2). Spheres 1, 3, and 4 are to be held fixed. The location of sphere 2 is specified by ρ_{12}, ρ_{23} and ρ_{24}. A cartesian coordinate system is erected with sphere 1 at the origin, sphere 4 along the x-axis and sphere 3 in the xy plane. ρ_{12} is given by the obvious relation

$$\rho^2_{12} = x^2 + y^2 + z^2. \tag{A.14}$$

From the law of cosines we can write,

$$\rho^2_{23} = \rho^2_{12} + \rho^2_{13} - 2\rho_{12}\rho_{13} \cos \gamma$$

where γ is the angle between ρ_{12} and ρ_{13}. Using spherical trigonometry, $\cos \gamma$ can be written as,

$$\rho_{12} \cos \gamma = x \cos \beta - y \sin \beta.$$

Substitution of this result into the previous equation yields,

$$\rho^2_{23} = \rho^2_{13} + x^2 + y^2 + z^2 - 2\rho_{13}x \cos \beta - 2\rho_{13} y \sin \beta. \tag{A.15}$$

The law of cosines can also be used to find ρ_{24}.

$$\rho^2_{24} = x^2 + y^2 + z^2 - 2\rho_{14} x + \rho^2_{14} \tag{A.16}$$

The Jacobian for tripolar coordinates is defined as

$$J_T = \partial(xyz)/\partial(\rho_{12}\rho_{23}\rho_{24})$$

$$= \det(\partial\xi_i/\partial\tau_j)$$

where the ξ_i are the cartesian components x, y, z and the τ_j are the tripolar coordinates $\rho_{12}\rho_{24}\rho_{23}$. The form of Eqs. (A.14), (A.15) and (A.16) suggests that the algebra will be simpler if one computes $(J_T)^{-1}$ instead of J_T directly.

$$J_T^{-1} = \det(\partial\tau_j/\partial\xi_i)$$

The required derivatives can be computed from Eqs. (A.14), (A.15) and (A.16).

$$J_T^{-1} = \begin{vmatrix} x/\rho_{12}, & y/\rho_{12}, & z/\rho_{12} \\ (x - \rho_{12}\cos\beta)/\rho_{23}, & (y - \rho_{13}\sin\beta)/\rho_{23}, & z/\rho_{23} \\ (x - \rho_{14})/\rho_{24}, & y/\rho_{24}, & z/\rho_{24} \end{vmatrix}$$

$$J_T^{-1} = \frac{-z\rho_{13}\rho_{14}\sin\beta}{\rho_{12}\rho_{23}\rho_{24}} \tag{A.17}$$

It is possible to express $\sin\beta$ in terms of the ρ's. Eqs. (A.15) and (A.16) can be solved for x and y. Substitution of these results into Eq. (A.14) leads to

$$z^2 \sin^2\beta = \rho^2_{12}(1 - \cos^2\beta)$$

$$- (\rho^2_{12} - \rho^2_{24} + \rho^2_{14})^2/4\rho^2_{14} - (\rho^2_{12} + \rho^2_{13} - \rho^2_{23})^2/4\rho^2_{13} \qquad \text{(A.18)}$$

$$+ 2(\rho^2_{12} + \rho^2_{13} - \rho^2_{23})(\rho^2_{12} - \rho^2_{24} + \rho^2_{14})\cos \beta/4\rho_{13}\rho_{14}.$$

$\cos \beta$ can be determined from the law of cosines.

$$\cos \beta = (\rho^2_{14} + \rho^2_{13} - \rho^2_{34})/2\rho_{13}\rho_{14} \qquad \text{(A.19)}$$

Eqs. (A.18) and (A.19) determine $\cos \beta$ in terms of the variables. The desired Jacobian is obtained from Eq. (A.17).

$$J_T = -\rho_{12}\rho_{23}\rho_{24}/Z \sin \beta\rho_{13}\rho_{14} \qquad \text{(A.20)}$$

APPENDIX V

NUMBER OF GRAPHS IN Z_{1N}

The number of graphs in Eq. (5.3) for Z_{1N} can easily be found in two steps.

1. Given a skeleton of N circles and (N - 1) δ-bonds, the number of available h-bonds M is given by the number of things taken two at a time minus the (N - 1) δ-bonds.

$$M = \binom{N}{2} - (N - 1) = (N - 1)(N - 2)/2$$

2. Any of the available h-bonds M may either be present or absent in a graph. The number of graphs in Eq. (5.3) is the number of possible combinations of h-bonds. This number is the same as the number of possible outcomes when a coin is flipped n times. Thus,

Number of graphs in $Z_{1N} = 2^M = 2^{(N-1)(N-2)/2}$

This result can be verified easily for short chains by direct counting.

APPENDIX VI

SIMPLIFICATION OF $y_{ij}(k)$ FOR THE HARD CORE POTENTIAL

The hard core potential implies that the function h_{ij} is

$$h_{ij} = 1 \text{ for } \rho_{ij} < b$$

$$h_{ij} = 0 \text{ for } \rho_{ij} > b.$$

Introducing this into Eq. (5.13) gives

$$\bar{kh}(k) = 4\pi \int_0^b \rho \sin k\rho \, d\rho$$

where the angular integrations have been performed using the method

of Appendix I. Integration by parts leads to the result

$$\bar{h}(k) = 4\pi(\sin kb - kb \cos kb)/k^3.$$

Using this result $y_{ij}(k)$ becomes,

$$2\pi^2 y_{ij}(k) = (4\pi)^{j-i} \int (\sin \ell/\ell)^{j-i} x^{-3}(\sin bx - bx \cos bx) d\vec{\ell}$$

where

$$x^2 = k^2 + \ell^2 - 2k\ell \cos \gamma$$

with γ the angle between $\vec{k}$ and $\vec{\ell}$. Introduction of spherical coordinates into the above equation produces the result

$$\pi k y_{ij}(k) =$$

$$(4\pi)^{j-i} \int_{0}^{\infty} (\sin \ell/\ell)^{j-i} \ell d\ell \int_{|k-\ell|}^{k+\ell} x^{-2}(\sin bx - bx)dx \ .$$

The integration over x can be done by parts to give

$$\pi k y_{ij}(k) = (4\pi)^{j-i} \int_{0}^{\infty} (\sin \ell/\ell)^{j-i} K_1(k, \ell, b)d\ell$$

where K_1 is defined in chapter 5.

APPENDIX   VII

CONVERSION OF $\sum_i \sum_j f(j - i)$ TO A SINGLE SUMMATION

Consider a series of the form

$$F(N) = \sum_{i=1}^{N-2} \sum_{j=i+2}^{N} f(j - i). \qquad (A.21)$$

Since the argument of f depends only on the difference (m = j - i), it is possible to change the above double summation to a single summation over m, provided an appropriate coefficient C(m) is included.

$$F(N) = \sum_{m=2}^{N-1} C(m) f(m)$$

C(m) can be found easily from Eq. (A.21) by changing one of the summing indices to m = j - i.

$$F(N) = \sum_{i=1}^{N-2} \sum_{m=2}^{N-i} f(m)$$

The order of the summation operations can be interchanged if the limits on the sums are adjusted to insure that m $\leq$ N - 1. This leads to

$$F(N) = \sum_{m=2}^{N-1} f(m) \sum_{i=1}^{N-m}$$

$$= \sum_{m=2}^{N-1} (N - m) f(m).$$

Hence the proper choice for C(m) is

$$C(m) = N - m$$

APPENDIX VIII

SUMMATION OF THE SERIES IN EQS. (5.29)

In chapter 5 the functions $\psi_0(N,\ell)$ and $\psi_1(N,\ell)$ arose.

$$\psi_0(N,\ell) = \sum_{m=2}^{N-1} (N - m)L^m \qquad (5.29a)$$

$$\psi_1(N,\ell) = \sum_{m=2}^{N-1} (N - m)(N - 1 - m)L^m \qquad (5.29b)$$

where

$$L = (\sin \ell/\ell).$$

Eq. (5.29a) can be put in the form

$$\psi_0(N,\ell) = N \sum_{m=2}^{N-1} L^m - L(d/dL) \sum_{m=2}^{N-1} L^m.$$

The summation $\sum_{m=2}^{N-1} L^m$ can be found easily from the geometric series.

$$\sum_{m=2}^{N-1} L^m = (L^2 - L^N)(1 - L)^{-1} \qquad (A.22)$$

This relation can be verified by expanding the denominator on the right

hand side for $L < 1$ and $L > 1$. Using L'Hospital's rule we have the limit

$$\lim_{L \to 1}[(L^2 - L^N)(1 - L)^{-1}] = N - 2 = \lim_{L \to 1} \sum_{m=2}^{N-1} L^m.$$

Thus Eq. (A.22) holds for all ℓ. Eq. (5.29a) now becomes

$$\psi_0(N,\ell) = L^2[N - 2 - L(1 - L^{N-2})(1 - L)^{-1}](1 - L)^{-1}$$

after performing the indicated differentiations.

Eq. (5.29b) can be summed in a similar manner. Expansion of the

(N - 1)(N - 1 - m) product in Eq. (5.29b) gives $\psi_1(N,\ell)$ in the form

$$\psi_1(N,\ell) = N(N - 1) \sum_{m=2}^{N-1} L^m - 2(N - 1)L(d/dL) \sum_{m=2}^{N-1} L^m$$

$$+ L^2(d^2/dL^2) \sum_{m=2}^{N-1} L^m .$$

Calculation of the required derivatives gives the result in Eq. (5.30).

The limit of $\psi_0(N,\ell)$ and $\psi_1(N,\ell)$ as $L \to 1$ can be found by invoking

L'Hospital's rule.

$$\lim_{L \to 1} \psi_0(N,\ell) = (1/2)(N - 1)(N - 2)$$

$$\lim_{L \to 1} \psi_1(N,\ell) = (1/3)(N - 1)(N - 2)(N - 3)$$

APPENDIX IX

EVALUATION OF $\Omega_0(b,m)$ AND $\Omega_1(b,m)$

In chapter 5 it was found that the first order corrective

term involved the functions Ω_0 and Ω_1 defined by

$$\Omega_0(b,m) = \int_0^\infty \exp(-m\ell^2/6)(1 - m\ell^4/180 + \ldots)K_2(k, \ell, b)d\ell \quad (5.34a)$$

$$\Omega_1(b,m) = \int_0^\infty \exp(-m\ell^2/6)(1 - m\ell^4/180 + \ldots)K_3(k, \ell, b)d\ell \quad (5.34b)$$

K_2 and K_3 are defined by Eq. (5.19). The integrals in Ω_0 are Fourier

sine and cosine transforms which are given by Bateman (29) as

$$\int_0^\infty \exp(-a\ell^2)(1 - m\ell^4/180)\ell^{-1} \sin \ell b d\ell = \quad (A.23)$$

$$(\pi/2)\mathrm{erf}(b/2a^{1/2}) + (m/180)(\pi/32)^{1/2}a^{-2}\exp(-b^2/4a)\mathrm{He}_3(b^2/2a)^{1/2}$$

$$\int_0^\infty \exp(-a\ell^2)(1 - m\ell^4/180)\cos \ell b d\ell = \quad (A.24)$$

$$(\pi/4a)^{1/2}\exp(-b^2/4a) - (m/180)(\pi^{1/2}/8)a^{-5}\exp(-b^2/4a)\mathrm{He}_4(b^2/2a)^{1/2},$$

where $\mathrm{He}_n(x)$ are the Hermite polynomials defined by

$$\mathrm{He}_n(x) = (-1)^m\exp(x^2/2)(d^n/dx^n)\exp(-x^2/2).$$

The first four Hermite polynomials can be computed to be

$$\mathrm{He}_0(x) = 1 \quad \mathrm{He}_1(x) = x \quad \mathrm{He}_2(x) = x^2 - 1$$

$$\mathrm{He}_3(x) = x^3 - 3x \quad \mathrm{He}_4(x) = x^4 - 6x^2 + 3.$$

$\Omega_0(b,m)$ can now be obtained from Eq. (5.34a) by using Eqs. (A.23) and (A.24).

$$\Omega_0(b,m) = (\pi/2)\text{erf}(3b^2/2m)^{1/2} -$$

$$(3\pi b^2/2m)^{1/2}\exp(-3b^2/2m)[1 + (20m)^{-1} + O(m^{-2})] \qquad (A.25)$$

$\Omega_1(b,m)$ can also be evaluated from Eq. (A.23) and (A.24), but we have the additional integral $\omega(b,m)$ to evaluate.

$$\omega(b,m) = \qquad\qquad\qquad\qquad\qquad\qquad\qquad\qquad (A.26)$$

$$\int_0^\infty \exp(-m\ell^2/6)(1 - m\ell^4/180 + \ldots)[(\sin \ell b/\ell^3) - (b \cos \ell b/\ell^2)]d\ell$$

This can be rewritten in the form

$$\omega(b,m) = \int_0^b \xi d\xi \int_0^\infty \exp(-m\ell^2/6)(1 - m\ell^4/180)\ell^{-1} \sin \xi\ell d\ell.$$

The inner integral is of the same form as Eq. (A.23). Thus

$$\omega(b,m) =$$

$$\int_0^b \xi d\xi\{(\pi/2)\text{erf}(3\xi/2m)^{1/2} - (3\pi\xi^2/2m)^{1/2}\exp(-3\xi^2/2m)[(20m)^{-1} + O(m^{-2})]\}.$$

$\omega(b,m)$ can now be found through integration by parts.

$$\omega(b,m) = (m\pi/3)[\text{erf}(3b^2/2m)^{1/2} - (2\pi)^{-1/2} \gamma(3/2,3b^2/2m)]$$

$$-\pi/120 + O(m^{-1})$$

where the incomplete gamma function is defined by,

$$\gamma(c + 1, x) = \int_0^x y^c \exp(-y) dy.$$

There is a recurrence formula (28) which relates the incomplete gamma functions $\gamma(c + 1, x)$ and $\gamma(c, x)$.

$$\gamma(c + 1, x) = c\gamma(c, x) - x^c \exp(-x)$$

Using this recurrence formula, $\omega(b,m)$ can be simplified.

$$\omega(b,m) = (\pi m/3)\{[(3b^2/4m) - (1/4)] \mathrm{erf}(3b^2/2m)^{1/2}$$

$$+ (1/2)(3b^2/2\pi m)^{1/2} \exp(-3b^2/2m)\} - (\pi/20) + O(m^{-1}). \qquad (A.27)$$

Using Eqs. (A.23), (A.24) and (A.27) we obtain the result

$$\Omega_1(b,m) =$$

$$(b/6)(b^2 + m)(3\pi/2m)^{1/2} \exp(-3b^2/2m) - (\pi m/12) \mathrm{erf}(3b^2/2m)^{1/2} + O(1).$$

APPENDIX   X

DEMONSTRATION OF APPROXIMATION EQ. (7.24)

FOR THE CASE $N = 4$.

Using Eq. (7.19), we can write $Z_{14}(\rho_{14};\lambda)$ in the graph formalism.

$$Z_{14}(\rho_{14};\lambda) = (1 + \lambda h_{14}) \sum_{i=0}^{2} \zeta_i(\rho_{14})\lambda^i$$

Similarly from Eq. (7.21b), $E_{14}(\rho_{14};\lambda)$ can be expanded as

$$E_{14}(\rho_{14};\lambda) = \sum_{i=1}^{3} \epsilon_i(\rho_{14})\lambda^i .$$

The graphs of the coefficients ζ_i and ϵ_i are given in Table A.1. The coefficients can now be calculated from approximation Eq. (7.24) by simply adding an h_{1N} bond across the $\zeta_{i-1}(\rho_{1N})$ graphs. These are also shown in Table A.1. It can be seen that all graphs except
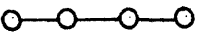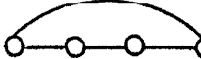
   are accounted for when $N = 4$. If the approximation is applied successively starting with $N = 3$, the graph
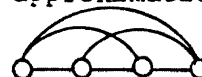
also will not be accounted for.

Table A.1
The coefficients obtained in the expansion of
$Z_{14}(\rho_{14};\lambda)$ and $E_{14}(\rho_{14};\lambda)$. The $\varepsilon_i(\rho_{14})$ calcu-
lated from approximation Eq. (7.24) are also shown.

$\underline{i}$	$\underline{\zeta_i(\rho_{14})}$	$\underline{\varepsilon_i(\rho_{14})}$	$\underline{\varepsilon_i(\rho_{14})}$ (approx. Eq. (7.24))

APPENDIX XI

METHOD OF EVALUATION OF THE SUMMATIONS IN EQ. (8.9)

$\phi_Z(\ell)$ is defined by,

$$\phi_Z(\ell) = \sum_{k=0}^{N-2} \binom{N-2}{k} z^k (-1)^k k^\ell.$$

Employing the binomial theorem, $\phi_Z(\ell)$ may be expressed as,

$$\phi_Z(\ell) = \frac{d^\ell}{d(\ell n\ Z)^\ell} (1 - Z)^{N-2}. \qquad (A.28)$$

By performing the differentiations in (A.28) one can generalize to,

$$\phi_Z(\ell) = \sum_{k=1}^{\ell} (-1)^k Z^k (1 - Z)^{N-2-k} \frac{(N - 2)!}{(N - 2 - k)!} a_{\ell k} \qquad (A.29)$$

$$a_{\ell k} = \begin{pmatrix} 1,\ 0,\ 0,\ 0\ \cdots \\ 1,\ 1,\ 0,\ 0 \\ 1,\ 3,\ 1,\ 0 \\ 1,\ 7,\ 6,\ 1 \\ \cdots \end{pmatrix}$$

The $a_{\ell k}$ satisfy the difference equation,

$$k\ a_{\ell k} + a_{\ell k-1} = a_{\ell+1 k}. \qquad (A.30)$$

From Eq. (A.29) as $z \to 1$ we have,

$$\phi(N - 2) = (-1)^{N-2}(N - 2)! \ a_{N-2 \ N-2} \qquad\qquad (A.31)$$

$$\phi(N - 1) = (-1)^{N-2}(N - 2)! \ a_{N-1 \ N-2}$$

$$\phi(N) = (-1)^{N-2}(N - 2)! \ a_{N \ N-2}$$

$$\phi(N + 1) = (-1)^{N-2}(N - 2)! \ a_{N+1 \ N-2} \ .$$

Using Eqs. (A.30) and (A.31), Eq. (8.9) can be shown to be

$$\langle \rho^2_{1N} \rangle = (N - 1)(N + 2)/4 \ .$$

APPENDIX XII

PARTICULAR SOLUTION TO EQ. (8.27)

A particular solution $\tau_{1N}^{(p)}$ to the equation

$$f(E_2)\tau_{1N-2} = (1/2)^N(1/3 - N/3),$$

is desired where:

$$f(E_2) = (E_2 - 1/2)^2.$$

From a theorem on difference equations (36), we can write

$$[f(E_2)]^{-1}a^N F(N) = a^N[f(aE_2)]^{-1}F(N).$$

The particular solution is given by

$$\tau_{1N-2}^{(p)} = [f(E_2)]^{-1}(1/2)^N(1/3 - N/2)$$

$$= (1/2)^N 4(E_2 - 1)^{-2}(1/3 - N/2).$$

Now assume that

$$(E_2 - 1)^{-2}(1/3 - N/2) = AN^3 + BN^2 + CN + D.$$

Then we have

$$(E_2 - 1)^2(AN^3 + BN^2 + CN + D) = 1/3 - N/2.$$

Comparing coefficients of like powers of N leads to the result

$$\tau_{1N-2}^{(p)} = -(1/2)^N N(N - 1)(N - 4)/3.$$

REFERENCES

1. Flory, P.J., J. Chem. Phys., 17, 303(1949).

2. Hermans, J., M. Klamkin and R. Ullman, J. Chem. Phys., 20, 1360(1952).

3. Rubin, R., J. Chem. Phys., 22, 241(1954).

4. Rubin, R., J. Chem. Phys., 20, 1940(1952).

5. Zimm, B. H., W. Stockmayer and M. Fixman, J. Chem. Phys., 21, 1716(1953).

6. Yamamoto, M., Busseiron Kenkyu, 44, 36(1951); Chem. Abstracts, 46, 1844(1952).

7. Grimely, T., J. Chem. Phys., 21, 185(1953).

8. Fixman, M., J. Chem. Phys., 23, 1656(1955).

9. Edwards, S. F., Proc. Phys. Soc., 85, 613(1965).

10. Reiss, H., J. Chem. Phys., 47, 186(1967).

11. Slater, J. C., Quantum Theory of Atoms II (1962).

12. Yamakawa, H., J. Chem. Phys., 48, 3845(1968).

13. Naghizadeh, J., J. Chem. Phys., 48, 1961(1968).

14. Born, M. and H. Green, Proc. Roy. Soc., A 188, 10(1946).

15. Kirkwood, J., J. Chem. Phys., 3, 300(1935).

16. Rice, S. and P. Gray, The Statistical Mechanics of Simple Liquids, Interscience, New York (1965).

17. Mayer, J. E. and M. G. Mayer, Statistical Mechanics, Wiley, New York (1940).

18. Montroll, E., J. Chem. Phys., 9, 626(1941).

19. Rayleigh, Lord, Phil. Mag., 37, 321(1919).

20. James and E. Guth, J. Chem. Phys., 11, 455(1943).

21. Wang, M. and E. Guth, J. Chem. Phys., 20, 1144(1952).

22. Treloar, L. R. G., The Physics Of Rubber Elasticity, Oxford Univ. Press, London (1958).

23. Zimm, B. and W. Stockmayer, J. Chem. Phys., 17, 130(1949).

24. Debye, P., J. Chem. Phys., 14, 636(1946).

25. Blatz P. and J. Curro, Polymer Preprints, A. C. S., 9, 272(1968).

26. Meeron, E., J. Math. Physics, 1, 183(1960).

27. Von Leeuwen, J., J. Groeneveld and J. DeBoer, Physica, 25, 792(1959).

28. Handbook of Mathematical Functions With Formulas, Graphs, and Mathematical Tables, National Bureau of Standards, (1966).

29. Erdelyi, A., W. Magnus, F. Oberhettinger and F. Tricomi, Tables of Integral Transforms, Bateman Manuscript Project, McGraw-Hill, New York (1954).

30. Curro, J. and P. Blatz, J. Chem. Phys., 48, 2832(1968).

31. Percus, J. and G. Yevick, Phys. Rev., 110, 1(1958).

32. Stell, G., Physica, 29, 517(1963).

33. Curro J., P. Blatz and C. J. Pings, J. Chem. Phys., 50 (1969).

34. Wertheim, M., Phys. Rev. Letters, 10, 321(1963).

35. Thiele, E., J. Chem. Phys., 39, 474(1963).

36. Brand, L.,Differential and Difference Equations, Wiley, New York (1966).

37. Tanford, C., Physical Chemistry of Macromolecules, Wiley, New York (1966).

38. Wall, F. and J. Erpenbeck, J. Chem. Phys., 30, 637(1959).

39. Gallacher, L. and S. Windwer, J. Chem. Phys., 44, 1139(1966).

40. Domb, C., J. Gillis and G. Wilmers, Proc. Phys. Soc., 28, 785(1958).

41. Percus, J., Phys. Rev. Letters, $\underline{8}$, 462(1962).

42. Krigbaum, W. and R. Godwin, J. Chem. Phys., $\underline{43}$, 4523(1965).

NOMENCLATURE

a_N	Number of nodal graphs in Z_{1N}
a	Segment length of the model chain
b_N	Number of elementary graphs in Z_{1N}
b	Hard core diameter scaled by the segment length a
$C(b)$	Coefficient defined on p. 112
c_N	Total number of graphs in Z_{1N}
$E_{1N}(\rho_{1N})$	Sum of the elementary graphs in Z_{1N}
E_1, E_2	Difference operators defined on pp. 104 and 105
$\bar{F}_{1N}(k)$	Fourier transform defined by Eq. (8.12)
$f(k)$	Fourier transform of the δ-function Eq. (4.2a)
h_{ij}	Analog of the Mayer function defined by Eq. (3.13)
H_{ij}	$1 - h_{ij}$
$K_1(k, \ell, b)$	Function defined in chapter 5
$K_2(k, \ell, b)$	Function defined by Eq. (5.19a)
$K_3(k, \ell, b)$	Function defined by Eq. (5.19b)
k	Boltzmann's constant and Fourier transform variable
n	Number of segments in the model chain ($N - 1$)
N	Number of subsystems in the model chain
$N_{1N}(\rho_{1N})$	Sum of the nodal graphs in Z_{1N}
P	Probability density
$\vec{p}_i$	Momentum of the ith subsystem
Q_N	Canonical partition function
$\vec{r}_i$	Position of the ith subsystem

$\vec{R}_G$	Radius of gyration of the model chain
$t_{ij}(\rho_{ij})$	Function defined by Eq. (8.1)
$u_{ij}(\rho_{ij})$	Function defined by Eq. (8.5)
v_{ij}	Potential between subsystems i and j
V	Total potential energy of the system
w_{ii+1}	Ordering potential between adjacent subsystems i and i + 1 defined by Eq. (3.10)
$W_{1N}^{(i)}$	Terms in $Z_{1N}^{(i)}$ due to graphs of "isolated" topology defined in Eq. (5.41)
$X_{1N}^{(i)}$	Terms in $Z_{1N}^{(i)}$ due to graphs of the "nested" topology defined in Eq. (5.41)
$Y_{1N}^{(i)}$	Terms in $Z_{1N}^{(i)}$ due to graphs of the "overlapped" topology defined in Eq. (5.41)
$y_{ij}(k)$	Fourier transform defined by Eq. (5.14)
$Z_{1N}(\rho_{1N})$	Restricted configuration integral or unnormalized probability distribution defined by Eq. (3.12)
Z	Unrestricted configuration integral defined by Eq. (3.5)
$Z_{1N}^{(i)}(\rho_{1N})$	Terms in the cluster expansion of $Z_{1N}(\rho_{1N})$ defined by Eq. (5.2)
$z_j(N)$	Coefficients in the power series expansion of $\bar{Z}_{1N}(k)$ defined by Eq. (5.7)
$z_{ij}(N)$	Coefficients in the power series expansion of $\bar{Z}_{1N}^{(i)}(k)$ defined by Eq. (5.7)
z	Function defined by Eq. (2.3)
α	Expansion coefficient of the model chain
β	1/kT
$\gamma(b)$	Exponent defined on p. 112.
$\gamma(C + 1, x)$	Incomplete gamma function

$\delta(x)$	Dirac delta function
$\varepsilon_i(\rho_{1N})$	Coefficients in the expansion of $E_{1N}(\rho_{1N})$ defined in Eq. (7.21b)
Γ_N	Product of delta functions defined by Eq. (3.15)
λ	Expansion parameter in Eq. (7.17)
η	Coupling parameter defined by Eq. (7.9)
$\nu_i(\rho_{1N})$	Coefficients in the expansion of $N_{1N}(\rho_{1N})$ defined in Eq. (7.21a)
$\zeta_i(\rho_{1N})$	Coefficients in the expansion of $Z_{1N}(\rho_{1N})$ defined in Eq. (7.17)
Ω_0, Ω_1	Functions defined by Eqs. (5.33)
ψ_0, ψ_1	Functions defined by Eqs. (5.29)
$\langle X \rangle$	Denotes the mean of X
$\bar{F}$	Denotes the Fourier transform of the function F